Chemical Reactivity and Structural Determination of Metal and Gaseous Adsorbates on Cu{100} using TPD and LEED

Hamid M. Younis Ahmed

Thesis submitted for the
degree of Master of Science

Supervised by:

Dr. Colin J. Barnes

Prof. Han Vos

School of Chemical Sciences

Dublin City University

2003

DECLARATION

I hereby certify this material, which I now submit for assessment on the programme of study leading to the award of M Sc in Chemistry, is entirely my own work and has not been taken from the work of others save and to the extent that such work has been cited and acknowledged within the text of my own work

Signed Hamid M Yousif Ahmed ID Number 99146150

Date 19/9/2003

ACKNOWLEDGEMENTS

I would like to thank my research supervisor the late Dr Colin Barnes and also Prof Han Vos for their help I would also like to thank Dr Ehab AlShamaileh for the great help in writing and correcting many parts of this thesis Also thanks to Dr Wasim Bashir for his encouragement

My thanks to all whom supported me

TABLE OF CONTENTS

* Carried in collaboration with Dr Ehab AlShamaileh

ABSTRACT

The structures formed by adsorbing thin-film platinum, formic acid and oxygen on Cu{100} single crystal are investigated by quantitative low-energy electron-diffraction (LEED) and Temperature Programmed Reaction Spectroscopy (TPRS) Symmetrized Automated Tensor LEED (SATLEED) calculations are used to determine the structure of the formed surface alloys and overlayers TPRS was used to probe the surface reactivity of the systems studied while surface composition was obtained using Auger Electron spectroscopy (AES)

The decomposition of a formate intermediate from a clean Cu(100) surface has been monitored through the use of TPD Spectroscopy CO_2 evolution was observed at ~440K The presence of repulsive lateral interactions between the adsorbates on the surface has been identified, through the shift of the peak temperature T_p to lower values, as the surface was exposed to increasing amounts of formic acid The T_p for 0 5L was observed at 458K,while that for 50L appears at 443K This shift means that the decomposition energy is reduced by 6%

It has also been evidenced that platinum has a destabilising effect on the formate intermediate The peak temperature (T_p) for the CO_2 desorption spectra from copper-platinum model surfaces, appear around 40K lower than those from clean copper This suggests a much less stable surface alloy compared to the clean surface In activation energy terms, this destabilisation can be expressed as a 13% decrease in the energy required for the formate to decompose It was also observed that desorption is much more rapid from the copper-platinum than from clean copper surfaces More study is needed to fully understand these results

A Cu{100}-c(2x2)-Pt surface alloy structure formed by deposition of 1ML mono layer of Pt and thermal processing to 550K is shown to correspond to a copper-capped bimetallic surface localised alloy with a sub-surface ordered c(2x2) CuPt layer The layerwise compositional profile has been extracted via ATA modelling resulting in an almost pure outermost copper monolayer with only a small Pt

impurity concentration (10±10 at%) Layers 3 and 4 contained higher Pt concentrations of 20±20 and 30±30 at% respectively

Substitution of platinum into the selvedge results in a significant expansion in the surface interlayer spacings relative to clean Cu{100} and switches the weak oscillatory relaxation of clean Cu{100} to a strongly and non-uniformly expanded interlayer separation The outermost three interlayer spacings are strongly expanded to 1 84±0 02Å (+1 9±1 1%), 1 91±0 03Å (+5 8±1 7%) and 1 89±0 03Å (+4 7±1 7%) respectively A slight rippling in the c(2x2) CuPt underlayer of amplitude 0 03±0 04Å, with Pt atoms rippled outwards towards the vacuum interface within the composite layer occurs

A Pt/Cu{100}-(2x2)-O surface alloy structure, formed by deposition of a high Pt loading and thermal processing in an oxygen atmosphere, is shown to correspond to an oxygen overlayer on a copper-capped bimetallic surface localised alloy with an ordered c(2x2) CuPt monolayer in layers 2 and 4 The selvedge structure within the LEED probing depth strongly resembles the {100} surface of the $L1_2$ phase of the bulk Cu_3Pt alloy Substitution of platinum into the selvedge results in a significant expansion in the surface interlayer spacings relative to Cu{100}-(2√2x√2)R45°-O due to the larger metallic radius of Pt and switches the weak oscillatory relaxation of Cu{100}-(2√2x√2)R45°-O to a strongly and non-uniformly expanded interlayer separation The outermost three interlayer spacings are expanded with a slight rippling in the first CuPt underlayer with Pt atoms rippled outwards towards the vacuum interface within the composite layer

INTRODUCTION

Many studies have been carried out on the adsorption of formic acid on copper This is of fundamental interest because formic acid represents the simplest carboxylic acid and it tends to form very stable intermediates on copper surfaces This system is of interest in particular to those concerned with methanol synthesis, which is an extremely important process as methanol is a very versatile chemical Methanol has many uses, e g to make formaldehyde, acetic acid, amines, chloromethane, etc Furthermore, methanol is an environmental friendly gasoline extender and it can also be used in the manufacture of methyl tetrabutyl ether, which is an octane enhancer in gasoline [1] The most popular method of methanol synthesis at present involves passing mixtures of CO, CO_2 and H_2 (syngas) over Cu/ZnO-based catalysts Studies into the mechanism and kinetics of methanol synthesis have shown that the adsorption of formate on copper is a very important step in the synthetic pathway

T Kakumoto and T Watanbe have attempted to calculate probable intermediates on the Cu/ZnO catalyst by *ab initio* molecular orbital calculations, (using the density functional method) [2] Their proposed mechanism for methanol synthesis using CO_2 and H_2 is in Scheme 1 1

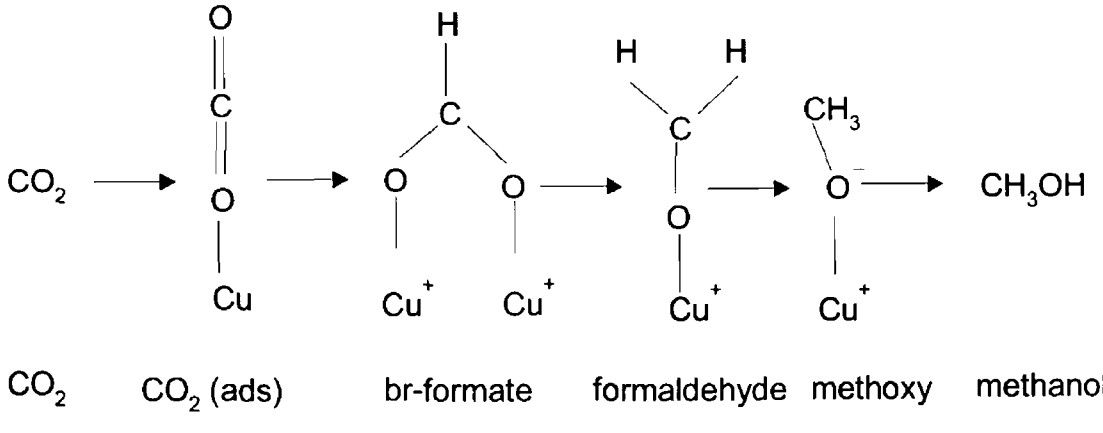

Scheme 1 1

In this mechanism, CO_2 is linearly adsorbed on the Cu^+ site A hydrogen atom attacks the carbon atom of the adsorbed CO_2 and a formate intermediate is formed Subsequently, hydrogen atoms attack the carbon and the oxygen atoms of the formate species, and the C-O bond is broken simultaneously A formaldehyde-type intermediate is formed on the Cu^+ site The H^- on Zn, which is adsorbed on ZnO as result of the heterogeneous dissociation of H_2, attacks the carbon atom of the formaldehyde-type species, and a methoxy intermediate is formed Finally, the H^+ on the oxygen atom of ZnO attacks the oxygen atom of the methoxy, resulting in the production of methanol J Li *et al* [1] have used Fourier Transform Infra Red Spectroscopy and H_2-Temperature Programmed Desorption to determine the following scheme for CO hydrogenation over the Cu-Zn based catalysts

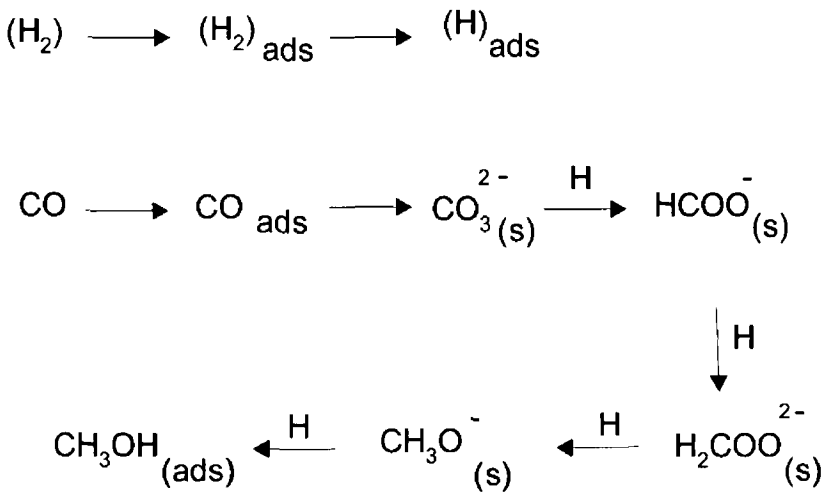

(ads) adsorbed species Scheme 1 2

(s) surface species

H_2 adsorbs on the surface of the catalyst and decomposes to H(ads) species Carbon monoxide is then adsorbed and reacts with the catalyst to form carbonate The carbonate subsequently reacts with H(ads) to produce $HCOO^-$ which becomes hydrogenated to form H_2COO^2 and CH_3OH Li *et al* [1] Deduce from FT-IR studies that the formate should be the intermediate in the synthesis of methanol S

Fujita *et al* have also used FT-IR spectroscopy and Temperatures Programmed Desorption in order to study the synthesis of methanol from CO_2 and CO [3] They found that no HCOO-Cu species were formed during synthesis from CO, only HCOO-Zn However, during synthesis from CO_2, both HCOO-Zn and HCOO-Cu species were detected Hence, only the results obtained by synthetic pathway from CO_2 will be discussed When a CO_2-H_2 mixture was fed over the Cu/ZnO catalyst, CH_3OH was produced together with CO and H_2O The methanol synthesis, $CO_2 + 3H_2 \rightarrow CH_3OH + H_2O$, occurred along with the reverse water gas shift reaction, $CO_2 + H_2 \rightarrow CO + H_2O$

Temperature Programmed Desorption (TPD) profiles obtained by Fujita *et al* [3] show two CO_2 peaks at 443K and 563K H_2 peaks at coincident temperatures accompanied these peaks, which is indicative of formate species One CO peak is observed at 553K with a coincident H_2 peak indicating the presence of a methoxide species, which is formed on the zinc component of the catalyst Further investigation into these results shows that the peak at 443K corresponds to the formate species on copper, while that at 563K corresponds to the formate species on zinc TPD profiles of CO_2 over a pure copper catalyst show only one peak at 440K

Hydrogenation of HCOO-Cu and HCOO-Zn species was conducted at temperatures below 400K, where these species are thermally stable and variation of the amount of the surface species in the hydrogenation was followed by the TPD method It was found that the amount of HCOO-Zn remains unchanged during the course of the experiment while the amount of CH_3O-Zn increases Hence, it can be deduced that CH_3O-Zn was produced through the hydrogenation of HCOO-Cu and not HCOO-Zn However, the HCOO-Cu decrease was not the same as the amount of CH_3O-Zn formed A reason for this might be the slow decomposition of HCOO-Cu to form CO_2 and H_2 Based on these findings, Fujita *et al* [3] have proposed the following mechanism for methanol synthesis from CO_2 (see Scheme 1 3)

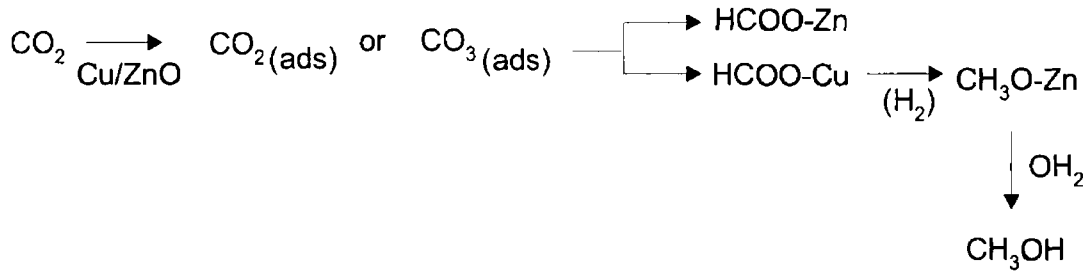

Scheme 1 3

Studies by R Burch *et al* [4] into the role of hydrogen in methanol synthesis provide results that do not quite complement those detailed above Their proposition is that following the generation of the copper formate by co-adsorption of CO_2 and H_2 it decomposes back to from these products Experiments were carried out at temperatures between 493K and 543K CO_2 is released into the gas phase, but atomic hydrogen tends to slipover and is loosely bound by ZnO These hydrogen atoms then diffuse back to the Cu where they attack another formate converting it into a dioxomethylene species This step is believed to be the rate-determining step, because it stabilises the preventing its decomposition back to CO_2 and H_2 Contrary to the beliefs of Fujita and his co-workers, Burch *et al* don't propose the formation of a CH_3O-Zn species that undergoes hydrolysis to form methanol They instead propose that the role of ZnO is merely to trap the hydrogen atoms that result from the decomposition of the formate These hydrogen atoms are those involved in both the hydrogen of another formate to dioxomethylene and hydrogenation of the dioxomehylene to methanol Work by K C Waugh [5] supports the findings of Fujita *et al*, rather than those of Burch *et al* Briefly, there are several theories regarding the exact mechanism of methanol synthesis from syngas over Cu/ZnO based catalysts Nevertheless, there is no doubt that a formate species forms on the copper, and that the hydrogenation of formate is the rate-determining step during methanol synthesis

References:

[1] J Li, W Zhang, L Gao, P Gu, K Sha, and H Wan, Appl Catal 165 (1997) 411

[2] T Kakumoto, and T Watanbe, Catalysis Today, 36 (1997) 39

[3] M Fujita, UsUi, H Ito, and N Takezawa, J Catal 157 (1995) 405

[4] R Burch, and S E Golunski, Catal Letters, 5 (1990) 55

[5] K C Waugh, Catalysis Today, 15 (1992) 51

CHAPTER 1

THEORY OF EXPERIMENTAL TECHNIQUES

1 1 Introduction to Temperature Programmed Desorption (TPD)

Temperature Programmed Desorption (TPD) has been mentioned as a technique that can be applied to the study of the adsorption and decomposition of formic acid on copper

TPD experiments are performed in a continuously pumped ultra-high vacuum chamber At a given temperature, gas is adsorbed on the adsorbent, and a temperature programme, preferably linear in time, is subsequently applied to it As the temperature is ramped up, enough thermal energy becomes available to break surface bonds, resulting in desorption being observed The amount of desorption into the gas phase is monitored as a function of temperature The most popular means of monitoring desorption is by employing a quadrupole mass spectrometer, tuned to the mass of the desorbed species The ioniser must be positioned close to and in direct line of sight of the sample surface The measured mass spectrometer signal directly represents the desorption rate, provided that the pumping speed of the chamber remains constant

The most usual method of heating the sample is by conduction from resistively heated support wires, which are spot-welded to edges of the sample The required temperatures are obtained by controlling the amount of electric current passed to the wires This method of heating ensures that the temperature ramp is linear in time and obeys the relationship

$$T_{(t)} = T_0 + \beta t \qquad \text{Eqn 1 1}$$

where T_0 = initial sample temperature, β = dT/dt (heating rate) in Ks^{-1}

The use of support wires results in the appearance of a "support" peak in a TPD spectrum, upon initiation of the temperature ramp This is because the wires heat up much more quickly than the sample, thus leading to rapid desorption from them

A thermocouple junction is spot-welded to the edge of the sample to measure the sample temperature

Interpretation of TPD spectra allows the determination of the kinetic desorption parameters which are the order (m), the activation energy (E_d) and the pre-exponential factor (A). Information regarding the nature and strength of any lateral adatom interaction, as well as the relative surface coverage and sticking probabilities of adsorbate can also be obtained. The rate of thermal desorption from surfaces can be represented in an ideal form by the Polanyi-Wigner equation:[1]

$$-dN/dt = A\exp(-E_d/RT) \qquad \text{Eqn. 1.2}$$

where N is the number of adsorbed molecules, A is pre-exponential factor. R = 8.31 $Jmol^{-1}$ K^{-1} and T is in Kelvin. A variety of methods are available for deducing values for the kinetic parameters from the experimental data, the two most important being the Redhead method and [1] the Leading Edge method. [2]

1.2 The Redhead method

Incorporation of the β term into the Polanyi-Wigner equation yields the expression

$$-dN/dT = (A/\beta)N\exp(-E_d/RT) \qquad \text{Eqn. 1.3}$$

which upon differentiation gives:

$$-d_2N/dT^2 = mNm\text{-}1(A/\beta)\exp(-E_d/RT)\text{-}E_d/RT^2. \qquad \text{Eqn. 1.4}$$

When $T = T_p$(thermal desorption peak maximum), $d_2N/dT^2=0$.

$$\text{Hence, } E_d/RT^2 = mNm\text{-}1(A/\beta)\exp(-E_d/RT_p). \qquad \text{Eqn. 1.5}$$

For first order desorption, m=1, which simplifies this equation to

$$E_d/R(T_p)^2 = (A/\beta)\exp(-E_d/RT_p). \qquad \text{Eqn. 1.6}$$

This equation can be further modified to $E_d = RT_p[\ln(AT_p/\beta)\text{-}3.46]$ if 108 $K\text{-}1<A/\beta<1013Ks^{-1}$.

Values for T_p and β can be readily deduced from experimental date, so provided that the pre-exponential factor A is known, the activation energy E_d can be calculated. For first order desorption, it is believed that A is of the same order of

magnitude as the molecular vibrational frequency and is usually assumed to be $10^{13}s^{-1}$ [4] It is obvious that the form of the Redhead equation detailed above is limited to applications where the activation energy and pre-exponential factor are independent of adsorbate coverage (i e the equation contains no terms in N) When m = 2 however, there is a coverage dependency In this case, the following form of the Redhead equation is used for the evaluation of activation energy

$$E_d/R(T_p)^2 = (2AN/\beta)\exp(-E_d/RT_p) \qquad \text{Eqn 1 7}$$

(N can be calculated from the integrated area under the peak, provided the pumping speed of the chamber remains constant) For second order desorption, T_p decreases with increasing coverage

1 3 The Leading Edge Method

A significant advantage of this method over the Redhead method is that no assumption of the pre-exponential factor is necessary This method involves construction of an Arrhenius plot based on the Polanyi-Wigner equation, [5] which may be arranged to give

$$\text{Ln } (N/Nm) = \text{Ln } A - (E_d/R)T_p \qquad \text{Eqn 1 8}$$

(N/Nm corresponds to the signal intensity (p))

If the activation energy and the pre-exponential factor are coverage independent, an Arrhenius plot of Ln (p) vs 1/T gives directly E_d from slope (slope = E_d/R) and A from its intercept (intercept = Ln A)

If E_d and A are coverage dependent however, the slope is no longer equivalent to $-E_d/R$

Instead,

$$\text{Slope} = \partial \text{Ln}(-N/Nm)/\partial(1/T)$$

$$= [-E_d(N)]/R + \partial N/(1/T)*[\partial \text{LnA}(N)/\partial N - 1/RT(\partial E_d(N)/\partial N)]T$$

As the second order terms in the above expression cannot be readily evaluated, only when these may be ignored, can the expression be applied
This can happen in one of three ways

1 If E_d and A are constant
2 If $\partial N/(1/T)$ is small This criterion is met at the onset of desorption when the coverage drops by no more than a few percent of its initial value
3 If there is compensation effect between the activation energy and the pre-exponential factor, i e if they vary in concert, in order to fulfil the conditions of the rate constant ($k = A\exp(-E_d/RT)$), thus cancelling the second order terms

Habenschaden and Kuppers [3] have evaluated spectra of CO adsorbed on Co(1010) to illustrate the applicability of the leading edge method The Co (1010) surface was exposed to varying amounts of CO from 0 1L to 1 5L Arrhenius plots of data from the low temperature tail of the various desorption peaks were obtained Good linearity is observed up to a coverage decrease of about 4% from the initial coverage This means that the desorption energies and pre-exponential factors can be evaluated quite accurately from the slope and intercepts, respectively, i e $\partial N/(1/T)$ is vanishingly small
Desorption energies extracted from the plots average at 25KJ/mol The pre-exponential factor for an exposure of 0 1L was found to be $1\ 87x10^{13}$ and that for 0 2L was found to be $2\ 0x10^{13}$ The work of Habenschaden and Kuppers also illustrates the limitation of applying the leading edge method, i e it is necessary to measure the p and T data of the experiment with high accuracy as the temperature region which may be used to extract E_d is rather small
Also, plots of poor linearity may be obtained if there is the problem of background noise interfering with the low temperature tail of the peak

1 4 The Effect of Desorption Order on TPD Spectra

The desorption order markedly affects the shape of the desorption curve and the behaviour of the peak temperature with variation of initial coverage The

characteristic thermal desorption spectrum for a first order process consists of asymmetric desorption peaks, whose maxima appear at the same temperature, regardless of coverage Second order desorption processes are characterised by a shift in peak maxima to lower temperature as a function of increasing coverage, with the peaks appearing symmetric First and second order kinetics are exhibited generally by chemisorbed monolayers, but multilayer systems tend to obey zero order kinetics

An example used to illustrate the latter phenomenon is deposition of palladium on tungsten [4] 2 7 monolayers palladium were adsorbed on W(110) The first monolayer is bound via a strong chemisorption bond, thereby causing desorption from this layer to obey first order kinetics and an asymmetric high temperature peak is observed In second and subsequent monolayers, the bonding is similar to that in a condensed solid of the pure adsorbate The influence of the bonding to the surface is insignificant, therefore, because of this lower bond strenth desorption from these monolayers is represented by peaks appearing at a lower temperature than that from the chemisorbed monolayer These peaks exhibiting zero order kinetics will continually increase in intensity as more and more adsorbate is condensed on the surface, i e they do not saturate Also the peak temperature shifts to higher temperature with increasing coverage and all desorption curves have a common leading edge

The movement of the peak maximum to higher temperature with increasing coverage is also characteristic of a fractional order desorption mechanism However, the curves will generally not have a common leading edge in such a case

In the above discussion on the effect of desorption order on TPD spectra, the presence of lateral interactions between adsorbates was not considered In reality however, these cannot be ignored as they influence the shape of the desorption peak as well as the behaviour of the peak temperature with variation of coverage They are also responsible in some cases for the appearance of multiple peaks in the spectrum Lateral intreactions may be attractive or repulsive in nature Attractive interaction result in the movement of desorption maxima to higher temperature with increasing

coverage It is believed that attractive interactions lead to the formation of islands of adsorbate making them increasingly stabilised Hence, more energy is required in order to stimulate their desorption This process which appears to obey fractional order kinetics may in fact have a first order reaction mechanism, but the peak maxima shifting to higher temperature with coverage is caused by attractive lateral interactions and not because of a fractional order mechanism R G Jones and D L Perry [5] have found that the above phenomenon exists when mercury desorbs from a tungsten (100) surface

Repulsive interactions, on the other hand, cause a shift of the peak maxima to lower temperatures with increasing coverage There is increasing interadsorbate repulsion as more and more material is adsorbed causing neighbouring atoms to become destabilised, and hence leading to a lowering in their adsorption energy It is possible, therefore, to incorrectly interpret a system displaying repulsive interactions as a second order process However, inspection of the peak shape for its symmetry may help to eliminate such misinterpretation In some cases, a great deal of destabilisation may be caused by the repulsive interactions, thereby causing a second low temperature peak to observe Again, there is a possibility of misinterpretation here, i e in such a case it could be wrongly considered that there is a multiplicity of binding sites on the surface Repulsive interactions have been observed on many systems, e g CO on Co (1010)[3] and H_2 on W (100) [6]

1 4.1 Multiple Peaks in TPD Spectrum

Some reference has been made to the various sources of multiple peaks in a TPD spectrum The existence of multiple desorption peaks may arise from

1 Multilayer systems, where one peak represents desorption from the first chemisorbed monolayer, and another set of curves represent desorption from the second and subsequent monolayers where the bonding is not as strong
2 The presence of more than one distinct binding site with differing activation energies for desorption (e g hollow, atop, etc)

3 The existence of coverage-dependent lateral interaction between adsorbates (especially repulsive interactions)

It is difficult to differentiate between (2) and (3), by employing only TPD Spectroscopy Indeed, it is often necessary to gain additional information about the spectroscopy methods, e g Reflection Absorption Infra-Red Spectroscopy or High Resolution Electron Energy Loss Spectroscopy

1 4 2 Effect of heating Rate

Typical heating rates range between 1 and 100K/s The temperature at which maximum desorption occurs will increase if the heating rate is increased Hence, the T_p obtained if a heating rate of 1K/s is used will be much lower than that obtained if 100K/s is used

1 5 Temperature Programmed Desorption (TPD) of Formic Acid on Copper Surfaces

This technique is a variant of thermal desorption, in which products from a surface catalytic reaction are desorbed and detected mass-spectrometrically Because adsorbed molecules can react to from a range of products with different masses, the simultaneous monitoring of several masses is necessary In order to do so the mass spectrometer is programmed to switch rapidly between several different masses Truly continuous monitoring is not possible, but such quasi-continuous outputs are sufficient D H S Ying and R J Madix [7] have used Temperature Programmed Desorption to study the decomposition of formic acid on a copper (110) crystal Following adsorption of the formic acid at 200K the temperature programmed reaction spectrum shown below was obtained

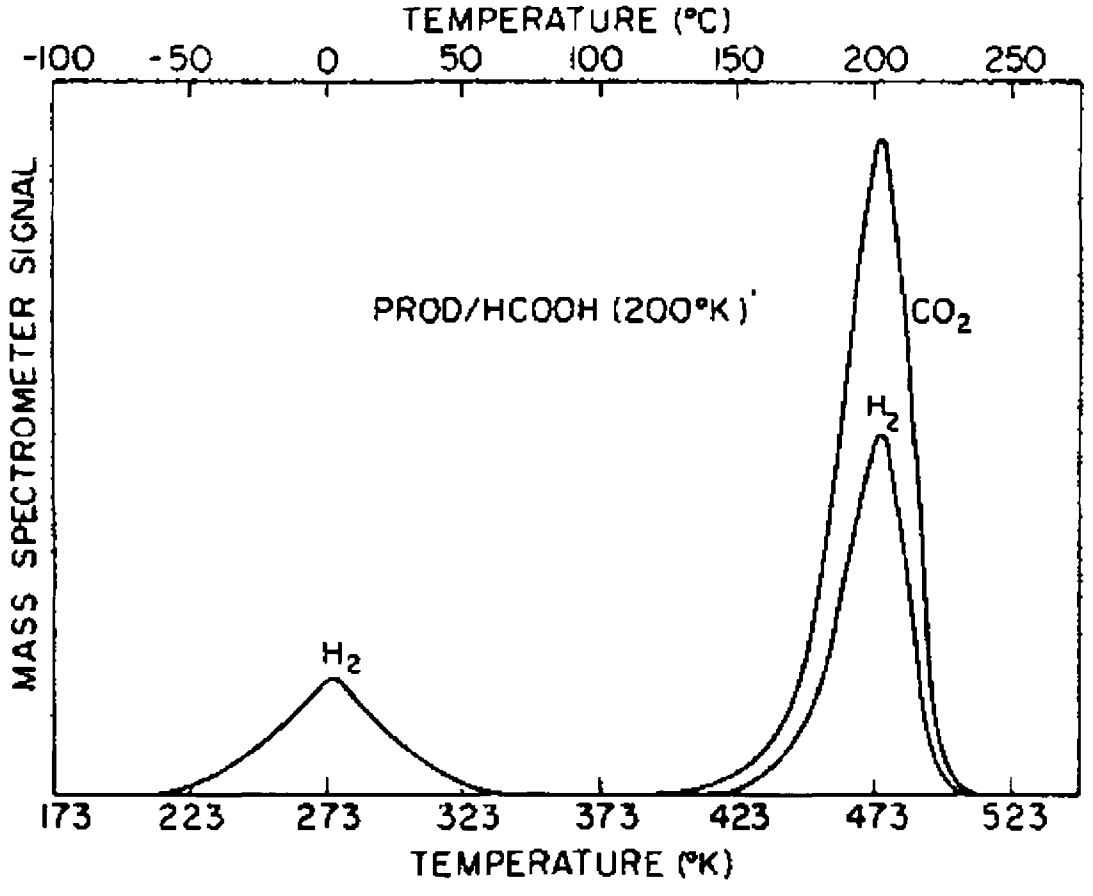

Figure 1 1 Temperature-programmed reaction spectroscopy results for formic acid adsorbed on Cu(110) at 200K [7]

It can be seen that hydrogen desorption occurs below room temperature, followed by the simultaneous evolution of CO_2 and H_2 at 473K Separate experiments studying CO_2 and H_2 adsorption alone, indicate that desorption of both $CO_2$and H_2 is complete below room temperature, as the above results can only be explained in terms of an intermediate being formed on the surface which decomposes to these products at the stated temperature

As a result of further investigations using deuterated formic acid, a formate species has been proposed as the intermediate The spectrum shown below was obtained, after adsorbing HCOOD at 200K [7]

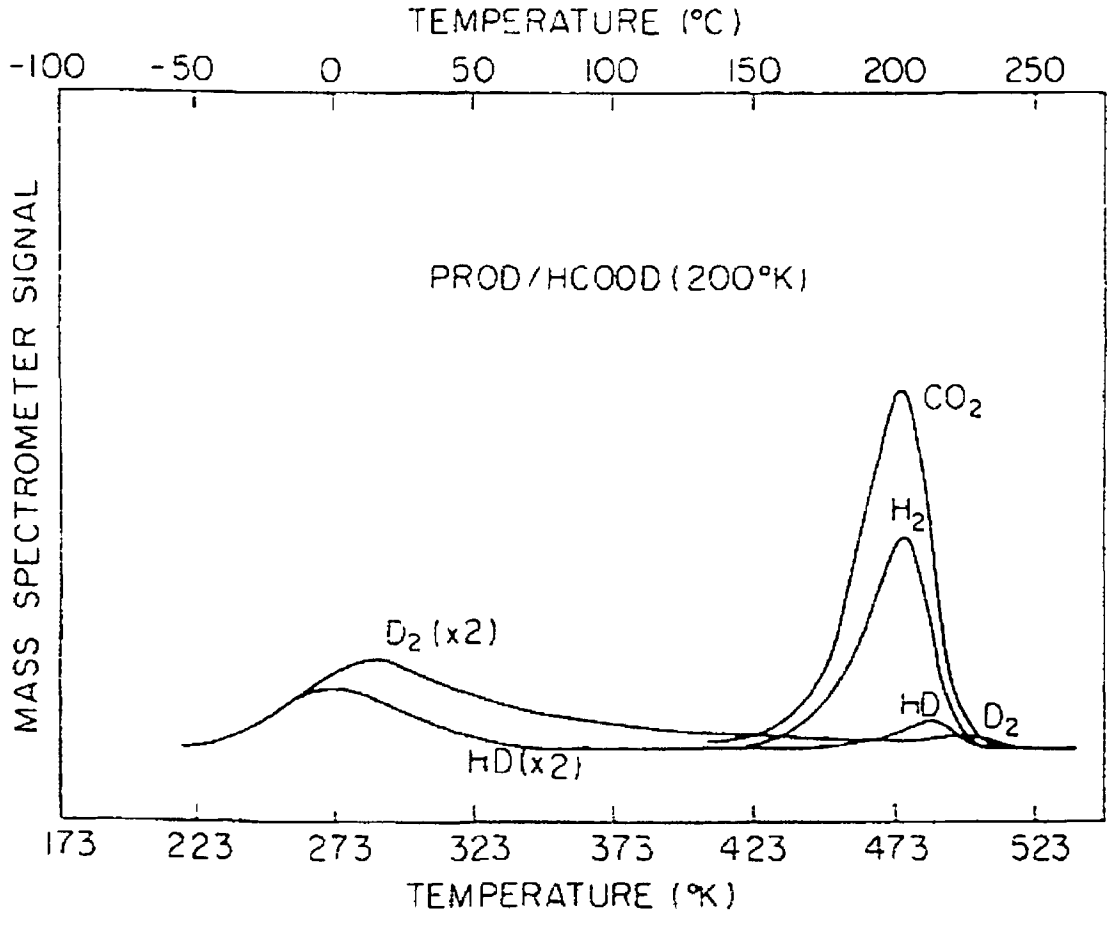

Figure 1 2 TPRS results for the products evolved from Cu(110) subsequent to HCOOD adsorption at 200K Some HCOOH was present [7]

The peaks observed can be accounted for in terms of the following mechanism

$HCOOD_{(ads)} \rightarrow HCOO_{(ads)} + D_{(ads)}$ Eqn 1 9

$2D_{(ads)} \rightarrow D_{2(ads)}$ 273K Eqn 1 10

and

$2HCOO_{(ads)} \rightarrow 2\,CO_{2\,(g)} + H_{2\,(g)}$ 473K Eqn 1 11

The evolution of HD is attributed to HCOOH impurities in the dosed gas

A quantitative evaluation of the amounts of H_2 and CO_2 evolved at 473K verified the H_2/CO_2 stoichiometry expected from decomposition of $HCOO_{(ads)}$

Another example of where TPRS has been applied in order to determine surface reaction mechanisms is formaldeyde on clean copper (110) surface, and an oxygen dosed Cu(110) surface The following is a spectrum obtianed by M Bowker and R J Madix [8]

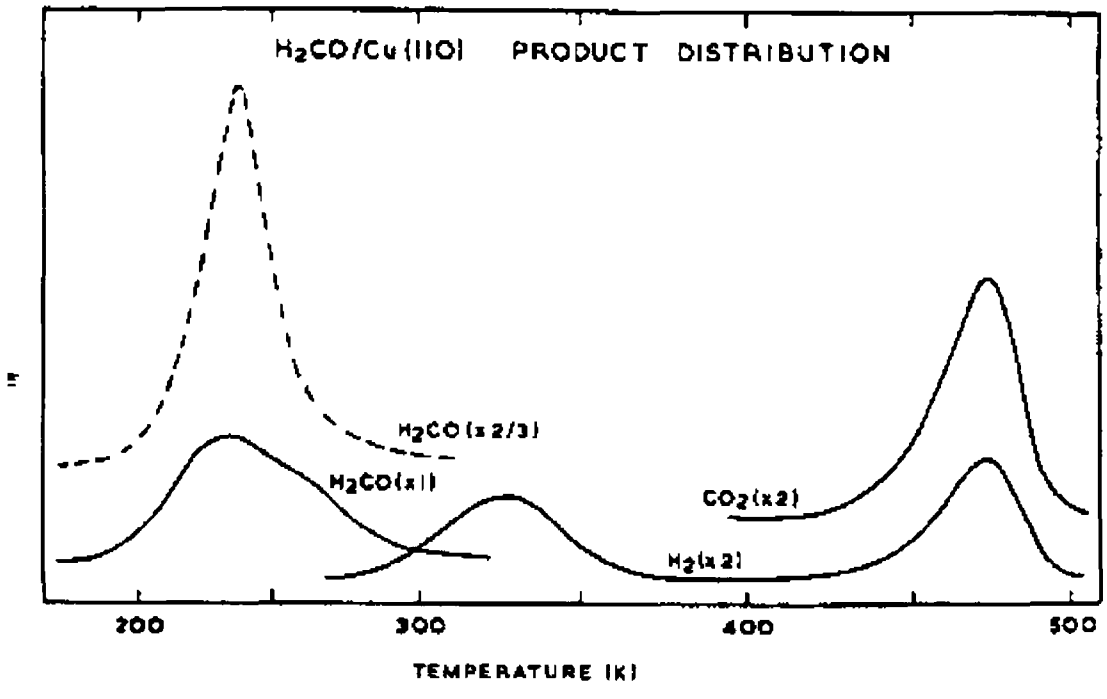

Figure 1 3 The product distribution seen in TPRS for formaldehyde adsorption on Cu(110) at 140K, (---) clean surface exposed to 5000 μs formaldehyde and (——) the surface pre-dosed with 2 5L of oxygen at 300 K and subsequently given a dose of 1000 ks H_2CO at 140K The heating rate was 4 Ks^{-1} [8]

It is evident that the only product desorbed from the clean Cu(110) surface was the formaldehyde itself which desorbed at 230K The proposed mechanism of the interaction of formaldehyde with the oxygen dosed Cu(110) surface is outlined below in Scheme 1 4

$H_2CO_{(g)} \rightarrow H_2CO_{(ads)}$ (1)

$H_2CO_{(ads)} \rightarrow H_2CO_{(g)}$ (2)

$H_2CO_{(ads)} + O_{(ads)} \rightarrow H_2COO_{(ads)}$ (3)

$H_2COO_{(ads)} \rightarrow HCOO_{(ads)} + H_{(ads)}$ (4)

$H_{2\,(ads)} + H_{(ads)} \rightarrow H_{2\,(g)}$ (5)

$HCOO_{(ads)} \rightarrow CO_{2\,(ads)} + H_{(ads)}$ (6)

$CO_{2\,(ads)} \rightarrow CO2_{(g)}$ (7)

$H_{(ads)} + H_{(ads)} \rightarrow H_{2(g)}$ (8)

Scheme 1 4

Step (2) is associated with the low temperature desorption of formaldehyde (235K), and it is presumed that step (3) takes place upon adsorption at 140K Step (4) takes place at 230K, and subsequently atomic hydrogen species remain on the surface until they desorb in second order fashion as molecular hydrogen at 320K The formate decomposition step (6) then occurs at 480K yielding co-incident decomposition limited peaks of H_2 and CO_2 in a 1 2 ratio (steps 7 and 8)

A further system which Madix and co-workers have studied in detail is methanol adsorbed on Cu(110) [9] Isotopic labelling was again used to ease the interpretation of the reaction mechanism on the surface by differentiating between C-bonded hydrogen and hydroxyl hydrogen and labelled $^{18}O_2$ to pre-dose the surface and distinguish it from the oxygen in methanol The reactions observed in this case are shown in Figure 1 4 and the mechanism is in Scheme 1 5

$CH_3OD_{(g)} \rightarrow CH_3OD_{(ads)}$ (1)

$CH_3OD_{(ads)} + {}^{18}O_{(ads)} \rightarrow CH_3O_{(ads)} + {}^{18}OD_{(ads)}$ (2)

$CH_3OD_{(ads)} + {}^{18}OD_{(ads)} \rightarrow CH_3O + D_2\,{}^{18}O_{(ads)}$ (3)

$D_2{}^{18}O_{(ads)} \rightarrow D_2{}^{18}O_{(g)}$ (4)

$CH_3O_{(ads)} \rightarrow H_2CO_{(g)} + H_{(a)}$ (5)

$CH_3O_{(ads)} + H_{(a)} \rightarrow CH_3OH_{(g)}$ (6)

$2H_{(ads)} \rightarrow H_{2\,(g)}$ (7)

Scheme 1 5

Steps (2) and (3) show the reaction of adsorbed alcohol with pre- dosed oxygen, $D_2{}^{18}O$ is the only water product evolved and desorbed at low temperature leaving two

methoxy species for every pre-dosed oxygen atom The products evolved at 350K are then desorbed in decomposition-limited peaks from the break- up of the methoxy

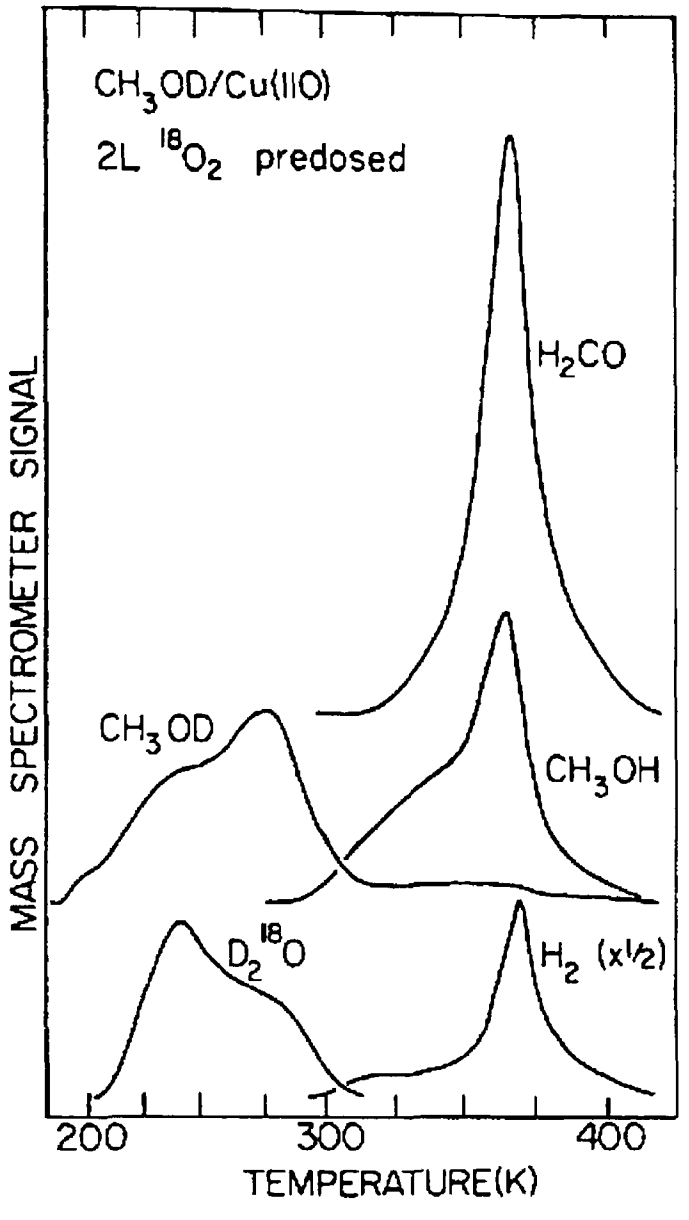

Figure 1 4 Thermal desorption product distribution after methanol adsorption on a Cu(110) face pre-dosed with 2L of $^{18}O_2$ [9]

1 5 1 Formic acid on copper single crystal surfaces

The work of D H S Ying and R J Madix [7] has been referred to briefly, in relation to Temperature Programmed Reaction Spectroscopy A more in-depth review of their work into formic acid decomposition on clean Cu(110) surface will now be given The purpose of their work was to determine the decomposition mechanism and the kinetics of the reaction Flash desorption spectroscopy was employed in order to do so As evident from Figure 1 1, the sole products observed from the decomposition of formic acid on a Cu(110) surface were carbon dioxide and hydrogen In order to characterise the order of the process, CO_2 flash desorption spectra were plotted as a function of formic acid exposure, Figure 1 5 As can be seen, the CO_2 peak position was independent of exposure over two orders of magnitude change in the initial exposure This independence is indicative of a first order process

Two different techniques were used to determine the activation energy of the CO_2 product The heating rate variation method and the leading edge method The heating rate variation method involves plotting $Ln(N_p)$ and $Ln(\beta/T_p^2)$, respectively as a function of reciprocal peak temperature (N_p is the maximum desorption rate) The slope of these plots was used for the evaluation of the activation energy values of CO_2 product A value of 31 89 KJ/mole was obtained using the $Ln(N_p)$ plot and 31 87 kcal/mole was obtained using the $Ln(\beta/T_p^2)$ plot

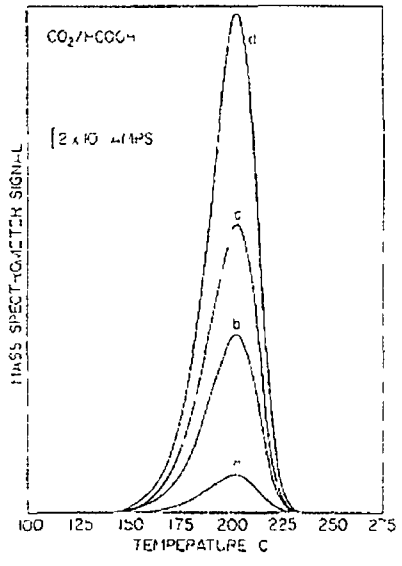

Figure 1 5 A coverage variation study for the CO_2/HCOOH product peak Relative exposures are given as pressure in the dosing line times, the exposure time (a) ~ 100 μ sec, (b) 500 μ sec, (c), 2000 μ sec (d) 10000 μ sec [7]

The Leading Edge Method yielded the following plot and activation energy of 139 3 KJ/mole

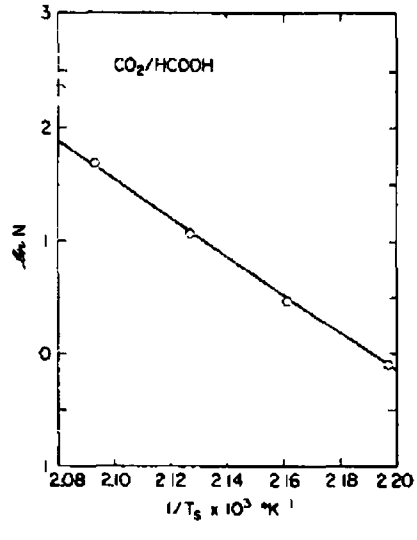

Figure 1 6 Determination of the activation energy of the CO_2/HCOOH peak by plotting Ln(N_p) versus the reciprocal temperature at constant coverage [7]

The activation energy obtained was used for the simulation of a first-order theoretical spectrum to fit the CO_2 peak The simulated spectrum obtained is shown below Figure 1 7

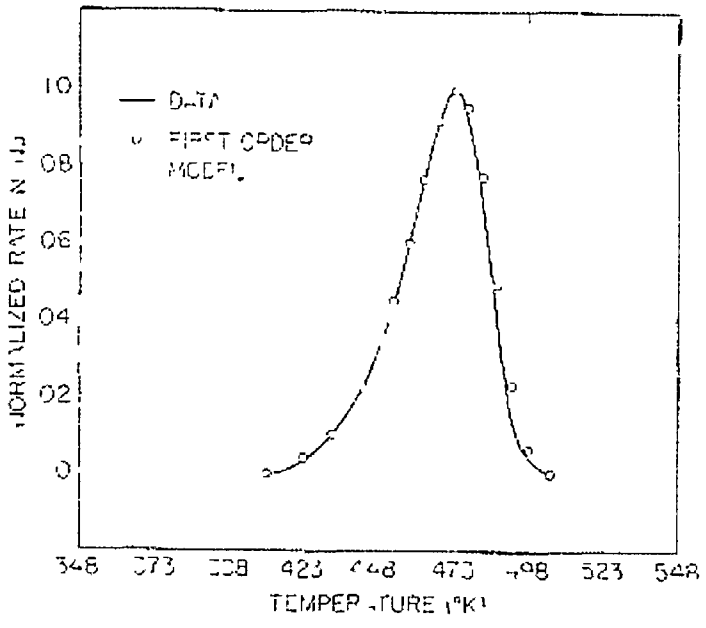

Figure 1 7 Computer simulation to fit the CO_2/HCOOH product spectrum Heating rate was 4 7K/s [7]

An Activation energy of 133 3KJ/mole and a pre-exponential factor of $9\ 4*10^{13}sec^{-1}$ were reported, utilising this method This pre-exponential value was reasonable considering results of infrared study, obtained by Ito and Suetaka [10]

The work of Ito and Suetaka also supports the findings of Ying and Madix, [8] in another respect, i e in terms of the formation of the formate ion as the intermediate Ito and Suetaka have used an infrared reflection method for the study of the adsorption of formic acid on evaporated copper surfaces, and confirmed the presence of formate ions The technique employed was capable of accurately determining the molecular orientation of formate on the copper surface Reflection spectra of the formate showed a $1360cm^{-1}$ band associated with the symmetric OCO stretching vibration but not the $1600cm^{-1}$ asymmetric OCO band The reverse was true of transmission spectra of smooth copper films deposited on polished KBr plates These

results lead to the conclusion that the chemisorbed formate molecules are oriented almost vertically on the smooth copper surface as shown

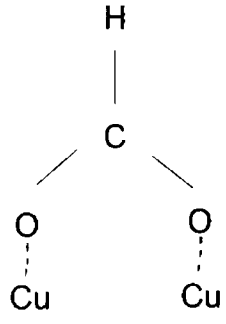

Figure 1 8 Geometry of formate on copper

M Bowker and R J Madix [8] have used a combination of XPS, UPS and thermal desorption techniques to study the reaction of formic acid on a copper (110) surface DCOOH was adsorbed at 140K Ultra-violet photoelectron spectra show that, although the formic acid adsorbs molecularly at 140K, its molecular structure is strongly perturbed by adsorption Dissociation of the acid hydrogen takes place during heating at around 250K The thermal desorption spectrum obtained, shows the desorption of the intact acid at a low temperature (~190K), followed by the desorption of H_2 at 280K Again as expected, the coincident desorption of D_2 and CO_2 in the ratio 1 2 is observed at 480K, indicative of the presence of the formate ion The most important point to note from the X-ray photoelectron spectra is that Ito and Suetaka s[10] proposition regarding the structure of the formate ion on Cu (110) is supported Oxygen 1s XPS linewidths indicated quite clearly that the two oxygen atoms in the formate molecule are equivalent, thereby supporting the suggestion that the formate is bound to the surface through both oxygen atoms, as illustrated above m Figure 1 8

The chemisorption and decomposition of formic acid on a copper (100) surface has been studied using high-resolution electron energy loss spectroscopy by B A Sexton [11] His findings provide futher evidence for the dissociation of formic acid upon adsorption, and also support the proposition that the formate binds in a bidentate

fashion with the copper surface At 100K, formic acid (HCOOH and HCOOD) was physically adsorbed on the clean Cu(100) crystal This was indicated by the appearance of C-O, C=O, C-H, O-H and O-D bands in the vibrational spectrum Annealing to 400K resulted in the formation of a strongly bound layer of formate species (HCOO) The observation of four prominent sets of vibrations at 340, 760 and 1330cm ^{1}, and a partially resolved doublet at 2840 and 2910cm ^{1} demonstrate this The 340cm ^{1} band is strongest in the spectrum and can be assigned to the copper-oxygen vibration of the formate-surface complex The 760cm ^{1} mode can be assigned to the deformation vibration of the OCO group The band at 1330cm ^{1} results from symmetric COO stretching and the doublet near 2900cm ^{1} can be identified as CH vibrations A complete absence of any bands due to υ(OH), υ(OD), or υ(C-O) CO confirms that both the physically adsorbed acids were converted to the same surface species HCOO The following digram shows the four possible symmetry groups for a bidentate copper formate surface complex

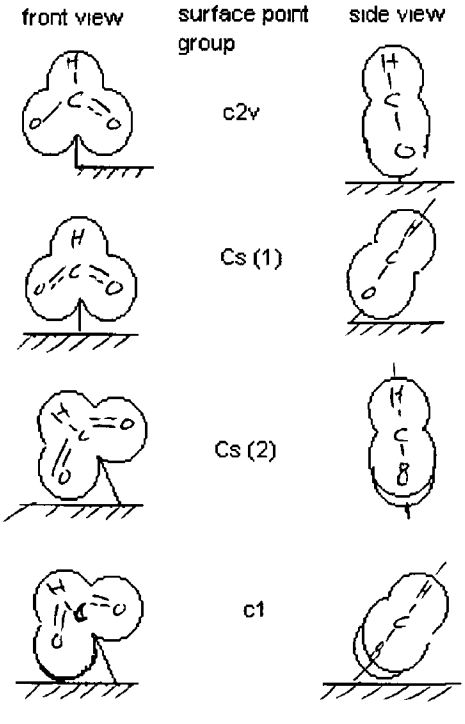

Figure 1 9 The four possible points groups for a bidentate copper- formate surface complex [11]

Sexton proposes that at 400K, the formate species possesses either C_{2v} or $C_s(1)$ symmetry (or possibly both) and at 100K, low symmetry orientations of the formate ($C_s(2)$ or C_1) exist Conversion between the low and high temperature states was found to be reversible

The reactive adsorption of formic acid on clean (110) and on oxygen dosed Cu(110) has been studied more recently by M Bowker *et al* [12] A combination of a molecular beam system, TPD, LEED and STM was employed to do so Figure 1 10 shows TPD profile of the two surfaces The data look similar to those reported earlier by Bowker and Madix [8] The desorption from the clean surface shows classical first order desorption kinetics, i e an asymmetric peak shape and a peak temperature which doesn't vary with coverage When oxygen was pre-adsorbed on the surface however, the CO_2 curve had a shoulder at the leading edge (~430K) This is thought to be due to a bidentate formate adsorbed in a different adsorption site from the more stable species The presence of the pre-adsorbed oxygen also results in the production of water, when the formic acid dissociated

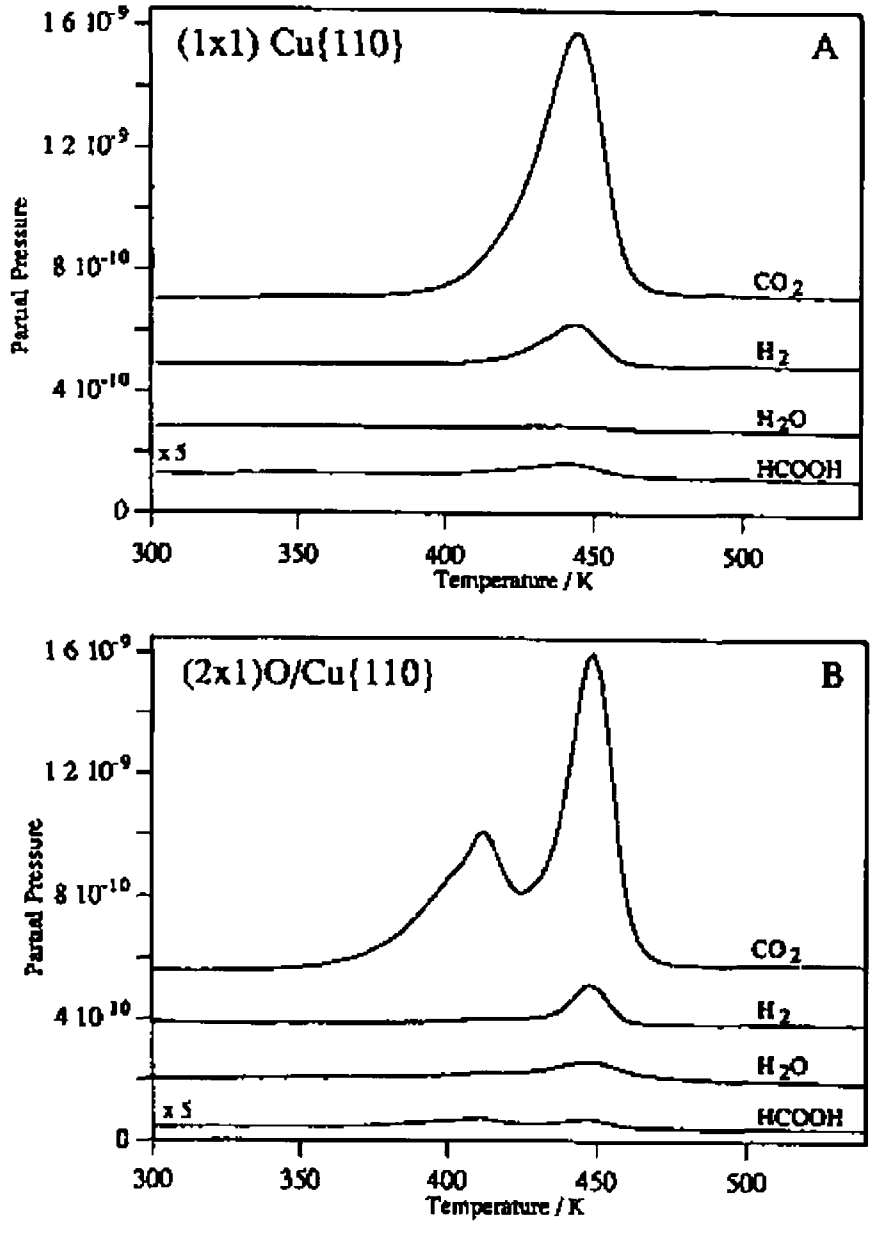

Figure 1 10 TPD Spectra for formic acid decomposition on (A) the clean Cu(110) surface at saturation coverage and from (B) the surface pre-dosed with 0 5 monolayers of oxygen [12]

Additional information was obtainable in the more recent work of Bowker [12] because of the incorporation of the molecular beam system This permits the study of surface reactions at high temperature where the formate intermediate is unstable As a result, it has been discovered that the mechanism of the reaction of formate with pre-adsorbed oxygen changes with substrate temperature As the surface temperature increases, the overall stoichiometry changes from (1) at ~450K to (2) at ~600K below

$[\sim 450K]\ 2HCOOH + O_{(ads)} \rightarrow 2CO_2 + H_2 + H_2O,$ (1)

$[\sim 600K]\ HCOO_{(ads)} + O_{(ads)} \rightarrow CO_2 + H_2O,$ (2)

The mechanism for the low temperature state is as follows

$HCOOH + O_{(ads)} \rightarrow HCOO_{(ads)} + OH_{(ads)}$ (1)

$HCOOH + OH_{(ads)} \rightarrow HCOO_{(ads)} + H_2O_{(g)}$ (2)

$2HCOO_{(ads)} \rightarrow 2CO_{2(g)} + H_{2(g)}$ (3)

However, at more elevated adsorption temperatures the following steps occur

$HCOOH + O_{(ads)} \rightarrow HCOO_{(ads)} + OH_{(ads)}$ (1)

$HCOO_{(ads)} \rightarrow CO_{2(g)} + H_{(g)}$ (2)

$H_{(ads)} + OH_{(ads)} \rightarrow H_2O_{(g)}$ (3)

The instability of the formate intermediate at temperatures above its desorption peak temperature, results in the rate of dehydrogenation of this species becoming fast, such that both hydrogen atoms from one molecule react with an oxygen to form water Bowker *et al* [12] have also presented values for the sticking probability of formic acid on the two copper surfaces A value of 0 1 was reported for the clean Cu(110) which increased to 0 8 at partially oxidised Cu(110) surfaces

One aspect of the work of Bowker and his co-workers that has not been convincingly explained is the appearance of the second (lower) CO_2 peak ~430K upon desorption from the oxidised Cu(110) surface It was proposed that it might be due to lateral interactions, or a formate being adsorbed in a different adsorption site from the more stable species However, if the latter was the case, a co-incident hydrogen peak should also be observed, and this is not so

A F Carley, P R Davies and G G Mariotti [13] have studied this system in more detail The Cu(110) surface was saturated with oxygen and following adsorption of formic acid, two CO_2 peaks were observed in the TPD spectrum, one at 440K and one at 400K Only the peak at 440K was accompanied by a H_2 curve The ratio of the

areas of these hydrogen and carbon dioxide peaks is approximately 1 2 as expected for the decomposition of formate Because the 400K CO_2 desorption peak has no hydrogen desorption associated with it, assignments to formate must be ruled out Earlier work by Carley and co-workers [14] had previously shown that carbonate can be formed at copper surfaces from the oxidation of carbon dioxide and that this carbonate decomposes above 370K to give chemisorbed oxygen and carbon dioxide The formation of a surface carbonate from the oxidation of formic acid at the copper surface would therefore account for the TPD data obtained in this case

1 6 Formic acid on CuPt CuPd surface alloys

J P Reilly *et al* [15] have studied formic acid adsorption and decomposition on palladium/Cu(110), in an attempt to establish the reactivity of the surface A range of Pd coverages were alloyed with Cu(110) surface, and the TPD spectra obtained after dosing with formic acid are shown below, Figure1 11

Coincident CO_2 and H_2 desorption is evident at ~430K, in the case of 1ML mono layer and 2 5ML Pd being alloyed with the surface This desorption is quite similar to that observed for clean Cu(110) However, the peak temperature is slightly shifted to a lower value This indicates a slight de-stabilisation of the formate intermediate due to the presence of the palladium For the higher coverages of palladium (4ML and 8ML), a remarkable decrease in the peak temperature is observed CO_2 evolution now occurs at ~360K This demonstrates that the formate has been significantly de-stabilised by the increased amounts of palladium Considering this destabilisation in terms of the activation energy, the decrease in T_p corresponds to a reduction of ~22KJ/mol ^{1} relative to pure copper

A possible explanation of the similarity of formate decomposition from the low Pd loadings and the clean Cu(110) may be due to the fact that the surfaces were annealed to 500K prior to dosing with formic acid It is quite possible that this pre-annealing leads to a pure Cu layer capping a mixed CuPd alloy Hence, the kinetics of formate decomposition are very similar to those on pure Cu(110) At the higher Pd

coverags however, the chemistry is remarkably different The CO_2 desorption peak in these cases, are neither Cu-like nor Pd-like This suggests the existence of an outermost mixed CuPd layer, which would explain the significant destabilisation of the formate The configuration of the formate on this alloyed layer is unknown, but Reilly *et al* have proposed that an interatom bidentate intermediate binds to both a Cu and a Pd atom simultaneously

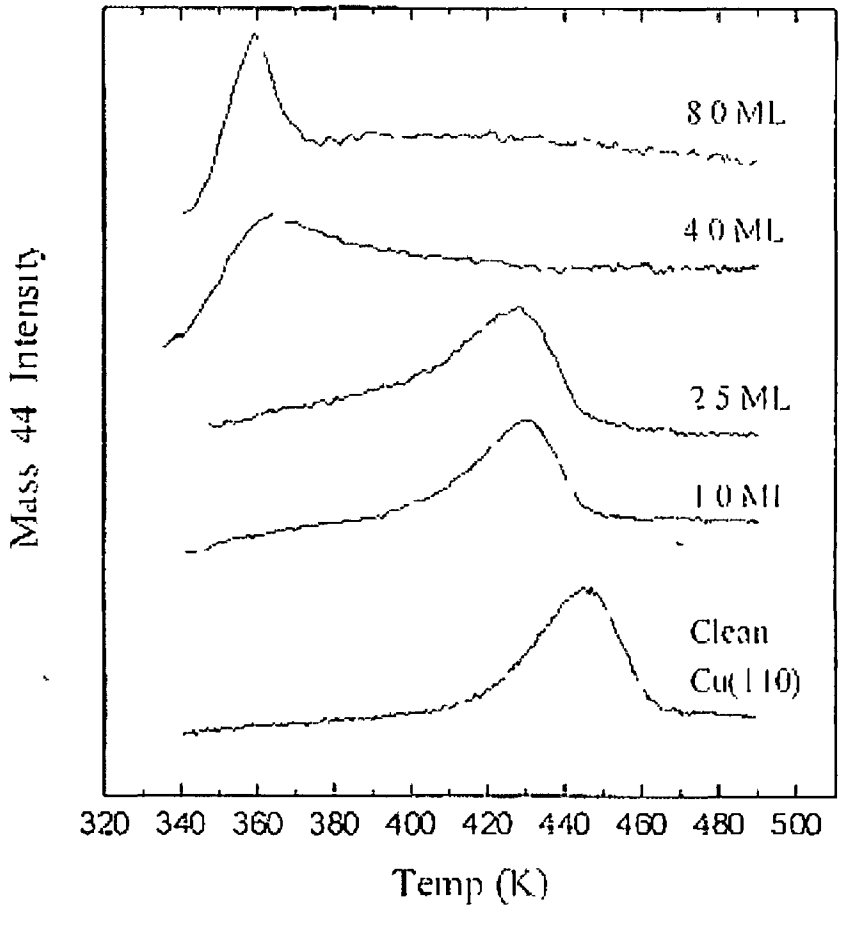

Figure 1 11 Mass 44 (CO_2) TPD spectra from clean Cu(110) and for Pd films of (a) 1 ML [coincident H_2 (mass 2) desorption (dotted line)], (b) 2 5 ML, (c) 4 ML, and (d) 8 ML All Pd films were preannealed to 500K and recooled to 300K prior to dosing with saturation formic acid coverage (~10L) [15]

Little other work has been done on the adsorption and decomposition of formic acid on copper-palladium surfaces It also appears that no investigations have been carried out to date, regarding formic acid decomposition on copper platinum surfaces

1 7 Surface alloy and overlayers in catalysis

A surface may be defined as the interface between a condensed phase of matter (solid or liquid) and another phase (solid, liquid or gas) In surface, a surface has a more precise picture represented by the top few atomic layers of a solid A single crystal surface is formed when a solid is cut paralled to a selected plane of atoms Surface atom properties are expected to be different from those of the bulk of the solid due to the forced interaction with another phase and also due to the loss of some neighbouring atoms Upon cutting, a rearrangement of atomic positions at the solid single crystal surface may take place such as atomic relaxation or reconstruction The region over which atoms relax or reconstruct (usually few atomic layers deep) is often called the selvedge [16]

The surface atoms of a single crystal are usually arranged in a regular repeating lattice structure Table 1 1 shows types of close-packed crystal structures adopted by metals with some examples of each type

Crystal structures	Abbreviation	Examples
Face-centred-cubic	Fcc	Cu,Pd,Pt, Au
Body-centred-cubic	Bcc	K, Cr, W, Fe
Hexagonal-close-packed	Hcp	Co, Ti, Cd, Mg

Table 1 1 Close-packed crystal structures adopted by metals

Figure 1 12 shows a unit cell of a fcc lattice with different cross-sections giving different surface atomic arrangement, which are identified by their Miller indices

The three planes illustrated in the figure correspond to the simplest and most studied low index Miller indices {100}, {110} and {111} This is due to their relatively uniform and known geometry (ignoring the Samuel percentage of defect sites present on these surfaces such as step sites, kinks, etc)

The structure at the surface is different from the bulk crystal because the surface atoms have lost some of their neighbour atoms For example, and as shown in Figure 1 12, compared to their normal bulk co-ordination number from X-ray diffraction, the {100} surface atoms have lost 4 nearest neighbours while the {110} and the {111} surface atoms have lost 5 and 3 nearest neighbours, respectively This simple fact makes the {110} surface atoms unstable and hence the most reactive while {111} is the most stable surface In order to compensate for the loss of bonding, surface atoms may undergo surface relaxation in the form of an oscillatory change in the mterlayer spacing

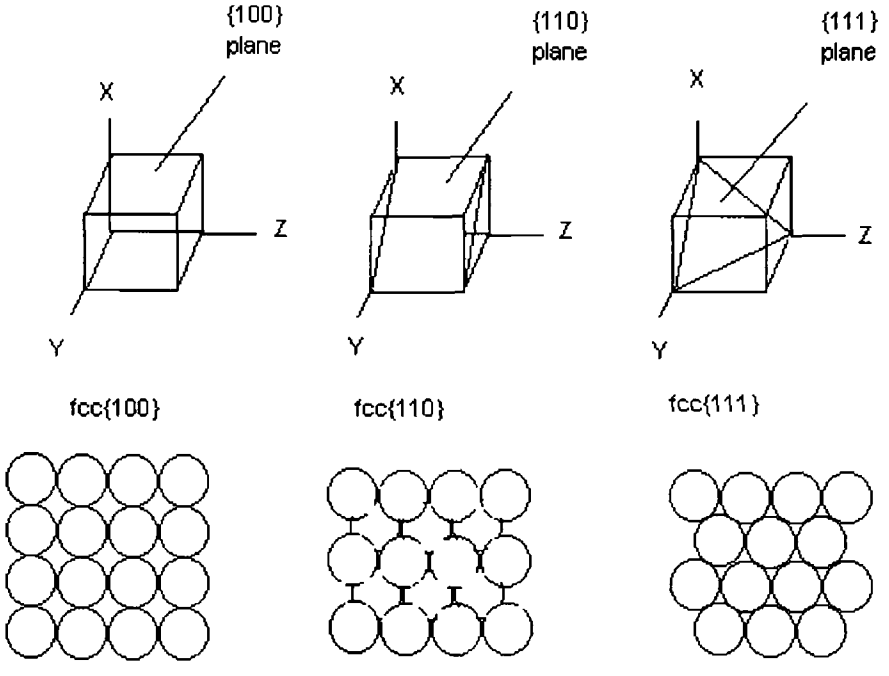

Figure 1 12 the fcc unit cell of a single cubic lattice illustrating the {100}, {110} and {111} planes and their corresponding real space atomic arrangement [1]

The Cu{100} selvedge undergoes a relaxation in which the first interlayer spacing is contracted by about 1% relative to the bulk value This can be explained by the presence of extra attraction forces exerted from the second atomic layer onto the top atomic layer (next to the vacuum) The attraction forces between first and second layer atoms in Cu{100} also pulls the second layer away from the third layer (towards the vacuum) resulting in an expansion of about 1 2% Therefore, the third interlayer spacing experiences a small contraction of about 0 5%

In the case of the {110} surface where the surface energy is relatively large, a surface reconstruction may take place to maximise surface atom co-ordination and to lower the surface energy Most metallic {110} surfaces undergo surface reconstruction, for example, the clean Au{110}-(1x1) surface becomes what is called the (1x2) missing-row reconstruction illustrated in figure 1 13 [17]

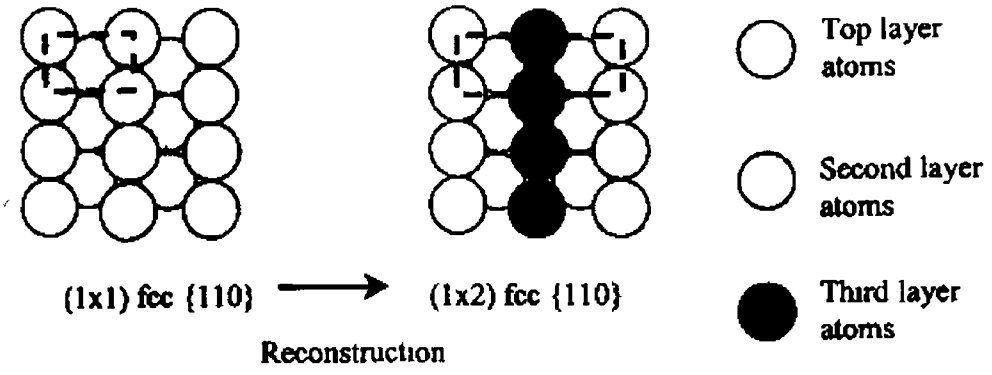

Figure 1 13 Reconstruction of the fcc{110} surface from a bulk truncated (1x1) structure to a (1x2) missing row surface Dashed lines show the unit cell in each case

An alloy is a solid mixture of two or more metals Surface alloys are made by the physical incorporation of one or more metals within the selvedge of a different metal (the substrate) Physical Vapour Deposition (PVD) is a common technique used to make surface alloys by the selective evaporation of metals onto the substrate [19] In some cases, the evaporated metals do not mix with the substrate but form surface overlayers instead

The first surface alloy was reported by Palmberg and Rhodin in the Au/Cu{100} system in 1968 [19] Despite the existence of Au/Cu bulk alloys, the formation of surface alloys do not require the bulk miscibility of the mixed metals (e g the Ni/Au system [20]) From a chemical point of view, metals and surface alloys and overlayers may be classified as heterogeneous catalysts (the catalyst is in the solid phase and the reactants are in different phases) The first industrial process based on heterogeneous catalysis was the synthesis of ammonia on modified iron as the catalyst in 1909 [20]

In the study of surface catalysis, surface alloy and overlayers utilising single crystals are considered as model catalysts because it is much easier to interpret their experimental results than polycrystalline surfaces Under controlled experimental conditions, the surface composition and structure of surface alloys and overlayers is studied in an attempt to either discover a new catalyst or to improve an existing catalyst s selectivity and /or activity The importance of catalyst development comes from their widespread use in many applications, for example automobile exhaust control [21], polymerisation [22], methanol synthesis [23] and reforming reactions [24]

1 8 Characterisations of surface alloys and overlayers

Surface science tries to understand the relationship between the physical and chemical properties of surfaces Since catalytic performance strongly depends on the surface properties of heterogeneous catalysts, several qualitative and quantitative techniques have been applied to study the structure and composition of surfaces

Table 1 2 presents a selection of the most commonly used surface-science techniques

Technique name	Acronym	Primary surface information
Low energy electron diffraction	LEED	Surface structure
Auger electron spectroscopy	AES	Chemical composition
Temperature programmed desorption or Thermal desorption spectroscopy	TPD TDS	Composition, heat of adsorption and structure
X-ray diffraction	XRD	Surface structure
Ion-scattering spectroscopy	ISS	Structure and composition

Low energy electron diffraction (LEED) and X-ray diffraction (XRD) techniques are used for structural studies The chemical reactivity is investigated by temperature programmed desorption/reaction spectroscopy (TPD/TPRS) By studying the structure and chemical reactivity of model catalysts, surface scientists aim at developing better techniques for making and testing stable and high under normal industrial operating conditions

1 9 The Cu{100} surface alloys and overlayers

The importance of copper as a heterogeneous catalyst is demonstrated by its use in some important large-scale industrial processes including the synthesis of methanol [25], and higher alcohols and ethers and in phenol oxidation [25]

The single crystal Cu{100}is usually chosen as a model substrate due its highly well-defined and stable surface structure and also due its relatively low cost Model systems like the Cu{100} single crystal and well-characterised Cu-based surface alloys and overlayers are studied to establish a link between the microscopic level of understanding the bonding and reactivity of adsorbates and the macroscopic measurements of kinetic rate and thermodynamic properties of the reacting system The knowledge is then exploited to create surfaces with the required microscopic structure to produce the desired catalytic properties

REFERENCE

[1] C J Barnes and Attard, "Surfaces", Oxford Chemistry Primers (1998) 72

[2] J B Miller, H R Siddiqui, S M Gates, J N Russell, and J T Yates, J Chem Phys , 11 (1987) 6725

[3] E Habenschaden and J Kuppers, Surf Sci 138 (1984) 147

[4] W Schlenk and E Bauer, Surf Sci 93 (1980) 9

[5] R G Jones and D L Perry, Surf Sci 82 (1979) 540

[6] T Toya, J Vac Sci &Tech 9 (1972) 890

[7] D H S Ying and R J Madix, J Catal 61 (1980) 48

[8] M Bowker and R J Madix, Surf Sci 102 (1981) 542

[9] M Bowker and R J Madix, Surf Sci 95 (1980) 190

[10] M Ito and W Suetaka J Phys Chem 79 (1975) 1190

[11] B A Sexton, Surf Sci 88 (1979) 319

[12] M Bowker, E Rowbotham, F M Leibsle, S Haq, Surf Sci 349 (1996) 97

[13] A F Carley, P R Davies, G G Mariotti, Surf Sci 401 (1998) 400

[14] A F Carley, A Chambers, P R Davies, G G Mariotti, R Kurian, M W Roberts, Faraday Disc 105 (1997) 225

[15] J P Reilly, C J Barnes, N J Price, R A Bennett, S Poulston, P Stone, M Bowker, J Phys Chem B 103 (1999) 6521

[16] C J Barnes and Attard, "Surfaces", Oxford Chemistry Primers (1998), p 31

[17] M Nijs, The Chemical Physics of Solid Surf & Heterogeneous Catalysis, (Editors D A King and D P Woodruff), Vol 7,Chapter 4, 1994

[18] M B Hugenschmidt, A Hitzke and R J Behm, Phys Rev Lett 76 (1996) 2535

[19] D Mattox, Handbook of Physical Vapour Deposition (PVD) Processing, William Andrews/Noyes Publications, New Jersey, 1998

[20] P W Palmberg and T N Rhodin, J Chem Phys 49 (1968) 134

[21] R Heck and R Farrauto, Appl Catal A, 221 (2001) 44

[22] B C Gates, J R Katzer and G C A Shuit, Chemistry of Catalytic Processes, McGraw-Hill, New York, 1979

[23] W G Frankenburg, in P H Emmet (Ed), Catalysis, Vol 3, NY, 1955, p 171

[24] G Natta, in P H Emmett (Ed), Catalysis, Vol 3, Reinhold, NY, 1955, p349

[25] R G Herman, Catal Today, 55 (2000) 233

CHAPTER 2

THE ADSORPTION AND DECOMPOSITION OF FORMIC ACID ON Cu {100} AND Cu {100}Pt SURFACES

2 1 Introduction

The adsorption and decomposition of formic acid at copper surfaces has been intensively studied over the years [1] This is partly because of the key role that formate is believed to play in methanol synthesis and partly because it is an ideal model system As a result of the attention it has received, the chemistry of the system is well understood Upon adsorption at 300K the formic acid dissociates to produce a bidentate formate intermediate, which bonds to adjacent sites on the copper surface through the two oxygen atoms Figure 2 1

Temperature Programmed Desorption (TPD)

Theory of TPD

TPD as a surface analysis technique was introduced by Apker [3] in 1948 Since adsorption on clean metal surfaces is generally a non-activated process, the desorption activation energy is then approximately equal to the differential heat of adsorption [3] This implies that TPD is a method of measuring the bond energy in adsorption In addition, the reaction order can be deduced by comparing the peak shapes of TPD spectra

Compared to other surface techniques, TPD is considered a straightforward and easy to interpret method Apart from some experimental parameters such as the heating rate β, a typical TPD spectrum provides the desorption peak maximum temperaure, T_p and a distinct trace shape that give information about the order of the desorption process

Several methods of analysis of TPD spectra have been described in the literature where the most convenient one is the Redhead method since it provides fairly accurate results and small computation time [4]

In the Redhead method, the frequency factor is assumed to be independent of coverage This approximation allows the application of a single equation to calculate

E_d, given that the desorption takes place under constant pumping speed and linear heating rate

$$E = RT_p [\ln (v T_p / \beta) - 3\ 64]$$

where E is the activation energy in Joules, R is the ideal gas constant of 8 314 $JK^{-1}mol^{-1}$, T_p is the desorption peak maximum temperature in Kelvin, v is the frequency factor of $10^{13}sec^{-1}$ and β is the heating rate in $Ksec^{-1}$

TPD spectra can also give some information about the relative surface coverage Provided the pumping speed is constant, the integrated area of a TPD peak is directly proportional to the adsorbate coverage Therefore, a method of calibration of the mean surface coverage can be obtained by comparing the integrated area under the TPD peak for surfaces with different exposures

Nowadays, TPD is widely used as a complementary method in studying surface structure and investigating simple chemical reactions on surfaces especially when gas adsorption behaviour is highly dependent on the constituents and morphology of surfaces

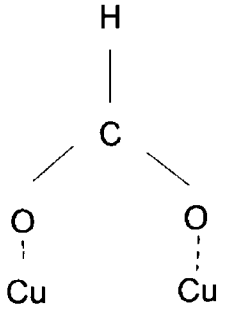

Figure 2 1 The geometry of formate on a copper crystal

It is generally accepted that the formate decomposes at ~470K to yield carbon dioxide and hydrogen [5]

$$2HCOO_{(ads)} \rightarrow CO_{2(g)} + H_{2(g)}$$

This has been evidenced through the use of Temperature Programmed Desorption Spectroscopy Following the adsorption of formic acid on a Cu(100) crystal, coincident peaks representing the evolution of CO_2 and H_2 are observed at~470K [6]

Furthermore, the behaviour of formic acid when adsorbed on a Pd/Cu(110) surface has also been studied It has been observed by J P Reilly *et al* [5], that palladium has a destabilising effect on the formate intermediate

The present work seeks to further examine the kinetics of the adsorption and decomposition of formic acid on a copper single crystal surface In addition, the effect that platinum has on the stability of the formate intermediate is also investigated

Temperature Programmed Desorption Spectroscopy is employed in order to do so A Cu(100) crystal is used for these studies, and platinum model surfaces were formed by depositing varying amounts of platinum onto the crystal

In a TPD experiment, an adsorbate, generally in its gaseous form, is dosed onto the surface to be studied at a certain pressure for a certain time Surface exposure is usually quoted in Langmuirs (L) where 1 L $=10^{6}$ Torr sec A linear temperature ramp is then applied to the sample where the amount of desorbed species is monitored as a function of temperature Figure 2 2 shows a schematic diagram of a simple TPD experiment set-up

In resistive heating, which is the usual method of heating, an electric current is applied to the sample support wires The heating rate β is the most important experimental variable in TPD experiments Higher β generally shifts the desorption peak to a higher temperature Analysis of TPD spectra requires that β is linear over the temperature range of interest Typical β values are in the range 1-10 K/s

Depending on reaction products and level of accuracy needed, mass spectrometers vary in specification The most common one is the quadrupole mass spectrometer (QMS) Different e/m fragments can be monitored upon desorption simultaneously by "multiplexing"
The distance between the sample and the detector (QMS) is minimised to ensure maximum detection efficiency but it is important to keep it fixed if integrated area of different TPD spectra are to be compared with each other

Since interference from gases present in the background vacuum and variable sensitivity of the QMS at different pressure values are some major problems in TPD experiment, it is important to maintain a constant base pressure in the vacuum chamber when TPD spectra are recorded In some cases where background gases interfere strongly with the recorded spectra, a background spectrum may be subtracted

Adsorption of various species on clean and alloyed Cu single crystal surface has been studied extensively by TPD Formic acid (HCOOH) and carbon monoxide (CO) are the most common simple gases used to probe surface reaction reactivity
Formic acid is the simplest carboxylic acid It forms a strong, stable bidentate formate intermediate on copper surfaces The formate is stable up to approximately 450K on Cu(100) before it decomposes to yield CO_2 and H_2 It has been found that this decomposition follows first order kinetics [8]

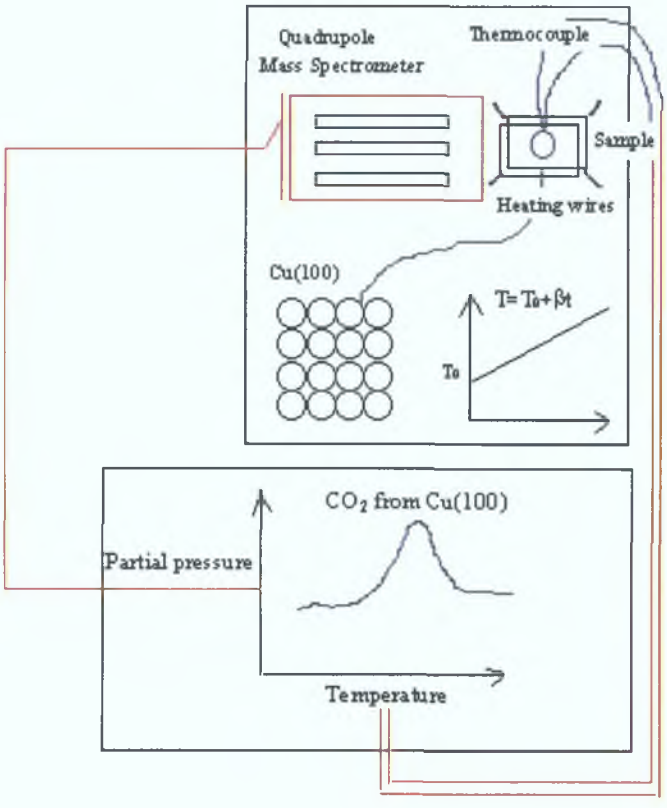

Figure. 2.2: Schematic diagram of a simple TPD experiment set-up.

Formic acid TPD on Cu

Madix and co-workers [9] were the first to study formic acid TPD from Cu in 1980. They found that formic acid adsorbs on a Cu(110) surface to produce a formate species. Using TPD, Bowker et al.[10] investigated the adsorption and decomposition of formic acid on Cu(110). A structural study of formate on Cu(111) by Sotiropoulos using normal incidence. X-ray standing wavefield absorption (NIXSW) suggested that the oxygen atoms of the formate were located in a top site and with the formate bridging two copper atoms [11]. Figure.2.3. shows the proposed bonding of the formate intermediate on Cu(100).

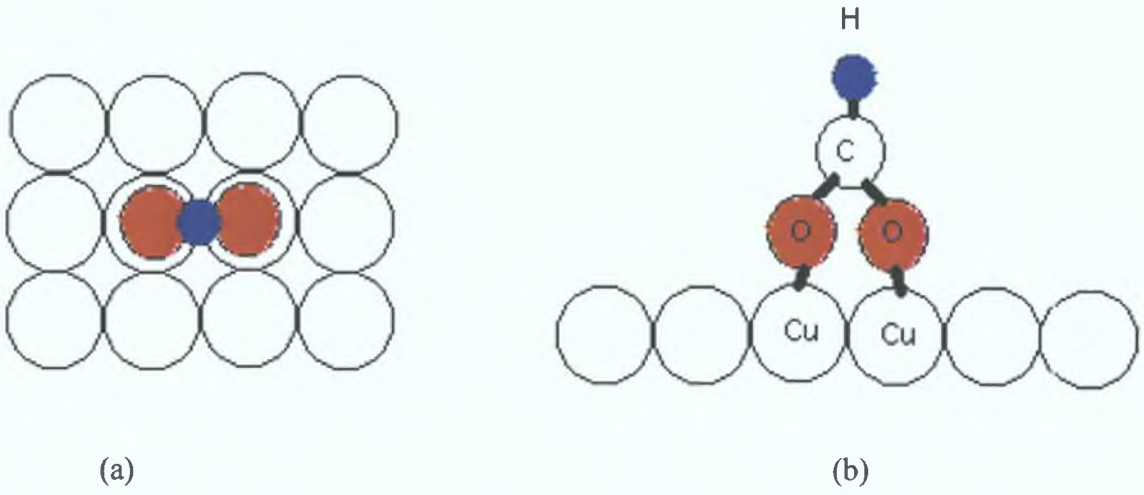

(a) (b)

Figure. 2.3: (a) Top view and (b) side view of the proposed bonding geometry of the formate intermediate on Cu(100).

2.2 Experimental

Experiments were performed in a stainless steel ultra- high vacuum chamber. The pressure of the chamber was maintained in the low 10^{-10} Torr region by means of an ion pump and a titanium sublimation pump. The chamber was equipped with a quadrupole mass spectrometer, an argon ion bombardment gun and 4-grid Low Energy Electron Diffraction (LEED) optics. The mass spectrometer is employed as detector for the temperature programmed desorption measurements. It is also utilised for residual gas analysis, and for checking the purity of the admitted formic acid.

Cleaning of the crystal involved repeated cycles of argon –ion bombardment, followed by annealing to ~700K. The surface crystallography was monitored by low-energy electron diffraction (LEED). A clean copper surface is indicated by the appearance of sharp, intense symmetric diffraction spots with a low background. The achievement of good quality platinum-copper model alloy surfaces was confirmed by the observation of a good c(2x2) pattern. Platinum was dosed from a home made evaporator consisting of a 0.3 mm diameter tungsten filament around which a 0.125 mm Pt wire was wound. The filament was mounted on a titanium sublimation pump feed through, and fitted with a stainless steel shield. Evaporation was achieved via the resistive heating of the filament.

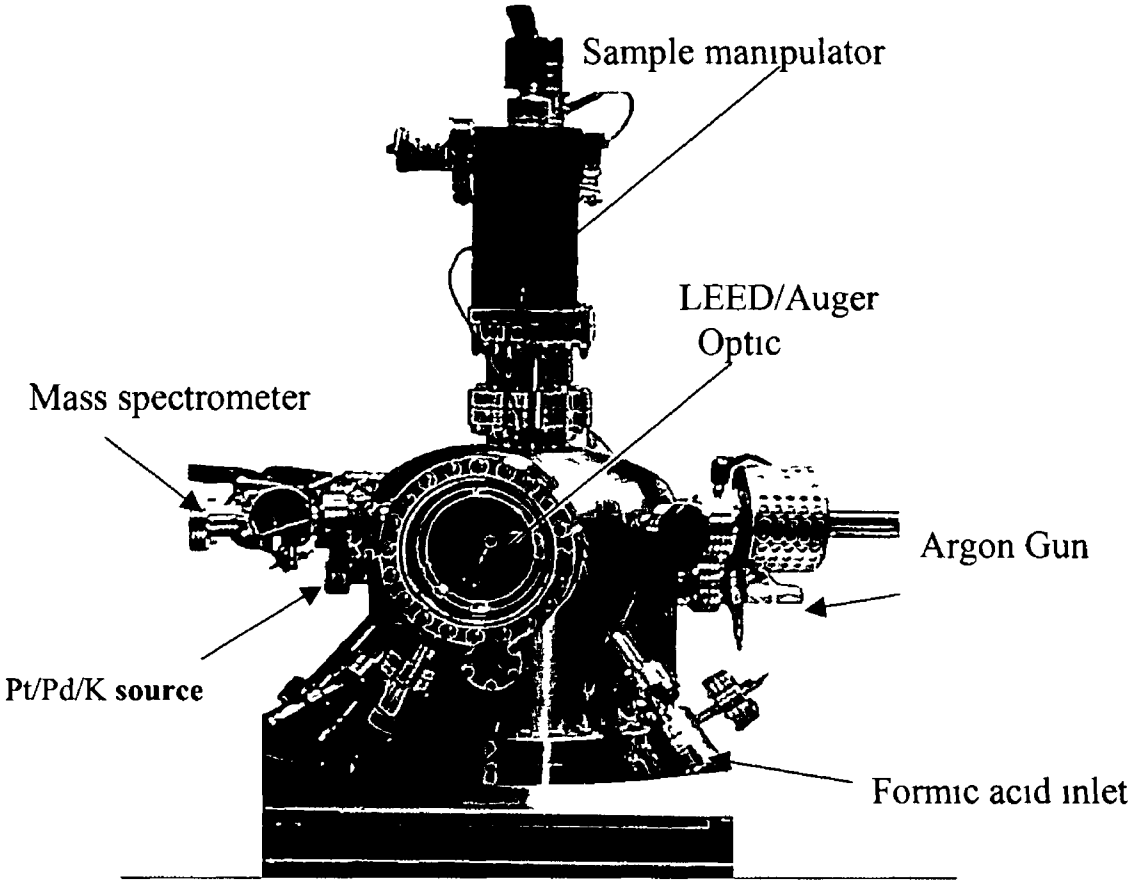

Figure 2 4 Photograph of the Dublin City University UHV chamber (now in School of Physical Sciences, DCU)

The formic acid (97% purity, Aldrich chemicals) was purified by several freeze-pump-thaw cycles, in order to remove any dissolved gases Dosing was performed through an all-metal leak valve with exposure measured with an uncalibrated Bayard-Alpert ionisation gauge Exposures are quoted in Langmuirs (1 Langmuir = 10^{-6} Torr sec)

The Cu(100) crystal was mounted via suspension between stainless steel blocks by tantalum wires The crystal was heated resistively, in linear fashion, by passing a direct current through the wires A thermocouple junction spot-welded to the edge of the sample provides a means of measuring the sample temperature The crystal is rotatable about the vertical chamber axis to position it for LEED analysis, argon ion bombarding, platinum evaporation and TPD measurements

2.3 Results and Discussion:

The Cu(100) surface was initially exposed to increasing amounts of formic acid, in an attempt to determine how the desorption peaks vary with coverage. The following sets of spectra were obtained. Figure.2.5

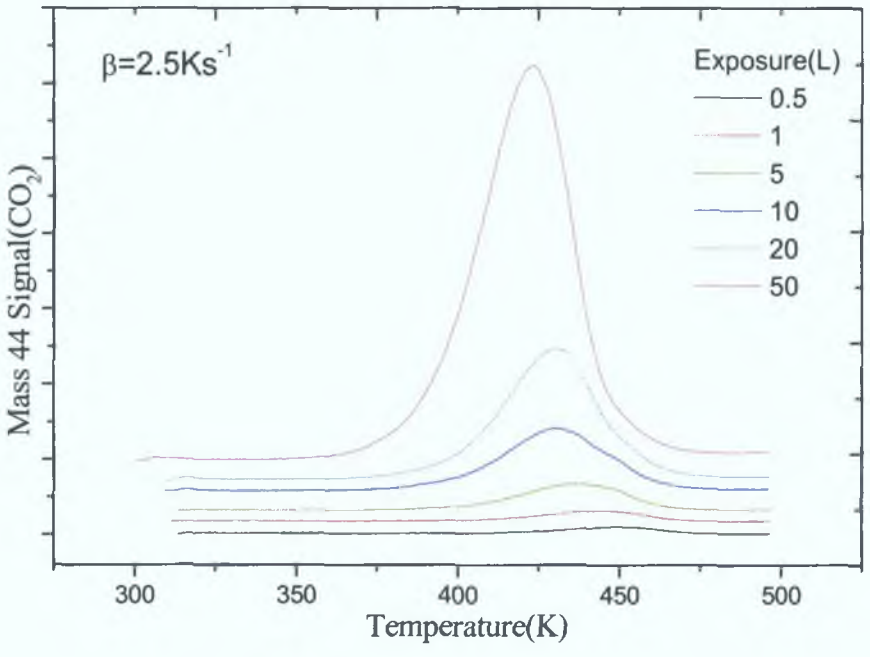

Figure. 2.5: Stack plot of CO_2 desorption spectra obtained, following exposure to 0.5,1,5,10,20 and 50L formic acid on Cu(100).

CO_2 evolution was monitored by tuning the mass spectrometer to detect species of mass 44-monitored. H_2 evolution was also observed at a coincident temperature to the CO_2. However, due to the inference of residual hydrogen in the chamber, poor quality mass 2 spectra were obtained. Hence, only CO_2 desorption was followed in this work.

It can be seen from the above plots that as the surface is exposed to increasing amounts of formic acid, the desorption peak increases in intensity, but it is also noted that the peak temperature for maximum desorption (T_p), shifts to lower temperatures It shifts from 458K for an exposure of 0 5L to 433K for 50L The activation energies for each exposure of formic acid were calculated using the Redhead equation and tabulated in Table 1 2

Table 1 2 Activation Energies for various Exposures of formic acid on pure Cu(100)

Exposure (L)	E_d (KJ mol^{-1})
0 5	121
1	119
1	118
10	116
20	115
50	114

It is generally accepted that the desorption of formate from single crystal surfaces is a first order process [5], and this is supported by the asymmetric shape of the peak observed Hence, the following form of the Redhead equation was used for evaluating the activation energy $E_d = RT_p[\log_e(AT_p/\beta)-3\ 46]$

where $R = 8\ 314\ Jmol^{-1}K^{-1}$, β is the heating rate and A is assumed to be $10^{13}\ s^{-1}$ The shift of the peak maxima to lower temperatures as a function of increasing exposure does not support the proposition of first-order kinetics It is proposed however, that this shift is as a result of repulsive lateral interactions between the adsorbed molecules It is well understood that repulsive interaction lead to the

destabilisation of the adsorbate. This is illustrated by the decrease in desorption energies, as given by the Redhead method.

In an attempt to investigate the effect of platinum on the stability of the formate intermediate, platinum model surfaces were formed by depositing varying amounts of platinum onto the Cu(100) crystal. The amounts of platinum decided upon for this study were 0.5, 1 and 1.5 monolayers. Fig.2.6 illustrates the spectra obtained following adsorption of 0.5, 1, 5 and 20L formic acid on Cu(100) surface alloyed with 0.5ML Pt.

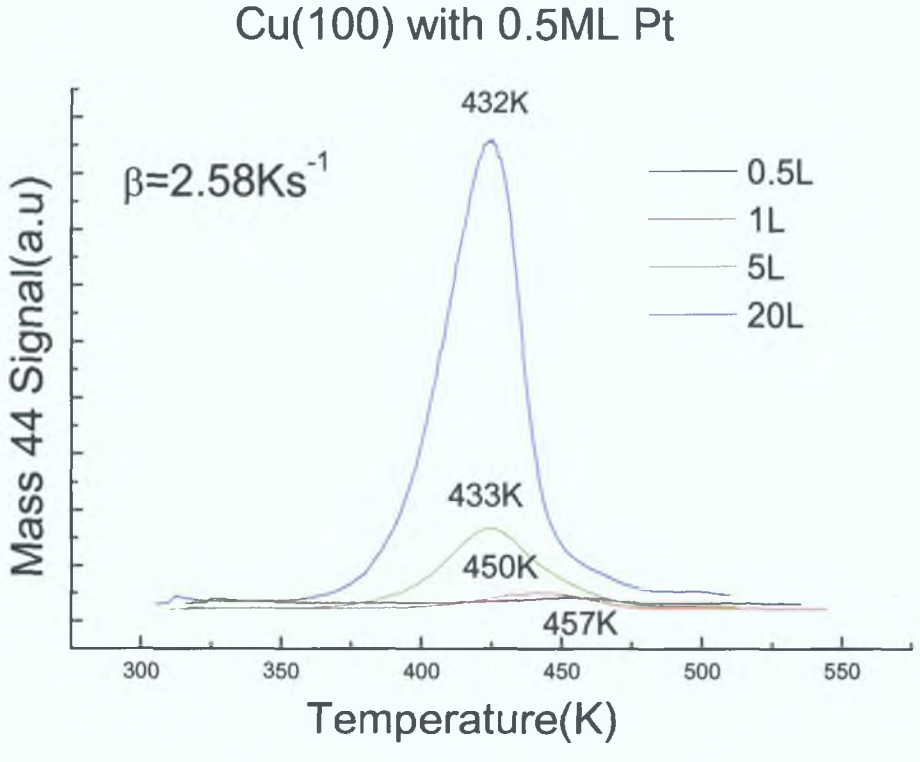

Figure. 2.6: Stack plot of CO_2 desorption spectra obtained form Cu(100) with 0.5MLPt

A comparison of the spectra obtained for the above system and for the pure copper system yields striking similarities. The peak temperatures are almost identical, as are the peak shape, and again there is a downward shift of T_p with increasing exposure. A possible explanation for these observations is that the desorption experiments were

performed the day after the layer was deposited. It is extremely likely that during this period, the platinum diffused from the surface into the bulk. Hence, it would be wrong to conclude from the above spectra that 0.5ML Pt has no affect on the stability of the formate. In contrast, the desorption spectra obtained when 1 ML Pt was deposited, shows that platinum results in a considerable destabilisation of the formate Figure.2.7.

The presence of 1 ML Pt leads to significant differences in the TPD spectra obtained, relative to those of pure copper (100). Considering the curve representing desorption of 20L for example from pure Cu(100), the T_p for this exposure was 438K compared to 393K with 1ML Pt. In activation energy terms, the decrease corresponds to a reduction of 12KJ mol^{-1}. Hence, the 1ML Pt has led to considerable destabilisation of the formate. It is also to be noted, that 1ML Pt results in a much narrower peak than that affined with pure Cu.

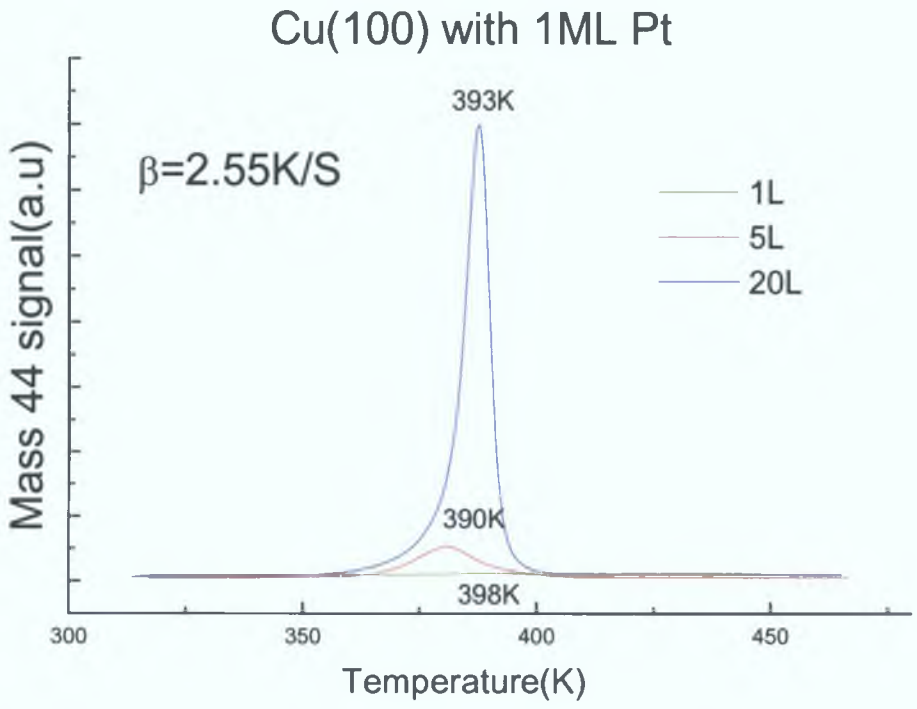

Figure. 2.7: Stack Plot of CO_2 spectra obtained following adsorption of 1, 5 and 20L formic acid from Cu(100) alloyed with 1 ML Pt.

It is difficult to deduce from the above spectra whether there exists any lateral interactions between the adsorbed molecules There is no systematic shift of T_p in this case A repeat of this experiment incorporating additional exposure of formic acid is necessary, in order to clarify the existence of lateral interactions The high quality of spectrum obtained for 20L formic acid on Cu(100) with 1ML Pt, (little noise) allows application of the Leading Edge Method Figures 2 8 and 2 9 illustrate the resulting coverage-dependent dissociative sticking co-efficient for both surfaces

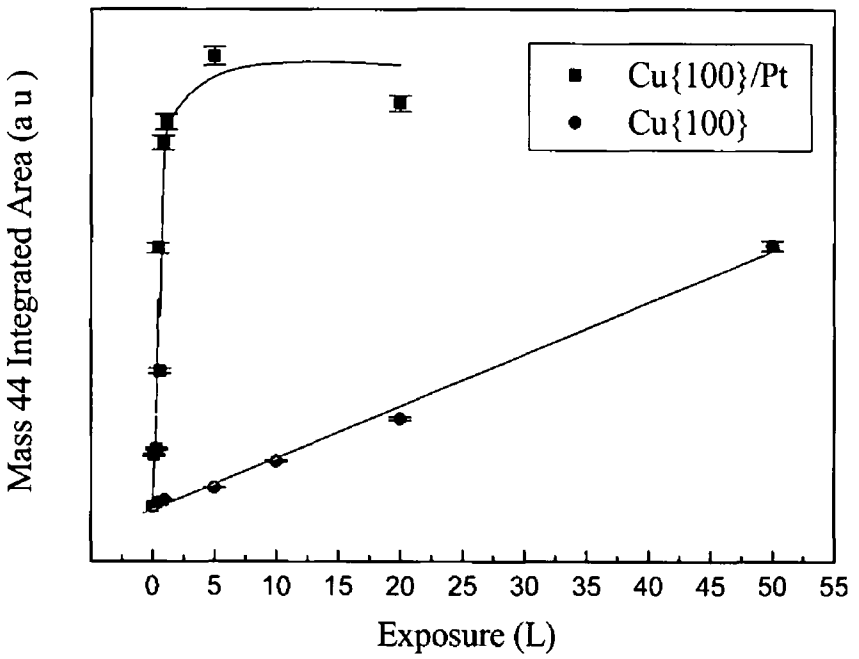

Figure 2 8 Integrated area of mass 44(CO_2) desorption from both Cu(100) and Cu(100)-c(2x2)-Pt surfaces as function of formic acid exposure

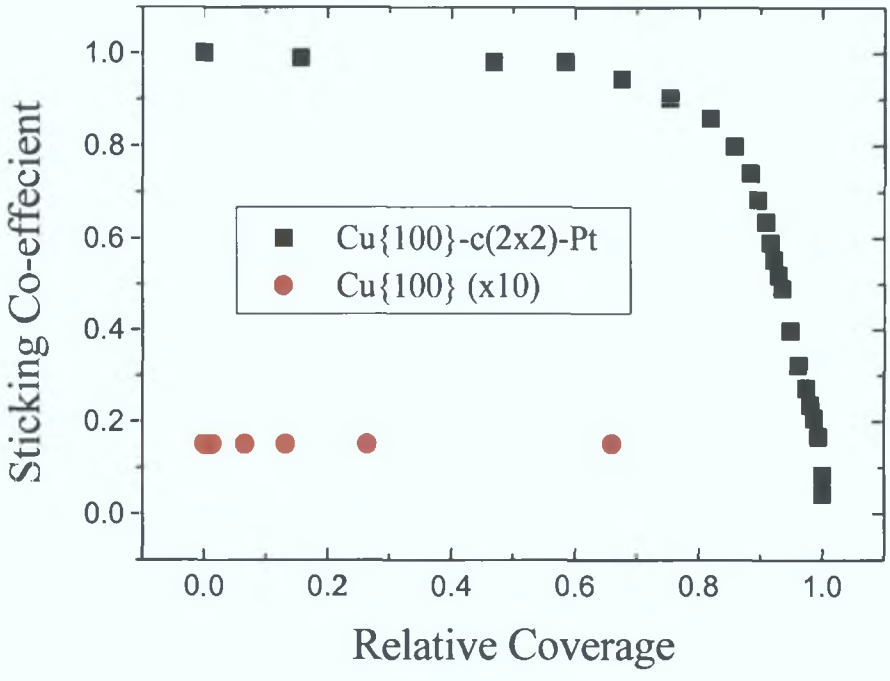

Figure. 2.9: Variation of formic acid sticking co-efficient with coverage on both Cu{100} and a Cu{100}-c(2x2)-Pt surface of intermediate Pt loading. (As HCOOH exposures were measured using a Bayard-Alpert ionisation gauge absolute sticking co-efficient may be in error. A formate saturation coverage of 0.5ML ($7.6x10^{14}$ molecules /cm^2) has been assumed on both surfaces).

Knowing that the slope of these plots is equivalent to $(-E_d)/R$, E_d could be calculated. It was found that when there was a coverage decrease of 8%, the desorption energy was found to be 124kJmol^{-1}, and in the case of 1%, the energy was found to be 100KJ mol^{-1}.

Values were also obtained for intermediate percentage decreases in coverage. These are tabulated in Table 2.2 (Pre-exponential factors (A) are also quoted. These were determined from the intercept of the plots, as the intercept is equivalent to Ln A).

Table 2 2 Desorption energies and pre-exponential factors obtained using the Leading Edge Method, for 20L HCOOH on Cu(100) with 1ML Pt

%Decrease in Coverage HCOO	Desorption Energy (KJmol ^{1})	Pre-exponential Factor
1	100	$4\ 5*10^{5}$
2	107	$4\ 6*10^{6}$
4	114	$5\ 3*10^{7}$
6	120	$3\ 6*10^{8}$
8	124	$1\ 3*10^{9}$

It can be seen that as the % of the leading edge from which the date taken decreases, the values obtained for the desorption energies approach that given by the Redhead method (104K)

Following deposition of 1 5ML Pt on the Cu(100) crystal and dosing with 0 5, 1, 5 and 20L formic acid, the TPD spectra shown in Figure 2 10 were obtained

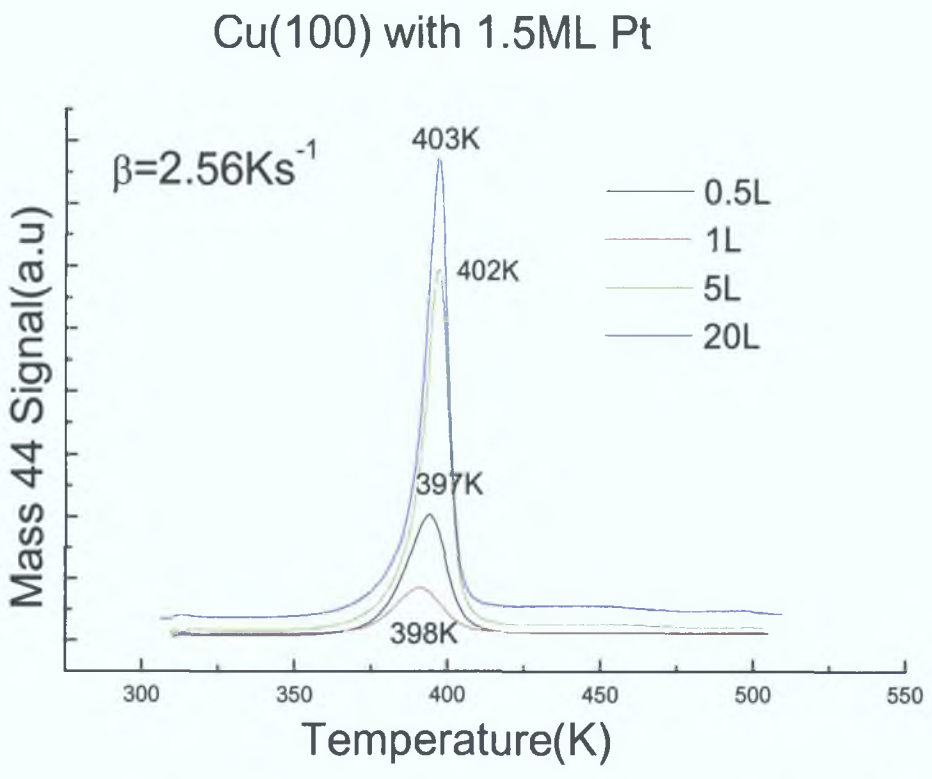

Figure. 2.10: CO_2 desorption spectra obtained from Cu(100) with 1.5ML Pt

Again, it is to be noted that T_p is much lower than those observed on pure Cu(100). Also, the desorption peak are much narrower. Another interesting observation is that in this case, the peak temperature appears to increase with increasing exposure to adsorbate. This is indicative of attractive lateral interaction. However, this cannot be conclusively stated because of the sige of the shift.

Considering the lowest and highest exposures, an overall shift of 7K is observed. It is impossible to make a conclusive deduction because the peak temperature is within a 5K error.

Utilising the Redhead Method, and assuming a pre-exponential factor of 10^{13}, average desoption energy of 105kJ mol^{-1} was obtained for the 1.5ML surface. As well as providing information regarding the stability of the formate intermediate on the various surfaces, the TPD experiments also allow the calculation of the sticking probability of formic acid.

Figure 2 11 shows plots of the integrated areas under the desorption peak obtained on clean Cu(100) (A) and on the 1 5ML Pt surface (B)

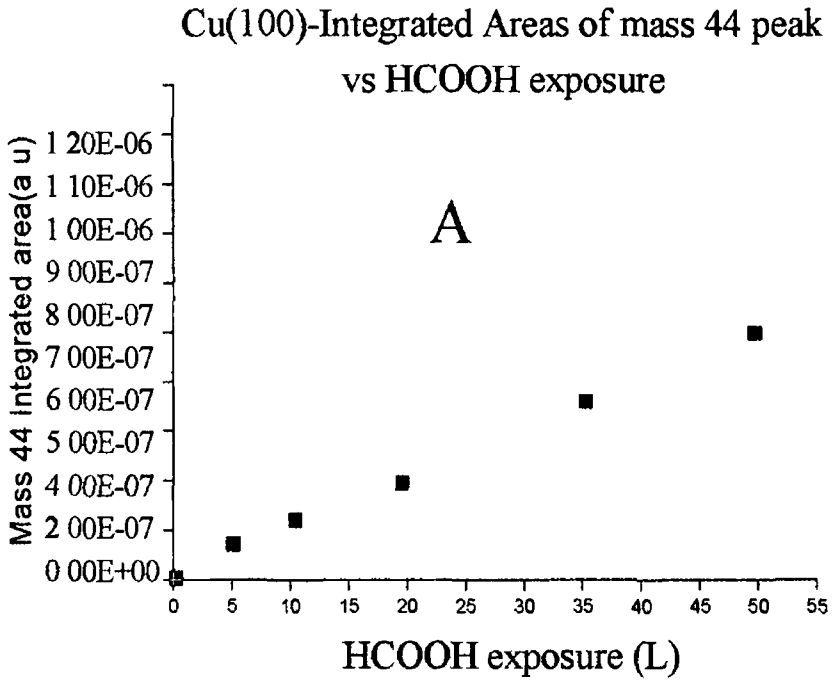

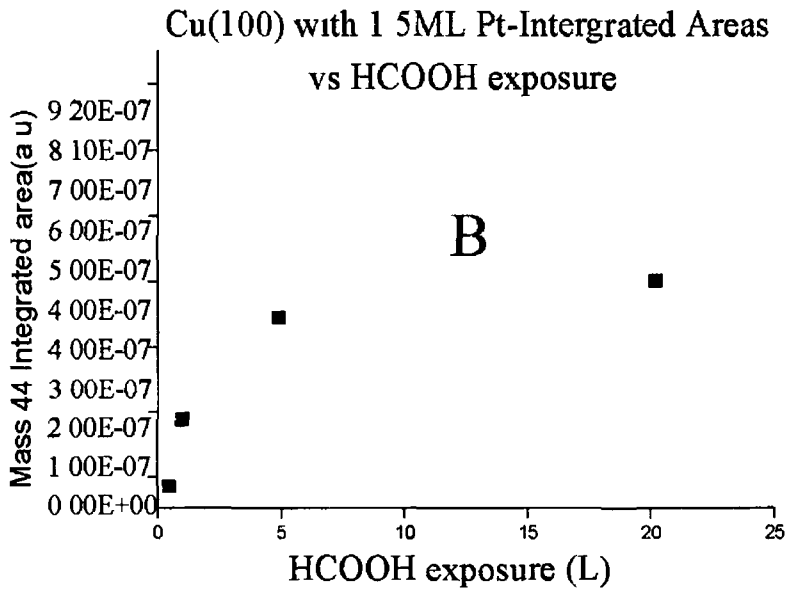

Figure 2 11 Plots of the integrated areas under the desorption peak obtained on clean Cu(100) (A) and on the 1 5ML Pt model system (B)

The linearity of the Cu(100) plot indicates the crystal does not become saturated with formic acid until it is exposed to at least 50L It cannot be said with certainty that saturation occurs upon exposure to 50L However, the linearity is a sign that precursor adsorption takes place This means that if a formic acid molecule collides with the surface at a filled adsorption site, it forms a weak Van der Waals type bond to the surface and diffuses for some finite length of time until it finds a vacant site and becomes chemisorbed

In the case of the 1 5ML Pt, it can be deduced from the plot that saturation occurs upon exposure to 10L formic acid Figure 2 12 illustrates the relative sticking probability of formic acid on this surface

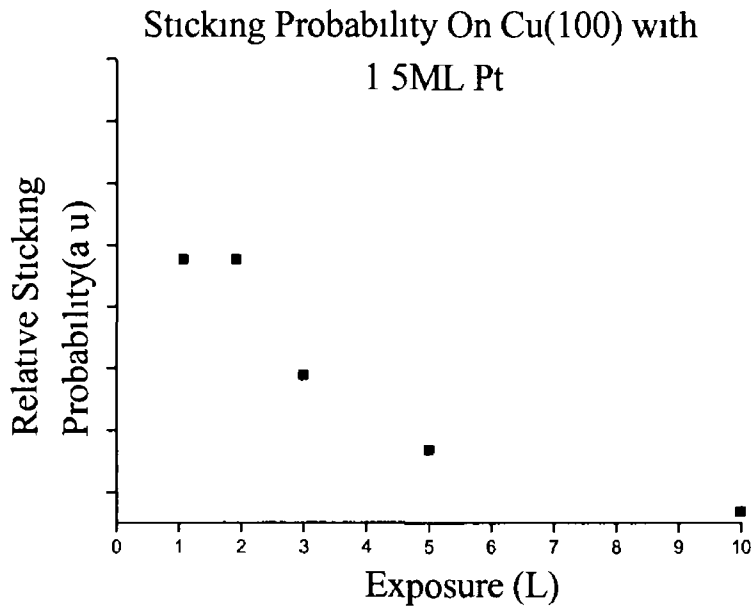

Figure 2 12 Relative Sticking Probability of formic acid on Cu(100) with 1 5ML Pt

It is likely that Langmuir adsorption is occurring in the case, whereby an adsorbate molecule, which collides with the surface at a filled adsoption site, rebounds back into the gas phase, and re-collides until it finds a vacant site

Absolute sticking probabilities were calculated using the relationship

$$S = \frac{\text{No of molecules adsorbed per cm}^2 \text{ surface}}{\text{No of molecules that collide with 1 cm}^2}$$

The number of molecules that were adsorbed by $1cm^2$ surface was calculated using the plots of integrated area vs exposure The number of molecules that collide with 1 cm^2 (z) was determined from the equation

$$Z = [p/(2\pi mkT)^{1/2}]t$$

Where p= pressure of dosing (Ncm^2)

t= dosing time (s)

m= molecular mass in kg molecule ^{1}

T= temperature of chamber in K

k= Boltzmann constant, in JK^{-1}

It was found as expected that the sticking probability of formic acid on pure Cu(100) remained constant, regardless of exposure This is because of the precursor type adsorption A value of 0 05 was obtained

The sticking probability on the 1 5ML Pt surface was found to be much higher, and decreased with increasing exposure 0 5L formic acid has a sticking probability of 0 67 and 10L has a sticking probability of 0 25 This is as expected because as more formic acid is put on, there are fewer vacant adsorption sites Hence it is less likely that the later molecules will adsorb

Figure.2.13: provides a comparison of the TPD spectra obtained for saturation coverage on each of the four surfaces studied. (It is assumed that pure Cu(100) saturates upon exposure to 50L formic acid).

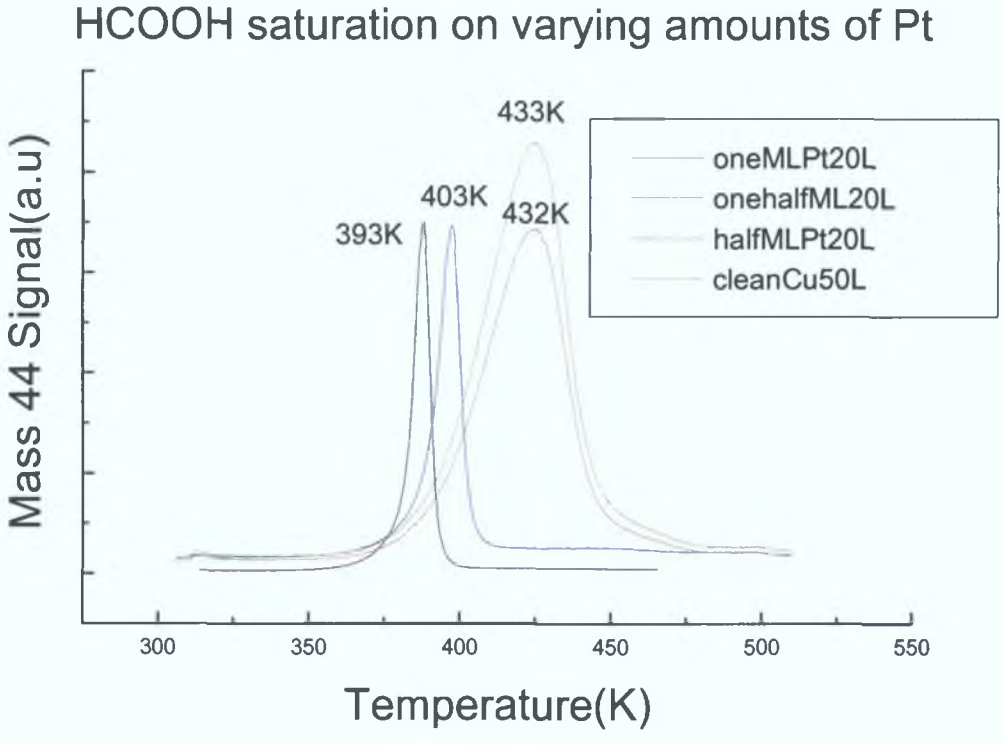

Figure. 2.13: CO_2 desorption spectra obtained following saturating pure Cu(100), and the 0.5ML, 1ML and 1.5ML Pt surfaces with formic acid.

This plot provides a clear illustration of the effect of platinum on the stability of the formate intermediate. It is evident that the platinum de-stabilises the intermediate. This is shown by the shift of T_p to a lower temperature as the amount of platinum was increased. (There is doubt about the validity of the result obtained for the 1ML and the 0.5 ML surfaces, the T_p is expected to fall between that of 0.5ML and 1.5ML).

Furthermore, Figure 2 13 clearly illustrates the difference in peak widths for the four surfaces It is evident that the platinum surface gives rise to much narrower peaks than clean copper Narrow peaks are indicative of rapid desorpton, hence it can be stated that for some reason the presence of platinum leads to an increase in the rate at which the adsorbed formate desorbs

The presence of repulsive lateral interaction on the clean Cu(100) surface as evidenced by the TPD spectra, shown in Figure 2 14, is a reasonable proposition, considering the geometry of the formate ion on the copper surface

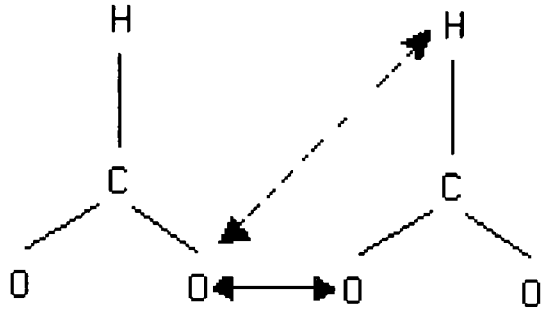

Figure 2 14 Geometry of formate on copper, illustrating lateral interactions

The oxygens of neighbouring molecules repel each other due to their electro-negativity and their competition for electron density from the copper This repulsion is much stronger than any hydrogen bonding that may exist between neighbouring formates This repulsive behaviour explains the 7kJ mol $^{-1}$ decrease in desorption energy, considering the adsorption of 0 5L and 50L formic acid In relation to the other surfaces, it has been proposed that following deposition of platinum, the surface structure consists of a pure copper layer capping a mixed CuPt alloy [7] This structure would not easily account for the remarkable differences observed between the clean Cu(100) TPD spectra and those of the copper-platinum model surfaces

Further investigation into the copper-platinum surfaces, using CO as a probe, has led to the identification of tiny platinum clusters It is believed that these clusters occupy around 5% of the outermost layer One possible explanation for the observation made on the copper-platinum surface, is that the platinum clusters promote the desorption of formate It is proposed that the adsorbed molecules diffuse towards the platinum clusters, where they undergo rapid decomposition This process would account for the lower desorption energy and narrower peak of the copper-platinum surfaces In addition, the affinity of the formic acid for the Pt clusters would explain why the sticking probability is greater on the copper-platinum surface than on the clean copper

The kinetic parameters deduced from the TPD spectra using the Redhead and Leading Edge Method, have been reported as desorption energies and pre-exponential factors It is important to highlight the fact that the desorption energy corresponds to the activation energy required for the decomposition of formate, and that the pre-exponential factor is of the same order of magnitude as the molecular vibrational frequency Therefore, it corresponds to the frequency with which the formate molecule goes to the transition state, where decomposition becomes favoured

The values of the E_d and A obtained from the Leading Edge Method as applied to the 1ML Pt system, exhibit a compensatory effect, i e E_d and A vary in concert to fulfil the conditions of the rate constant

$k_d = A\exp(-E_d/RT)$

where E_d is the activition energy for desorption, A is a pre-exponential factor A maximum is observed because, although k_d increase exponentially with temperature, the surface coverge decreases simultaneously [12]

2 4 CONCLUSIONS

The decomposition of a formate intermediate from a clean Cu(100) surface has been monitored through the use of TPD Spectroscopy CO_2 evolution was observed ~440K The presence of repulsive lateral interactions between the adsorbates on the surface has been identified, through the shift of peak temperature to lower value, as the surface was exposed to increasing amounts of formic acid The T_p for 0 5L was observed at 458K,while that for 50L appears at 443K This shift means that the decomposition energy is reduced by 6%

It has also been evidenced that platinum has a destabilising effect on the formate intermediate Peak temperature (T_p) for the CO_2 desorption spectra from copper-platinum model surfaces, appear around 40K lower than those from clean copper this suggests a much less stable surface alloy compared to the clean surface In activation energy terms, this destabilisation can be expressed as a 13% decrease in the energy required for the formate to decompose It was also observed that desorption is much more rapid from the copper-platinum than from clean copper More study is needed to fully understand these results

References:

[1] R J Madıx, Surf Scı 89 (1979) 540

[2] L Apker, Ind Eng Chem 40 (1948) 846

[3] L J Clarke, Surface Crystallography, An ıntroductıon to LEED, Wıley&Sons, 1985

[4] P A Redhedad, Vacuum 12 (1962) 203

[5] D A Kıng, Surf Scı 47 (1975) 384

[6] D H S Yıng and R J Madıx, J Catal 61(1980) 48

[7] J R Reılly, C J Barnes, N J Prıce, R A Bennett, S Poulston, P Stone, M Bowker J Phys Chem B 103 (1999) 6521

[8] J P Reılly, PhD thesıs, Dublın Cıty Unıversıty, (2000)

[9] R J Madıx, J Catal 61 (1980) 48

[10] M Bowker and R J Madıx, Surf Scı 102 (1981) 542, M Bowker, E Rowbotham, Surf, Scı 349 (1996) 97

[11] C J Barnes and Attard, Surfaces, Oxford Chemıstry Prımers (1998) p 61

CHAPTER 3

A TENSOR LEED DETERMINATION OF THE STRUCTURE AND COMPOSITIONAL PROFILE OF A Cu{100}-c(2X2)-Pt SURFACE ALLOY *

3 1 Introduction

The bimetallic combination Cu{100}/Pd is one of the best studied examples of surface alloy formation [1] In contrast, the closely associated Cu{100}/Pt system has received much less attention, despite the application of Cu_xPt_{1-x} alloys as a working catalyst for both CO oxidation [2] and hydrocarbon reforming reactions [3]

The earliest study of the Cu{100}/Pt system was carried out by Graham, Schmitz and Thiel [4] using Auger Electron Spectroscopy (AES), Low Energy Ion Scattering Spectroscopy (LEISS) and Low Energy Electron Diffraction (LEED) illustrating that Pt grows at room temperature in a somewhat disordered overlayer as Pt clusters with some intermixing with the underlying Cu substrate Auger spectroscopy was used to calibrate the Pt surface coverage via comparison of the AES intensities of Pt and Cu to those of Au and Cu from the Cu{100}-c(2x2)-Au surface alloy (Θ_{Au}=0 5ML) Formation of a weak diffuse c(2x2) LEED pattern was reported for coverages of 0 8ML and above for room temperature deposition Annealing of the Cu{100}/Pt interface to 525K at a Pt coverage of 0 8ML was indicative of strong copper segregation and formation of a well-ordered c(2x2) LEED pattern Graham et al determined that for Pt coverages up-to 1ML, annealing to 525K leads to surfaces with a pure or almost pure Cu layer outermost [4] In contrast, Shen and co-workers, using a combination of He^+ and Li^+ LEISS, report that thermal activation of a 1ML Pt film to the slightly lower temperature of 450K for 10 minutes led to formation of a c(2x2) structure with adjacent layers with Pt concentrations of 46 at% and 41 at% in layers 1 and 2 respectively [5] Clearly the compositional profile of the Cu{100}-

c(2x2)-Pt surface alloy with Pt loading of around 1ML is highly sensitive to the thermal treatment utilised It would appear that "low temperature" thermal activation (⟨450K) lead to surfaces with considerable Pt content in the outermost layer, while "high temperature" (⟩525K) annealing leads to surfaces with a pure or almost pure Cu termination at low Pt loadings Thermal processing at temperatures above 600 K leads to rapid destruction of the c(2x2) superstructure due to Pt interdiffusion into the bulk of the Cu{100} sample Hence, the Cu{100}-c(2x2)-Pt surface alloys reported by Graham *et al* [4] and Shen et al [5] correspond to kinetically trapped meta-stable states with face-centred-cubic dilute substitutional $Cu_{1-x}Pt_x$ alloys being the true thermodynamically favoured structure Nevertheless, once formed, the Cu{100}-c(2x2)-Pt alloy is stable for prolonged operational temperatures below 500K and as such is useful to probe the effect of surface alloying of Cu and Pt on a range of reactions including hydrocarbon reforming, CO oxidation and methanol synthesis For example, in a recent study of the Cu{100}-c(2x2)-Pt system, Reilly et al reported that Cu{100}-c(2x2)-Pt surface alloys formed by "high temperature" (550K) thermal activation of a Pt films of loadings of 1 to 1 5ML led to significant changes in the decomposition kinetics of a formate catalytic intermediate [6]

To date no quantitative structural work has been carried out on the Cu{100}/Pt bimetallic interface The Cu/Pt system is a favourable bimetallic combination to utilise the technique of tensor LEED (TLEED) in combination with the average T-matrix approximation (ATA) to determine both the surface geometric structure and the layerwise compositional profile In this paper we report the results of a TLEED-ATA analysis of a Cu{100}-c(2x2)-Pt surface alloy formed by "high temperature"

thermal activation of Pt films of monolayer coverage, illustrating that the c(2x2) periodicity arises from chemical ordering in a mixed CuPt underlayer with an essentially Cu-terminated surface with a concentration profile similar to the outer bilayer of a $Cu_3Pt\{100\}$ bulk alloy surface which adopts a Cu-terminated $L1_2$ structure consisting of alternate layers of pure Cu and c(2x2) mixed CuPt [7]

3 2 Experimental

All experiments were performed in an ion and titanium sublimation pumped ultra-high vacuum chamber with facilities for LEED, AES and thermal desorption spectroscopy and a base pressure of $1x10^{-10}$ torr The Cu{100} sample was cleaned by standard procedures involving argon ion bombardment and annealing to 800K until no contaminants were observed in the AES and LEED I(V) spectra from the clean Cu{100}-(1x1) surface which were in excellent agreement with previous literature reports [8] Platinum was evaporated from ultra-high-purity (99 99%) 0 125mm Pt wire wrapped around a shrouded and collimated 0 3mm tungsten filament The platinum evaporation rate was estimated using the method of Reilly *et al* [6] which consisted of periodic momtoring of the intensity and full-width-at-half-maximum (f w h m) of the (1,0) and (1/2,1/2) LEED reflexes as a function of Pt evaporation time Spot profiles were collected at constant temperature (~330K) with the surface being briefly thermally activated to 550K using a temperature ramp of 2 5Ks^{-1} after each Pt dose in order to promote c(2x2) surface alloy formation Reilly et al [6] have argued that the co-incident maximum in the intensity and minimum in f w h m of the (1/2,1/2) beam corresponds to formation of a well-ordered c(2x2)

CuPt underlayer (θ_{Pt}=0 5ML) Titration experiments with CO indicated that a small (0 1ML) coverage of Pt remained in the outermost layer, hence the evaporation time required to reach a maximum in the (1/2,1/2) beam intensity and minimum in f w h m was set to a Pt coverage of 0 6ML This method was adopted rather than the traditional methods of coverage calibration such as construction of Auger signal versus deposition time plots, as it is known that the room temperature growth mode for the Cu{100}/Pt bimetallic combination involves Pt clustering and surface alloy formation making definitive coverage calibration by Auger spectroscopy difficult

The Cu{100}-c(2x2)-Pt structure was formed by deposition of 1ML of Pt onto Cu{100} with the sample held at room temperature, resulting in a high background LEED structure with weak broad c(2x2) reflexes The procedure adopted to determine the optimal thermal treatment to form a well-ordered c(2x2) surface alloy was as follows a 1ML Pt film was evaporated on to a clean Cu{100} surface at room temperature and a spot profile across the (1,0), (1/2,1/2) and (0,1) beams was recorded The surface was then heated to increasing temperature in increments of between 20 and 25K with the crystal held at the anneal temperature for 1 minute duration before cooling to a constant temperature and acquiring a spot profile The optimal annealing temperature was decided by plotting both the integrated intensity and f w h m of the (1/2,1/2) reflex as a function of annealing temperature the optimal anneal temperature of 550K was that required to bring the (1/2,1/2) beam to a co-incident maximum intensity and minimum f w h m Annealing to temperatures above 600K led to destruction of the c(2x2) structure due to interdiffusion of Pt deep in-to the Cu{100} sample

The LEED I(V) measurements were made at room temperature under conditions of normal incidence using a CCD video camera and collecting data by automatic spot tracking Normal incidence was attained by variation of the sample alignment until the four (1,0) beams had identical spectral structure and highly similar relative intensities over the energy range 50-350eV Symmetry equivalent beams were co-added to reduce effects of residual sample misalignment Prior to symmetry addition, each beam was individually background subtracted by fitting an exponential background to chosen minima in the I(V) curves The data was then normalised to constant incoming beam current The data set utilised in the analysis corresponded to a total energy range of 1260eV

LEED calculations were performed with the Barbieri/Van Hove Symmetrized Automated Tensor LEED package [9] Up-to 9 phase shifts were used for both copper and platinum initially taken from the Van Hove/Barbieri phase shift package Other non-structural parameters included bulk Debye temperatures of 315K for Cu and 233K for Pt [10] In the initial stage of analysis these values where fixed while in the final optimisation of the favoured structures both the Pt and Cu Debye temperatures were allowed to vary in order to obtain optimal theory-experiment agreement An energy independent imaginary part of the inner potential of -5eV was utilised throughout the initial stage of the analysis with this parameter again being optimised in the final refinement stage The energy independent real part of the inner potential was allowed to vary via a rigid shift in the LEED calculations with theory-experiment agreement being tested with the Pendry R-factor [11] Error bars were

calculated based on the variance of the Pendry R-factor using the standard prescription [11]

3 3 Results and Discussion

The initial models tested were limited by the following assumption that the c(2x2) structure observed upon thermal activation was due to chemical ordering of Cu and Pt in c(2x2) sub-layers with composition CuPt Based on the structure of the {100} surface of a bulk Cu_3Pt $L1_2$ alloy, a natural suggestion for the structure of the surface alloy would be alternate CuPt and Cu layers initially confined to the in-plane Cu{100} periodicity [7] To test this structure, we allowed up-to 3 layers of CuPt stoichiometry to be distributed within the selvedge Inclusion of one, two and three c(2x2) CuPt layers would lead to creation of top two, four and six layer slabs respectively of average stoichiometry Cu_3Pt As LEED is insensitive to deeper lying layers, a 6 layer slab should correctly model to a good level of approximation the entire LEED probing depth as a distorted Cu_3Pt $L1_2$ type structure In each case, two possibilities exist in which the surface terminates either in a mixed CuPt layer or a pure Cu layer Structures were also tested in which two-or three-ordered CuPt sub-planes (Θ_{Pt}=1 and 1 5ML, respectively) were stacked in adjacent layers Again terminations with either a mixed CuPt layer or pure Cu layer outermost were tested The structural parameters allowed to vary included the first five interlayer spacings and rippling within mixed CuPt layers and in pure Cu layers (when allowed by symmetry) The range of rippling amplitudes considered was ±0 2Å which is in excess of the difference in metallic radius between Pt and Cu of 0 11Å Layer

spacings were also allowed to vary by ±0 3Å from the bulk Cu value of 1 805Å, which represents a variation of 17% with respect to the bulk interlayer spacing To preserve the experimentally observed 4-fold rotational symmetry observed in the LEED pattern, calculations were performed for two domains rotated by 90^0 and co-added where appropriate

Table 3 1 illustrates the results of this screening stage of the analysis The results collated in Table 3 1 clearly illustrate that the favoured model consists of a mixed c(2x2) CuPt underlayer capped by a pure Cu monolayer (R_p=0 25) Of all models tested, only two give a comparable level of agreement and consist of Cu_3Pt $L1_2$-like structures with the ordered CuPt layers extending deeper into the selvedge Slabs of Cu_3Pt-like structure of four and six atomic layers thick both yield Pendry R-factors of 0 29, which he just on the limit of acceptable structures based on the RR-value for the favoured structure of 0 04 The four layer thick Cu_3Pt slab has what initially appears to be an advantage it corresponds to a net Pt loading of 1 0ML, in agreement with the experimental coverage calibration However, as the favoured model based on the Cu/CuPt/Cu/Cu/Cu stacking sequence contains only 0 5ML Pt, hence there exists the potential to further increase the level of agreement by distributing additional Pt as a substitutionally disordered alloy within Cu layers within the LEED probing depth

Table 3 1 Minimum Pendry R-factors for stacking patterns tested in the initial screening stage of the analysis In each case the total Pt loading is given All mixed CuPt layers were assumed to be chemically ordered with a c(2x2) periodicity

Θ_{Pt}(ML)	Stacking pattern	R_P
0.5	PtCu / Cu / Cu / Cu / Cu	0.51
0.5	Cu / PtCu / Cu / Cu / Cu	0.25
1	PtCu / Cu / PtCu / Cu / Cu	0.53
1	Cu / PtCu / Cu / PtCu / Cu	0.29
1	PtCu / PtCu / Cu / Cu / Cu	0.51
1	Cu / PtCu / PtCu / Cu / Cu	0.45
1.5	PtCu / Cu / PtCu / Cu / PtCu / Cu	0.53
1.5	Cu / PtCu / Cu / PtCu / Cu / PtCu	0.29
1.5	PtCu / PtCu / PtCu / Cu / Cu / Cu	0.55
1.5	Cu / PtCu / PtCu / PtCu / Cu / Cu	0.48

Two structures were selected for final structural optimisation corresponding to stacking sequences Cu/CuPt/Cu/Cu/Cu/Cu (model A) and Cu/CuPt/Cu/CuPt/Cu/Cu (model B) The modelling of Pt atoms in the disordered substitutional alloy layers was achieved through application of the ATA approximation [12] In this final refinement stage the Pt and Cu phase shifts utilised were also re-calculated for models consisting of ordered c(2x2) CuPt underlayer alloys Total Pt loadings in the coverage range between 0 50 and 1 8 ML were considered, with the excess Pt distributed in layer 1, 3 and 4 in steps of 10 at % (model A) and in layers 1 and 3 (model B) again in steps of 10 at % For each compositional profile tested, the tensor LEED allowed a full geometrical optimisation Addition of extra Pt within the model B structure did not lead to any significant decrease in R_p below the value of 0 29 obtained for the ideal stacking sequence In contrast, the R-factor for model A was reduced from 0 25 to 0 20 leaving this model alone as the clearly favoured structure

Figure 3 1 illustrates schematically the favoured geometry and layerwise compositional profile and corresponds to a Pt coverage of 1 1±0 6ML Figure 3 2 illustrates the level of theory-experiment agreement obtained, corresponding to a Pendry R-factor of 0 20 Non-structural parameters included Debye temperatures of 155K for Pt and 300K for Cu and an imaginary part of the inner potential of -5eV

Incorporation of such large quantities of Pt into the outermost four atomic layer slab yields an average stoichiometry close to Cu_3Pt Due to the larger metallic radius of Pt, it is possible that Pt induces an in-plane lateral expansion, however, no experimental evidence was found for Pt-induced in-plane expansion Sharp circular LEED spots were always obtained with the in-plane periodicity of the c(2x2) surface alloy being identical to that of Cu{100} within the resolution of the measurements In order to further examine whether lateral relaxation leads to an increased level of theory-experiment agreement, a series of calculations were performed in which the in-plane spacing was increased in steps of 0 03Å (≈1% of the Cu-Cu m-plane nearest neighbour separation) While small (1%) expansions yielded no significant change in R_p expansions of 2% or more led to a monotonic increase in the R-factor, with expansions equal to or in excess of 3% being outside the Pendry RR value of 0 04 Thus, any Pt-mduced lateral expansion must be below 2% (≈0 05Å)

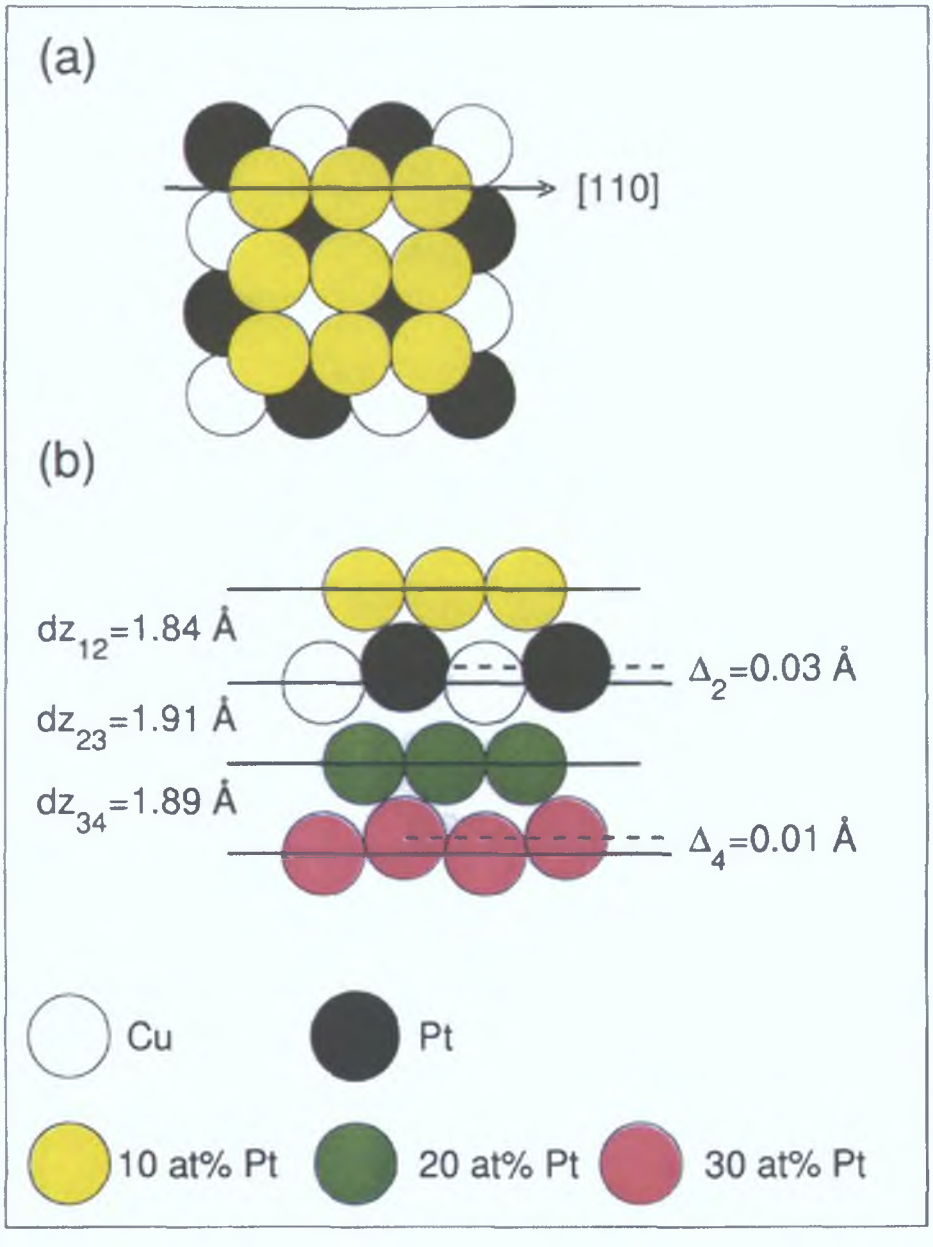

Figure. 3.1: Model of the favoured geometry for the Cu{100}-c(2x2)-Pt surface alloy (a) top view (outermost two layers only shown); (b) side view along the [110] azimuth defining the major geometric parameters varied within the analysis (the buckling in layers 2 and 4 is over-emphasised for clarity as is the z-spacing between adjacent layers). Note that the second and fourth layers are out of plane with respect to the pure copper layers.

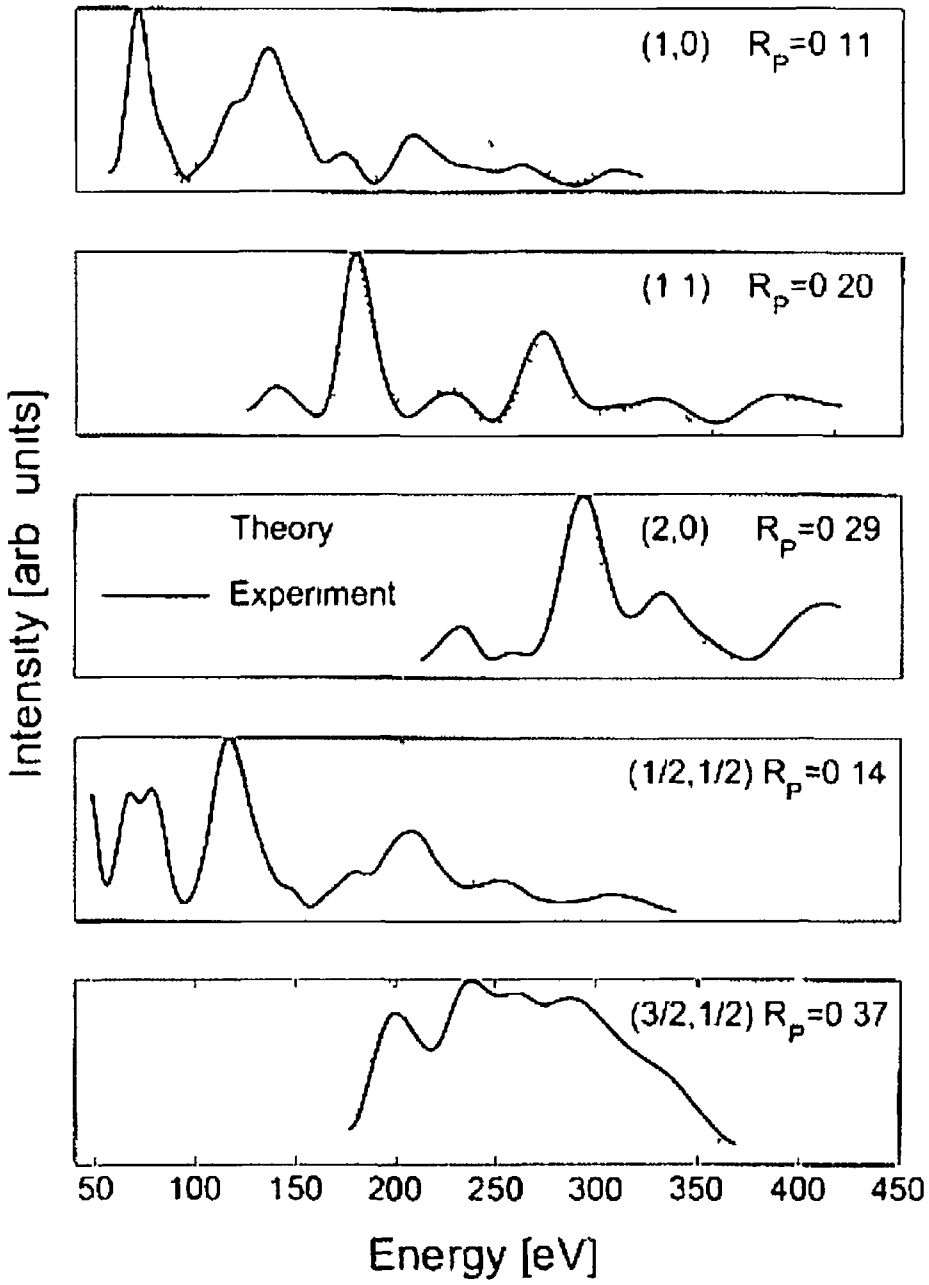

Figure 3 2 Optimal theory-experiment agreement Experimental data is shown as full lines and theory as dotted lines

Figure 3 3 illustrates the response of the Pendry R-factor to the main geometric variables, including the first three interlayer spacings and the buckling within the mixed CuPt monolayer (layer 2) with all other structural and non-structural variables held at their optimal values The optimal value for each parameter is given at the top of each panel along with the estimated error Substitution of Pt into the outermost four atomic layers leads to a significant expansion of the outermost three interlayer spacings, particularly dz_{23} which is expanded to 1 91 Å (+5 8%) A small Cu-Pt buckling amplitude of 0 03±0 04Å occurs in the ordered mixed c(2x2) CuPt underlayer, with Pt rippled outwards towards the vacuum interface

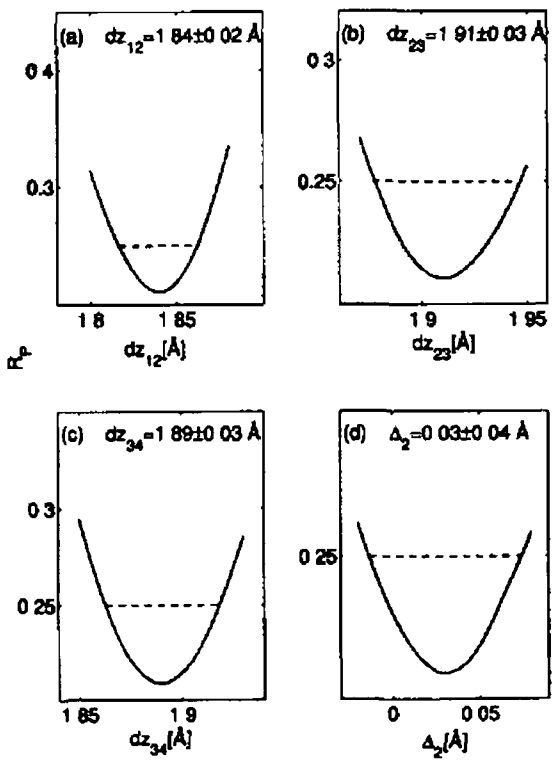

Figure 3 3 Variation of the Pendry R-factor with the first three interlayer spacings and buckling in the mixed CuPt second layer Positive buckling amplitudes correspond to Pt atoms rippled outwards towards the solid-vacuum interface

The optimal value for each parameter is given at the top of each panel along with the estimated error Substitution of Pt into the outermost four atomic layers leads to a significant expansion of the outermost three interlayer spacings, particularly dz_{23} which is expanded to 1 91 Å (+5 8%) A small Cu-Pt buckling amplitude of 0 03±0 04Å occurs in the ordered mixed c(2x2) CuPt underlayer, with Pt rippled outwards towards the vacuum interface

The layer spacings within the surface alloy are strongly modified from those of pure copper the structure of the clean Cu{100}-(1x1) surface determined for the same Cu{100} sample used in this study yielded a first layer contraction of −1 0±1 5% and a second layer expansion of +1 2±1 5% with third and deeper layers at their bulk truncated positions (R_p=0 15) [13] Confining Pt two-dimensionally to a Cu{100} lattice leads to a 17% increase in the effective Pt two-dimensional density The surface alloy may be expected to relieve the lattice strain by an expansion of the layer spacing in the z-direction This effect would be expected to be considerably less than 17%, as such a large interlayer spacing increase would lead to significant Cu-Cu bond weakening A compromise will be adopted, as was recently found in the case of a Cu{100}-c(2x2)-Pd underlayer alloy structure [14] In the case of the Cu{100}-c(2x2)-Pd underlayer alloy a net expansion relative to clean Cu{100} of the outermost three layer slab of 0 18Å (6%) resulted [14], compared to the value of 0 14Å (8%) in the case of Cu{100}-c(2x2)-Pt-1ML structure

The composition profile adopted appears to be driven by the tendency of the system to form a layerwise composition profile similar to that of the {100} surface of a Cu_3Pt $L1_2$ bulk alloy which consists of alternate pure Cu and mixed c(2x2) CuPt

layers with a Cu terminated surface [7] While layers 2 (50 at%) and layer 4 (30±30 at%) have high Pt concentrations and layer 1 a very low Pt content (10±10 at%) as expected, a considerable quantity of Pt is located in layer 3 (20±20 at%) which would correspond to a pure Cu layer in a $Cu_3Pt\{100\}$ bulk alloy Formation of the surface alloy requires interdiffusion of significant quantities of Pt from the Cu/Pt interface through many copper layers It is thus perhaps not unsurprising that quantities of Pt are kinetically trapped in layer 3 As transport of Pt from layer 3 to 4 corresponds to a bulk interdiffusion process, minimising the Pt concentration in layer 3 competes with loss of Pt from layer 4 deeper into the bulk of the sample, thus making it extremely difficult to prepare a Cu{100}-c(2x2)-Pt surface alloy with a perfect layerwise composition While the favoured Pt loading determined by ATA analysis of 1 1±0 6ML agrees rather well with the experimental estimate of 1ML based on the methodology of Reilly et al [6], the relative insensitivity of LEED to layerwise composition, even for a relatively favourable bimetallic combination such as Cu and Pt leads, to a correspondingly large uncertainty in the exact Pt loading

Figure 3 4 illustrates a plot of the Pendry R-factor as a function of the concentration of Pt in layers 3 and 4, demonstrating this rather weak sensitivity of the analysis to the layerwise composition In order to test the reliability of the analysis to the details of the layerwise composition, a second experimental data set was collected The experimental data consisted of the same beams as the original analysis and a slightly larger data range of 1500eV The layerwise composition, geometric parameters and non-structural parameters were optimised based on the favoured model illustrated in Figure 3 1 Table 3 2 illustrates the results of the two analyses There is excellent

agreement both in terms of structural parameters such as interplanar spacings and buckling amplitudes and the layerwise Pt concentration extracted via ATA analysis The only significant difference is in the outermost layer composition for which analysis of the second data set favours a pure Cu layer outermost, although both analyses fall within the estimated error of 10 at% for the outermost layer composition This appears to suggest that the structure and compositional profile of the Cu{100}-c(2x2)-Pt-1ML alloy may be formed rather reproducibly

A copper-capped geometry is in full agreement with the ion scattering studies of Graham et al [5] who have determined the surface of a Cu{100} doped with Pt and thermally processed to 525K to be essentially copper terminated up to Pt loadings of 1ML Copper capping is clearly favoured based on surface energy considerations due to the significantly lower surface energy of Cu{100} (2 17 Jm^{2}) compared to that of Pt{100} (2 73 Jm^{2}) [15] This difference is further enhanced if the surface energy per surface Cu or Pt atom is considered, due to the higher atomic density adopted by Cu{100} compared to Pt{100}

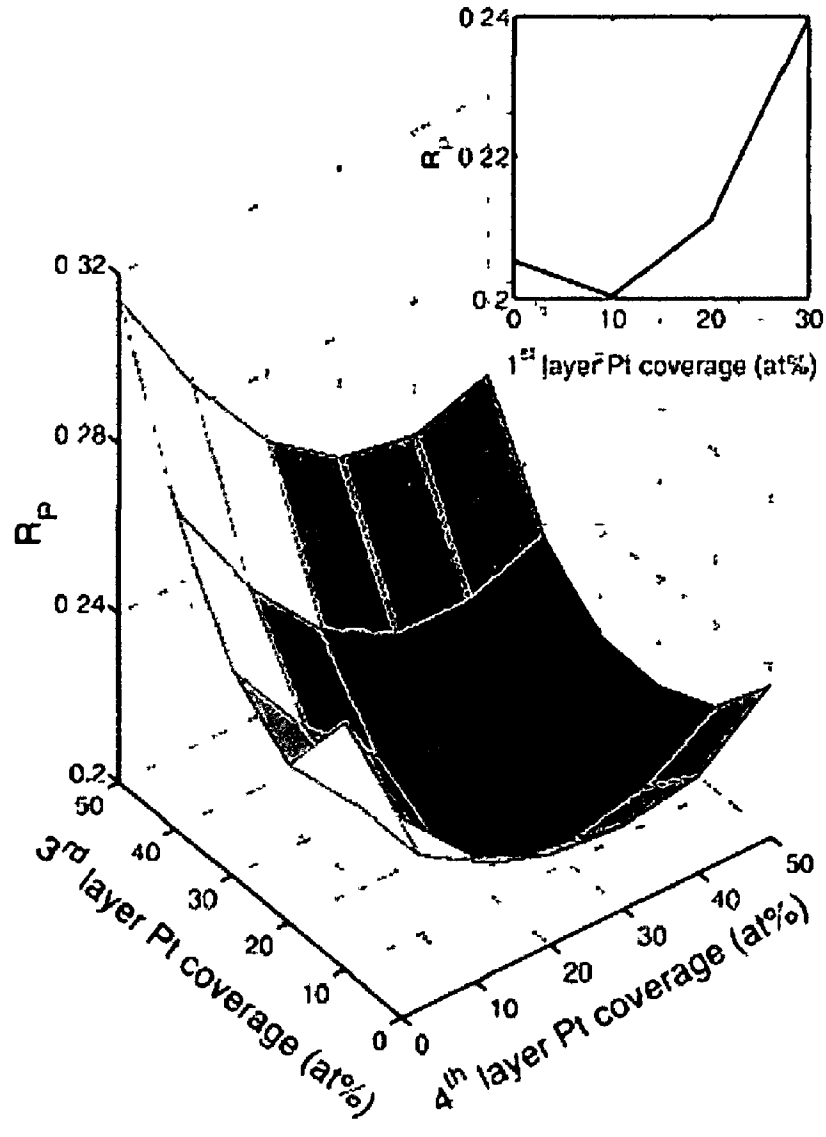

Figure 3 4 Variation of the Pendry R-factor with layerwise Pt concentrations in layer 3 and 4 with all structural parameters held at their favoured values and the first layer concentration held at the optimal value of 10 at% The inset at the top of the figure illustrates the response of the Pendry R-factor to the outermost layer composition, again with all structural parameters held at their optimal values and third and fourth layer Pt compositions at 20 and 30 at% respectively

Table 3 2 Comparison of geometric parameters and layerwise Pt concentration for the favoured model illustrated in Figure 3 1 obtained from two independently prepared Cu{100}-c(2x2)-Pt (1ML) surfaces Layer spacings are quoted with respect to copper atom positions in mixed CuPt layers

Parameter	Data set 1	Data set 2	Average
d_{12}(Å)	1.84	1.86	1.85
d_{23}(Å)	1.91	1.91	1.91
d_{34}(Å)	1.89	1.86	1.88
Δ_3(Å)	0.03	0.03	0.03
$(\Theta_{Pt})_1$(at%)	10	0	5
$(\Theta_{Pt})_2$(at%)	20	20	20
$(\Theta_{Pt})_4$(at%)	30	30	30

Reports of formation of a Cu{100}-c(2x2)-Pt surface alloy with Pt loading of 1ML via annealing to the lower temperature of 450K in which significant quantities of Pt are present in both layer 1 (46 at%) and layer 2 (41 at%) clearly indicate the possibility of formation of a second metastable ordered surface alloy [5] consisting of two adjacent c(2x2) CuPt layers with a mixed CuPt termination However, the primary technique involved in this study was LEISS which is primarily sensitive to atomic composition, it is also possible that the structure corresponds simply to a

heterogeneous surface consisting of domains of a Cu-terminated c(2x2) CuPt underlayer co-existing with areas of Pt clusters in the correct ratio to yield the measured top layer composition Further work is required using both TLEED-ATA and chemical probes of the top layer local composition to establish the identity of the intermediate Cu{100}-c(2x2)-Pt phase reported by Shen and co-workers [16]

3.4 Conclusions

A Cu{100}-c(2x2)-Pt surface alloy structure formed by deposition of 1ML of Pt and thermal processing to 550K is shown to correspond to a copper-capped bimetallic surface localised alloy with a sub-surface ordered c(2x2) CuPt layer The layerwise compositional profile has been extracted via ATA modelling resulting in an almost pure outermost copper monolayer with only a small Pt impurity concentration (10±10 at%) Layers 3 and 4 contained higher Pt concentrations of 20±20 and 30±30 at% respectively

Substitution of platinum into the selvedge results in a significant expansion in the surface interlayer spacings relative to clean Cu{100} and switches the weak oscillatory relaxation of clean Cu{100} to a strongly and non-uniformly expanded interlayer separation The outermost three interlayer spacings are strongly expanded by 1 84±0 02Å (+1 9±1 1%), 1 91±0 03Å (+5 8±1 7%) and 1 89±0 03Å (+4 7±1 7%), respectively A slight rippling in the c(2x2) CuPt underlayer of amplitude 0 03±0 04Å, with Pt atoms rippled outwards towards the vacuum interface within the composite layer occurs

References

[1] U Bardı, Rep Prog Phys 57 (1994) 939

[2] P Praserthdam and T Majıtnapakul, Appl Catal A 108(1) (1994) 21

[3] J Yoshınbu and M Kawaı, J Chem Phys 103 (1995) 3220

[4] G W Graham, P J Schmıtz and P A Thıel, Phys Rev B 41 (1990) 3353

[5] Y G Shen, J Yao, D J O'Connor, B V Kıng and R J MacDonald, Solıd State Commun, 100 (1996) 21

[6] J P Reılly, D O'Connell and C J Barnes, J Phys Condensed Matter 11 (1999) 8417

[7] Y G Shen, D J O'Connor and K Wandelt, Surf Scı 406 (1998) 23

[8] H L Davıs and J R Noonan, J Vac Scı Technol 20 (1981) 842

[9] M A Van Hove, W Morıtz, H Over, P T Rous, A Wander, A Barbıerı, N Materer, U Starke and G A Somorjaı, Surf Scı Rep 19 (1993) 191

[10] N W Ashcroft and N D Mermın, Solıd State Physıcs , CBS Publishıng, Japan, 1981

[11] J B Pendry, J Phys C Solıd State Physıcs 13 (1980) 937

[12] Y Gauthıer and R Baudoıng, ın "Segregatıon and Related Phenomena" Edıtors P Dowben and A Mıller, CRC Press, Boca Raton (1990) p169

[13] E AlShamaıleh and C J Barnes, submıtted to Phys Rev B

[14] C J Barnes, E AlShamaıleh, T Pıtkanen, P Kaukasoına and M Lındroos, Surf Scı 492 (2001) 55

[15] L Vıtos, A V Ruban, H L Skrıver and J Kollar, Surf Scı 411 (1998) 186

[16] C J Barnes and E AlShamaıleh, work ın progress

CHAPTER 4

COVERAGE DEPENDENT STRUCTURE AND REACTIVITY OF Cu{100}- c(2X2)-OXYGEN

4.1 Introduction

The decomposition of formic acid on metal surfaces has long been regarded as a model for catalytic reactions due to the simplicity of the intermediates and products involved. [1]. The adsorption of formic acid on copper surfaces has been intensively studied because of the key role that the formate is believed to play in methanol synthesis. As a result of the attention it has received, the chemistry of the system is relatively well understood. The prominent decomposition pathway for copper catalysts is the dehydrogenation of the formate intermediate to produce H_2 and CO_2 [2].

The dissociation of the parent molecule occurs below room temperature to leave a stable formate, $HCOO_{(a)}$, as the surface intermediate. Using temperature programmed reaction spectroscopy (TPRS) it was found that this formate species is held on the surface until around 400K when it starts to decompose forming CO_2 and H_2 product [3]. The formate species is chemisorbed on the copper surface in a bidentate fashion though the two oxygen atoms as shown below:

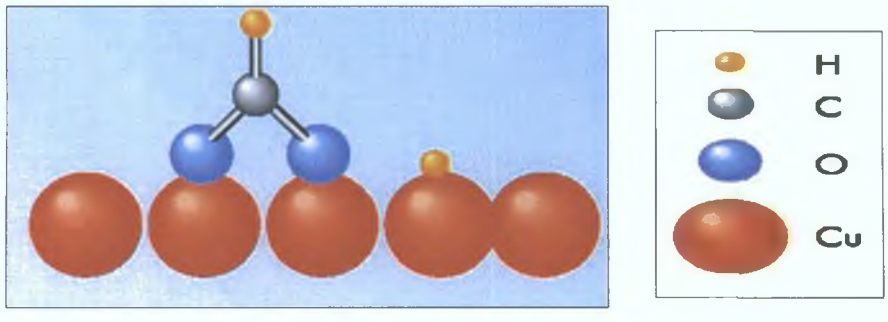

Figure. 4.1: Formate intermediate on a Cu surface (atoms not drawn to scale).

The decomposition of the formate species was also shown to be the rate-limiting step [4]

The behaviour of formic acid when adsorbed on the oxidised Cu(110) surface has also been studied It was observed that the formate was more stable because of the presence of the oxygen [5] When oxygen is preadsorbed on to the copper surface with formate, the oxygen is cleaned off as H_2O by reaction with atomic hydrogen released during formate decomposition [6] Large doses of oxygen (over 1000 L) on the Cu(100) surface yields the $(2\sqrt{2} \times \sqrt{2})R45°$-O structure, ($\theta_0$ = 0 5 ML) See Fig 4 2 [7]

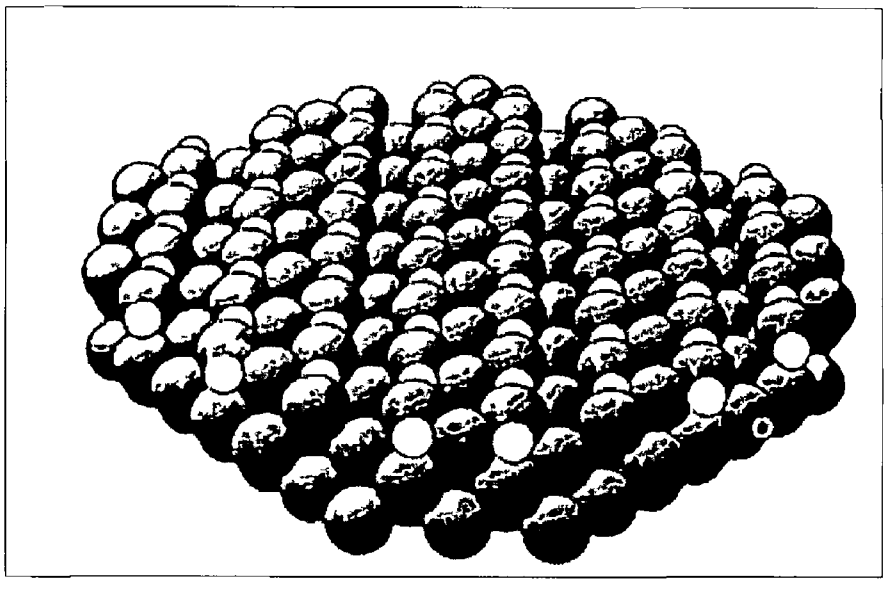

Figure 4 2 The $(2\sqrt{2} \times \sqrt{2})R45°$-O structure on Cu(100) The larger shaded balls represent the Cu atoms and the smaller shaded balls represent the O atoms [8]

The following TPRS experiments are performed under ultra-high vacuum (uhv) conditions The use of uhv conditions or of single copper crystals as catalysts is not viable in the commercial production of methanol However, using such systems as models can provide valuable information As the copper catalyst used in industry will be subject to oxidation is it important to study the effect that adsorbed oxygen has on the formate intermediate The kinetics of the adsorption and decomposition of formic acid on the clean Cu(100) surface is examined Using a variety of oxygen coverages, the decomposition of formic acid on thermally oxidised Cu(100) surface is also

investigated To increase the oxygen coverage above 0 5 ML a more aggressive exposure to oxygen is needed An oxygen plasma is therefore used and in this work formic acid decomposition is studied on an oxygen plasma processed Cu(100) surface

Plasma is loosely defined as a partially or wholly ionised gas with a roughly equal number of positively and negatively charged particles Low temperature plasmas work within a vacuum chamber where atmospheric gases have been evacuated These low pressures allow for a relatively long free path of accelerated electrons and ions Since the ions and neutral particles are at or near ambient temperatures and the long free path of the electrons, which are at high temperature or electron-volt levels, have relatively few collisions with molecules at this pressure the reaction remains at low temperature Because of the high energy involved, the gas molecules are excited enough to fluoresce This fluorescence allows the beam to be easily aimed at the sample for cleaning or processing

The aim of this project is to investigate the thermal oxidation of Cu(100) and to compare its chemistry to that of the oxygen plasma treated surface

4 2 Experimental

Experiments were performed in an UHV chamber with a base pressure in the Figure 4 3 low 10^{-10} Torr region The stainless steel chamber was equipped with a quadrupole mass spectrometer and facilities for Ar^+ ion bombardment A diffusion pump, filled twice daily with liquid nitrogen, was used to help keep the uhv conditions The crystal was mounted in the uhv chamber using tantalum wires The manipulator used to mount the sample crystal provided motion in three dimensions and permitted heating and accurate positioning for Ar^+ bombardment and TPRS measurements

The crystal was heated resistively, in a linear fashion by passing a direct current of 13 5 amps through the Ta wires The linearity of the heating rate was examined graphically, as seen in figure 4 4 From 300-322 K the rate is slower than for at higher temperatures and above 442 K the linearity is questionable and in fact begins to slow down once more The region between 322 K and 442 K is however linear in its heating rate and coincidentally all of the experiments were performed at this temperature range The average heating rate is 3 Ks^{-1} A Chromel Alumel thermocouple was embedded in a hole of 0 25mm diameter drilled into the sample and provided a means of measuring the sample temperature

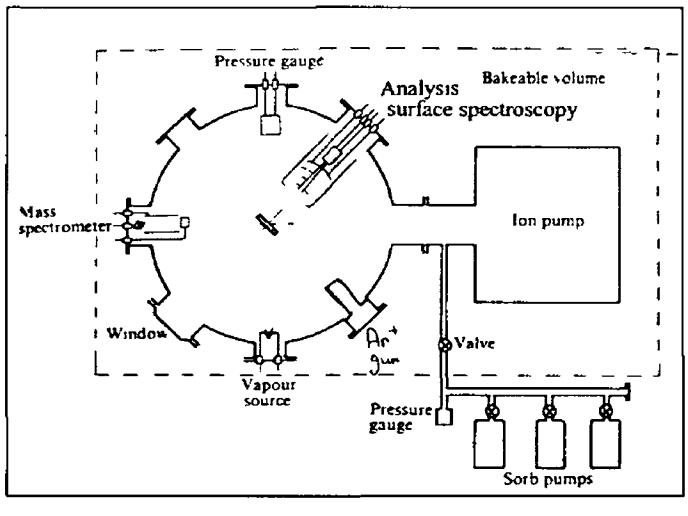

Figure 4 3 Schematic of an uhv chamber equipped for surface science experiments

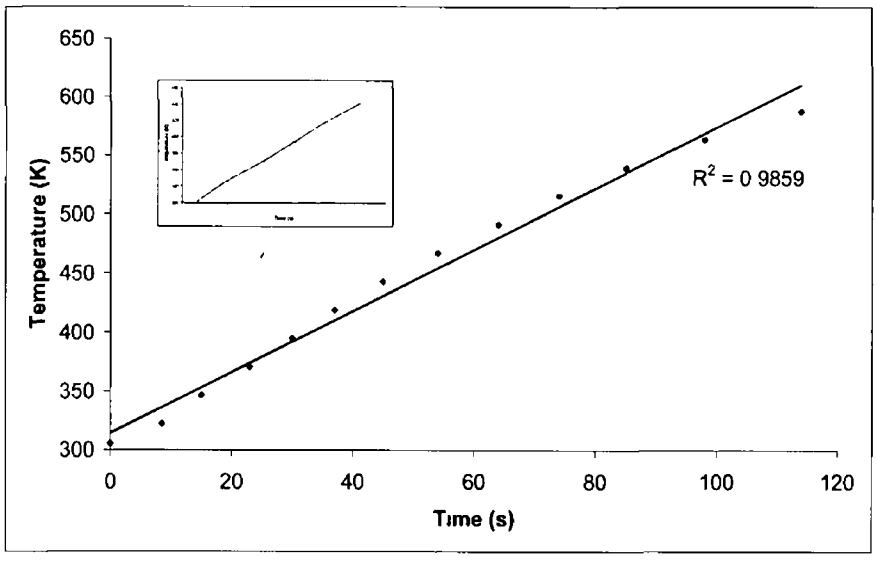

Figure 4 4 Plot of temperature versus of time showing the relatively linear heating rate The inset shows the region between 322 K and 442 K where the heating rate is most linear

The mass spectrometer was employed as the detector for the TPD measurements, for gas analysis and verifying the purity of the admitted formic acid Fragmentation patterns from the mass spectrometer data are used to identify molecules desorbing from the surface The TPD data were acquired using the MASsoft Hiden software package By opening the MASsoft main window as seen in figure 4 5 and then clicking on Gallery figure 4 6 a range of different scan types are displayed

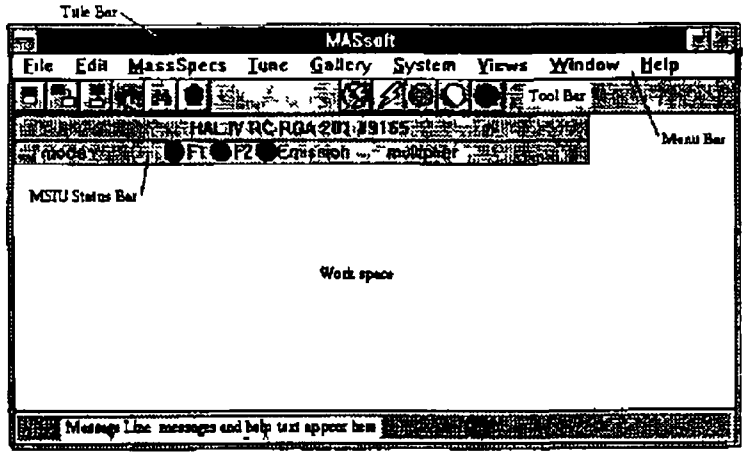

Figure 4 5 MASsoft window

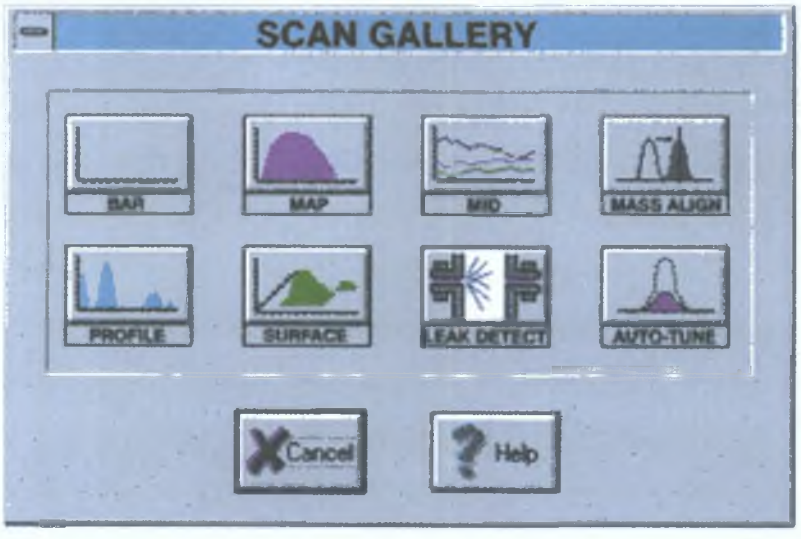

Figure. 4.6: Scan Gallery

PROFILE was used to perform background mass spectra and to check gas purities (Figures 4.8-4.11). The MID scan was used for all our TPD experiments. This scan type allows single mass analysis as well as multi-masses to be monitored. Masses can be added or deleted. When the required masses have been added, a simple click on OK commences the scan. After 5 minutes, when the baselines are level, the TPRS experiments can be carried out. The mass spectrometer settings used in all experiments are given in Figure 4.7.

Saving the raw data involves simply clicking on *Save As* under *File* and entering the file name. One word of warning: the files should never be closed from the right hand part of the screen, as the data displayed will be permanently erased! As all the graphs were plotted using the ORIGIN software package it was necessary to export the raw data from MASsoft. The exported data can then be opened up in Microsoft Excel and subsequently copied and pasted into ORIGIN. The X component (time in ms) and the Y component(s) (pressure at a given mass) are then plotted. As TPD measures the mass spectrometer signal as a function of temperature it is necessary to convert the X-axis from time to temperature. Assuming a linear heating rate and knowing the starting time and temperature, this can be easily achieved.

Parameter	Unit
Mode-change-delay	1000 ms
Energy	1.35V
Focus	54 V
Suppressor	363 V
Cage	3.0 V
Electron-energy	70.0 V
Emission	20.000 uA
Resolution	0%
1st Diode	1200 V
Multiplier	1800 V

Figure. 4.7: Mass spectrometer parameters used.

Cleaning of the crystal was typically performed by Ar^+ ion bombardment. The sample was positioned in front of the sputter gun. The Ar leak valve was carefully opened to leak in the gas. To check its purity 1 x 10^{-7} Torr of Ar was introduced into the chamber and a mass scan was run. The major peak (Ar^+) was at m/z = 40 and the secondary peak (Ar^{++}) was at m/z = 20. The mass spectrometer was turned off before increasing the pressure to 2 x 10^{-6} Torr. With energy of 4 keV, the beam was focussed until the fluorescent Ar^+ beam covered the entire crystal. After a 15-minute bombardment, the crystal was annealed for 5 minutes at 700 K with a current of 10 amps.

With the sample facing the plasma gun, the oxygen plasma processing was carried out with a beam energy of 1.9keV for times varying between 30 and 120 seconds.

The formic acid (97% Aldrich Chemicals) was further purified by several freeze-pump-thaw cycles in order to remove any dissolved gases. The formic acid sample was frozen using liquid nitrogen. Then the valve was opened to vacuum and pumped off to atmosphere. Impurities were pumped away while the formic acid defrosted. A sudden rise to atmospheric pressure was observed on the Pirani pressure gauge as the

gases were being pumped away The valve was then closed and the formic acid reservir was allowed to completely defrost After the formic acid had thoroughly defrosted, the freeze-pump-thaw procedure was repeated twice more

Prior to dosing, the gas-handling lines were flushed with that gas three times and then pumped out Dosing of the formic acid and oxygen was performed through an all-metal leak valve In all experiments dosing was performed with the ion gauge filament set to 1 0 mV except when dosing at high oxygen coverages when 0 1 mV was used, to prevent possible burn out of the filament Prior to experimentation, mass spectra of the gases were taken to check for purity In all experiments the formic acid was dosed at 305 ± 12 K and the oxygen was dosed at 346 ± 5 K For the 3000 L thermal oxygen exposure, three doses of 1000 L were used with successive brief annealing to 600 K to give the $(2\sqrt{2} \times \sqrt{2})$ R 45°-O structure
Exposures are reported in Langmuirs, (1 Langmuir = 1 x 10^{-6} Torr s) and are based on readings of an uncalibrated Bayard-Alpert ion gauge

4 3 Results and Discussion

4 3.1 Decomposition of Formic Acid on a Clean Cu(100) Surface

The Cu(100) surface was exposed to increasing formic acid coverages Figure 4 8 shows multi-mass spectra of the products decomposed from 20 L of formic acid The CO_2, H_2, H_2O and HCOOH evolution was monitored by tuning the mass spectrometer to detect species of mass 44, 2, 18 and 46, respectively The dissociation of the parent molecule occurred at room temperature leaving a stable formate $HCOO_{(a)}$ as the surface intermediate This formate species was held on the surface until above 400 K when it starts to decompose forming the CO_2 and H_2 product It is this decomposition that is believed to be the rate-determining step The formic acid decomposition products observed in the current study agreed with those reported in literature [9,10]

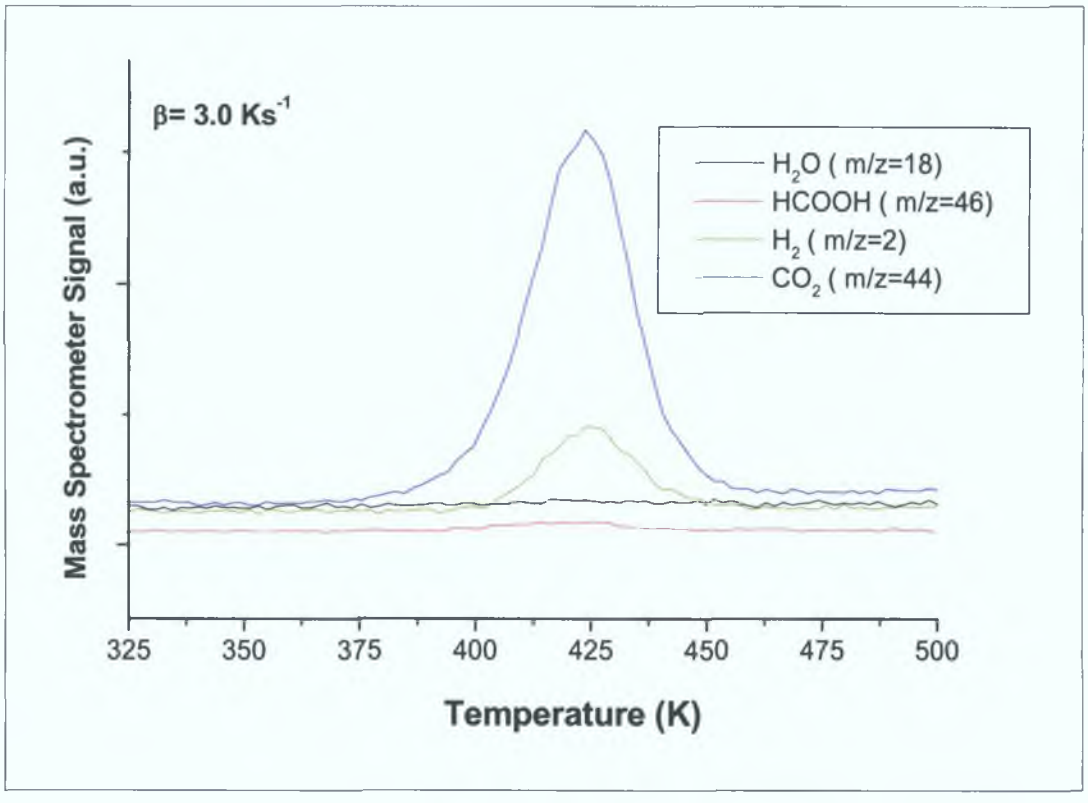

Figure. 4.8: TPRS spectra of the decomposition of 20L of formic acid dosed at 300K on the clean Cu(100) surface.

Carbon dioxide and hydrogen were the sole products observed. The CO_2 and H_2 products showed coincident leading edges and identical peak temperatures of 427 K with a heating rate of 3 Ks^{-1}. When the gavin was multiplied by 5 a small formic acid peak was also observed. This can be accounted for by the recombination of the formic acid from the formate intermediate and adsorbed atomic hydrogen. The water decomposition was negligible. The following reaction mechanism is proposed:

$HCOOH_{(g)} \rightarrow HCOO_{(a)} + H_{(a)}$

$2H_{(a)} \rightarrow H_{2\,(g)}$

$HCOO_{(a)} \rightarrow CO_{2\,(g)} + H_{(a)}$ (slow) - the rate-determining step

$2H_{(a)} \rightarrow H_{2\,(g)}$ (fast)

Figure 4 9 shows a stacked plot of the decomposition to CO_2 on Cu(100) at various formic acid coverages From the plots it can be seen that, in general, as the formic acid exposure increases, so too does the intensity of the desorption peak As more formic acid is adsorbed on the surface, more CO_2 is formed There is a clear shift in the desorption peak to lower temperatures with increased formic acid exposures It shifts from 432 K for the 0 1 L exposure to 423 K for the 20 L exposure The activation energy for the desorption also shifts from 115 KJ/mol for the 0 1 L exposure to110 KJ/mol for the 20 L exposure

This shift is possibly a result of the increase in the repulsive lateral interactions between the adsorbed molecules with increasing exposure As the formic acid exposure increases, the adsorbed molecules are held closer together on the copper surface The electronegative oxygen atoms of neighbouring molecules repel each other This repulsion is much stronger than the hydrogen bonding that may exist between adjacent formates

Interestingly, the peaks do not display the typical asymmetric shape normally associated with first order reactions This could be because of a slow down in the heating rate with time

4 3 2 Decomposition of Formic Acid on a Thermally Oxidised Cu(100) Surface

The study of the decomposition of formic acid on the clean Cu(100) surface is a well understood system and our experiments only confirm what is already known for the last 20 years [9] However, this fundamental TPRS experiment sets the foundations for the following experiments on the O/Cu(100) system Figures 4 10, 4 11 and 4 12 show the effect adsorbed oxygen has on the decomposition of 20 L of formic acid on Cu(100) When the oxygen exposure increases, the adsorbed formate behaves less like the formate adsorbed on clean Cu(100) In fact, water begins to form and its decomposition increases with oxygen exposure Hydrogen formation, on the other hand, is seen to decrease with the amount of oxygen adsorbed

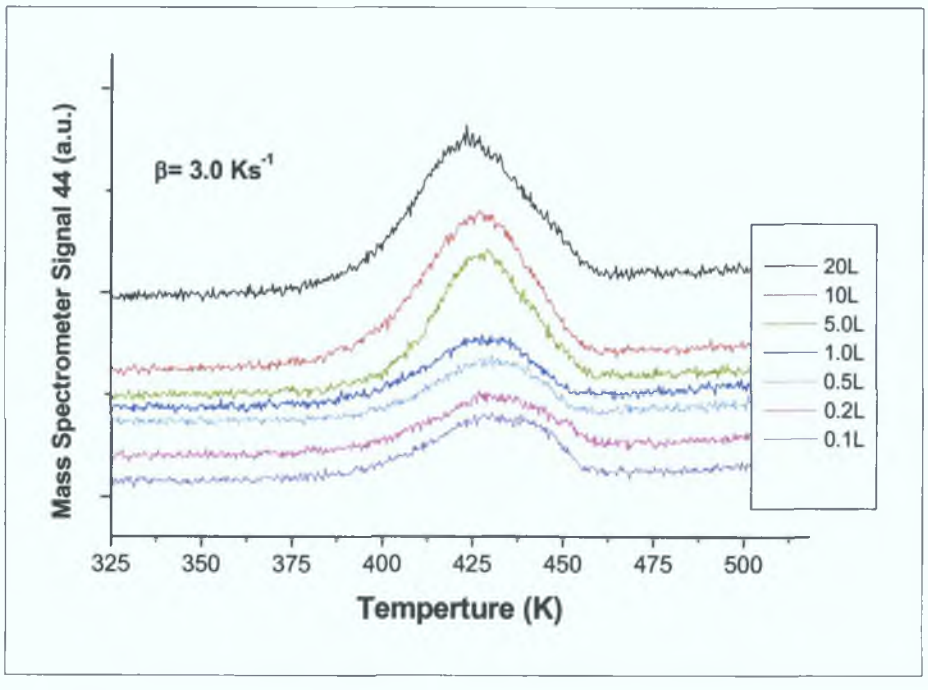

Figure. 4.9: The desorption of CO_2 on Cu(100) at various formic acid exposures dosed at 300 K.

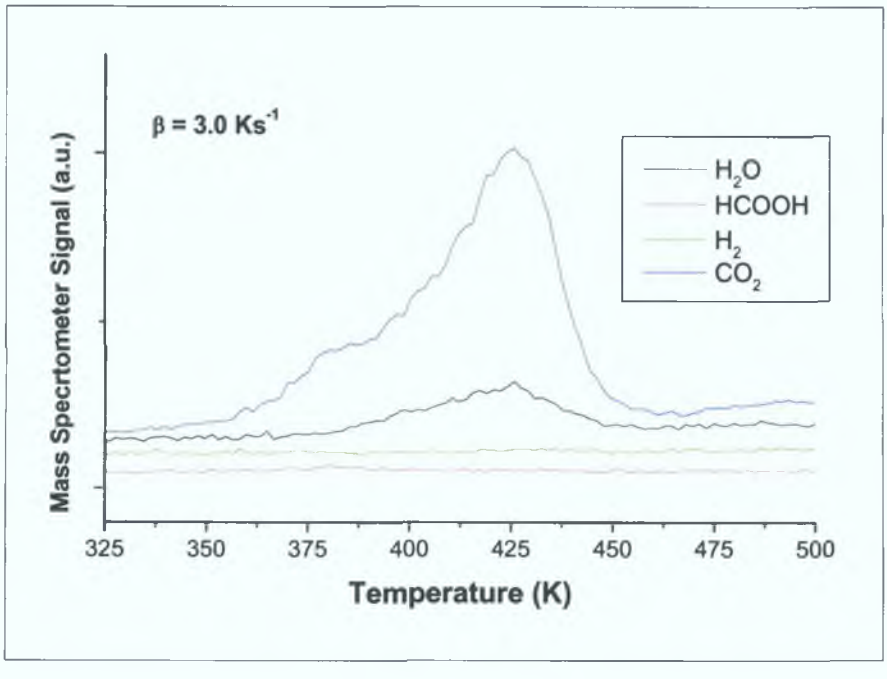

Figure. 4.10: TPRS spectra from 20 L of formic acid decomposition on a Cu(100) after exposure to 1000 L of oxygen.

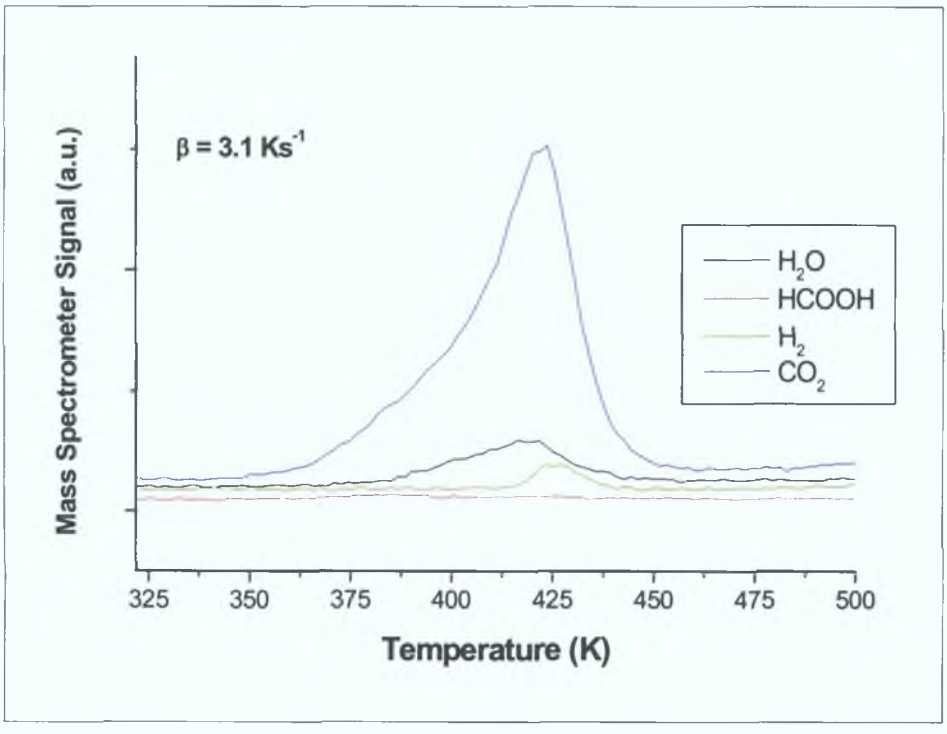

Figure. 4.11: TPRS spectra from 20 L of formic acid decomposition on a Cu(100) after exposure to 200 L of oxygen.

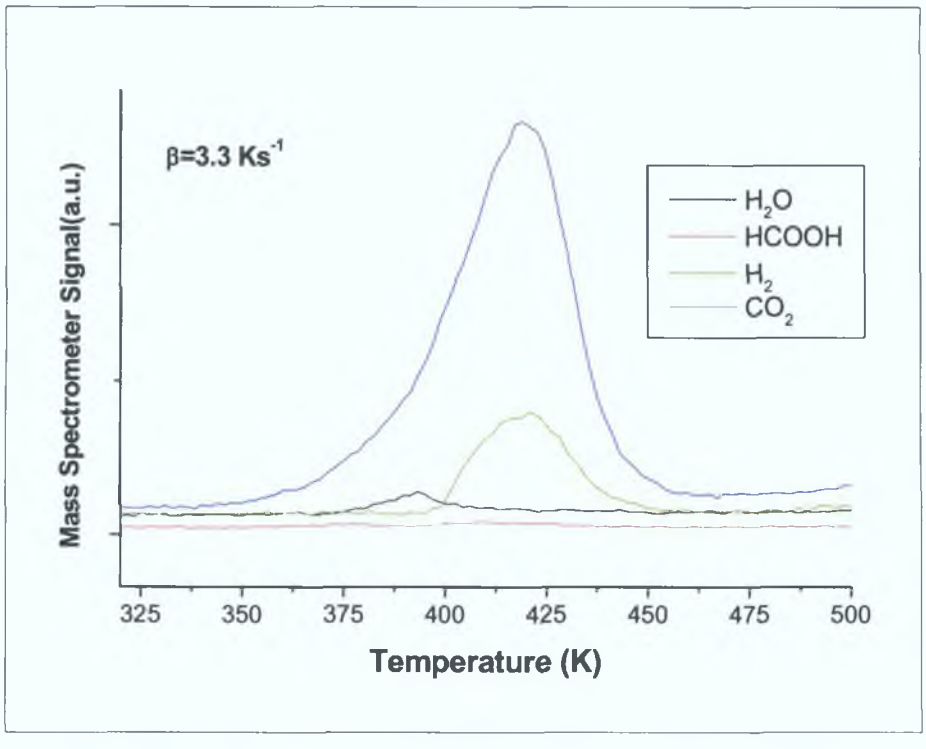

Figure. 4.12: TPRS spectra from 20 L of formic acid decomposition on a Cu(100) after exposure to 25 L of oxygen.

From Figure 4 10 it can be seen that the sole decomposition products from 20 L of formic acid adsorbed after a 1000 L oxygen exposure on Cu(100) were CO_2 and H_2O Both molecules displayed peak maxima at 426 K Hydrogen desorption was not observed Interestingly, a clear shoulder on the CO_2 peak could be seen at around 370 K

At the 200L oxygen exposure CO_2 and H_2O were the major decomposition peaks, Figure 4 11 although a small hydrogen peak was also observed The CO_2 and H_2O peak maxima were no longer coincident This time the peak maxima of H_2O appeared at 417 K, CO_2 at 422 K and the peak maxima of the H_2 was at a higher temperature still at 425 K The CO_2 peak also displayed a strange shoulder at around 380 K

For low oxygen exposures, only small water peaks were observed In Figure 4 12 the major decomposition products from 20 L of formic acid on Cu(100) exposed to 25 L of oxygen, are H_2 and CO_2, similar to the decomposition of formate on the clean Cu(100) Only a small H_2O peak is observed

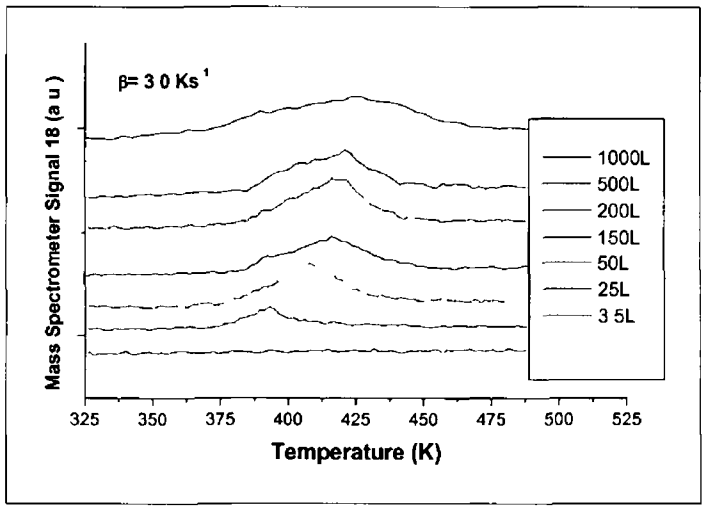

Figure 4 13 H_2O desorption from 20L of adsorbed formic acid after various oxygen exposures

Figure 4.13 shows a stack plot of the desorption of H_2O from 20 L of adsorbed formic acid after various oxygen exposures. The relationship between oxygen exposure and water desorption is evident. The water intensity increases with oxygen exposure. At the 3.5 L oxygen exposure little or no water is given off, compared to at the 1000 L oxygen exposure when the intensity of the water peak is at a maximum. There is also a shift to a higher T_{max} of over 40 K from the 25 L to the 1000 L oxygen exposure.

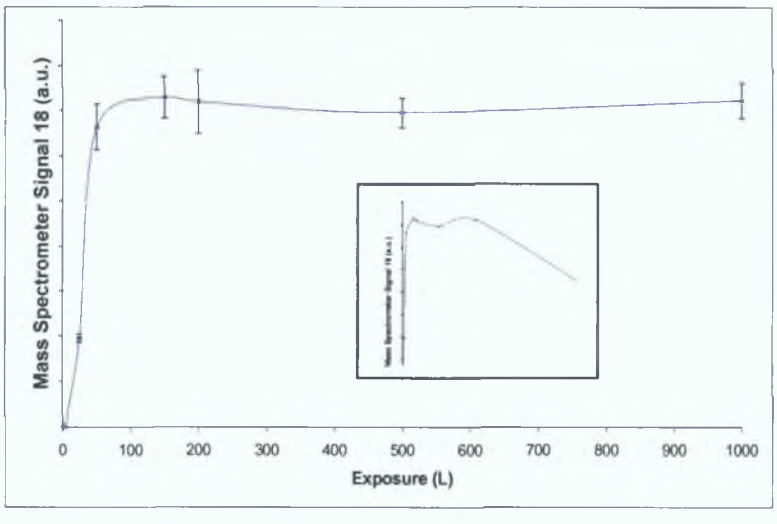

Figure. 4.14: Integrated area of water desorption for Cu(100) exposed to varying oxygen dosages up to 1000 L with error bars associated with the integration. The inset shows oxygen coverages up to 3000 L. In all cases the surface was exposed to 20 L of formic acid.

This increase in water desorption with oxygen exposure is illustrated clearly in Figure 4.14. A sharp rise in water desorption can be seen until the 500 L oxygen coverage after which it starts to level out. Surprisingly, there is a decrease in water desorption from the 1000 L to the 3000 L oxygen exposure. Perhaps at oxygen exposures higher than 1000L the oxygen adsorbed becomes unreactive and less water is desorbed as a result.

The hydrogen desorption, in contrast to the water desorption, decreases with oxygen exposure as can be seen from the stack plots in Figure 4.15. The peak maxima are shifted to higher temperatures with oxygen exposure. Figure 4.16 shows the rapid drop in hydrogen desoption with increasing oxygen exposures. In going from the 1.5 L to the 3.5 L oxygen exposure there appears to be an increase in hydrogen desorption and not a decrease as expected. It is conceivable this may be an experimental error or it may be due to a change in pumping speeds in the vacuum chamber.

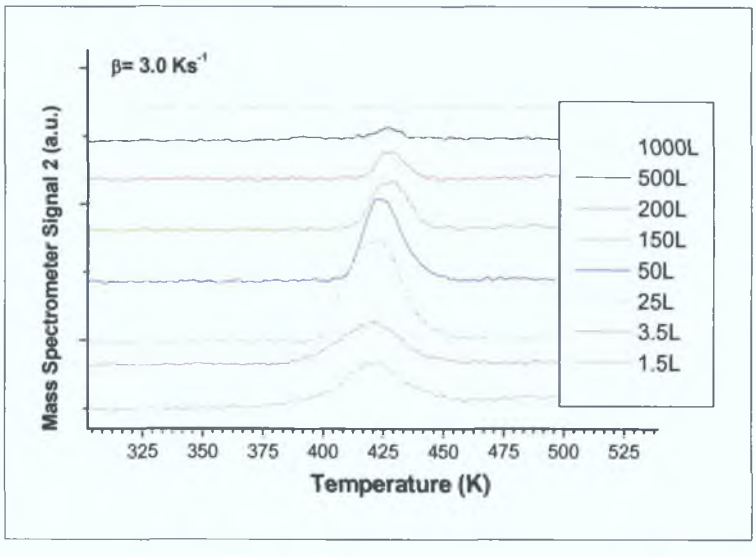

Figure. 4.15: H_2 desorption from 20L of adsorbed formic acid after various oxygen exposures.

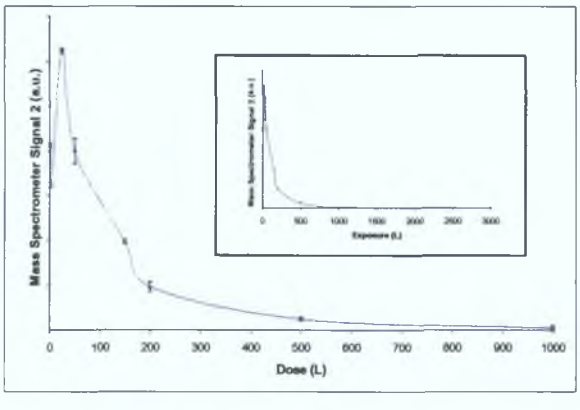

Figure. 4.16: Integrated area of H_2 desorption for Cu(100) exposed to varying oxygen dosages up to 1000 L with error bars associated with the integration. The inset shows oxygen coverages up to 3000 L. In all cases the surface was exposed to 20 L of formic acid.

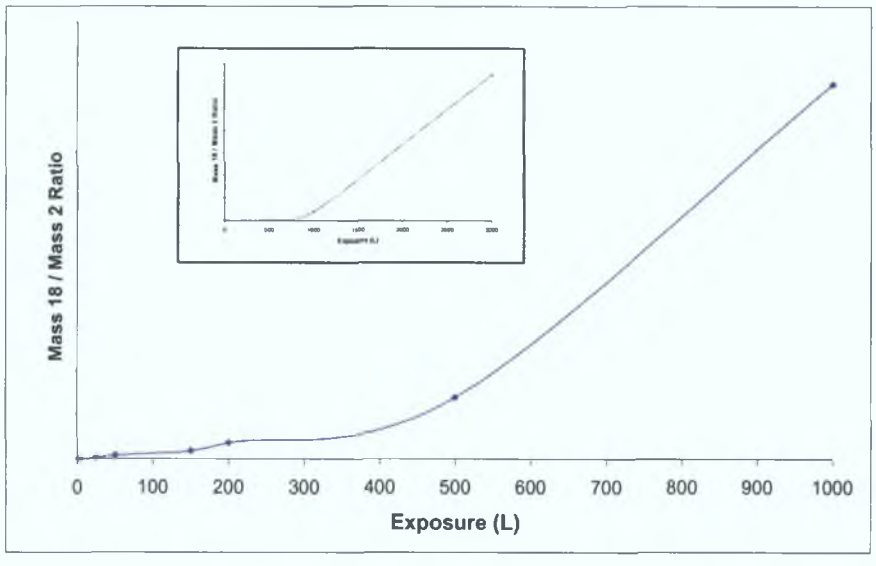

Figure. 4.17: Ratio of water and hydrogen desorption for Cu(100) exposed to varying oxygen dosages up to 1000 L. The inset shows oxygen coverages up to 3000 L. In all cases the surface was exposed to 20 L of formic acid.

Figure 4.17 illustrates the ratio of the water / hydrogen integrated areas. An increase in water over hydrogen as a function of oxygen exposure is evident.

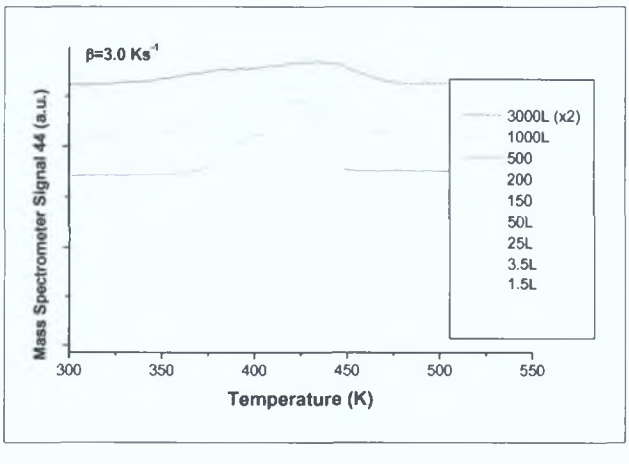

Figure. 4.18: CO_2 desorption from 20L of adsorbed formic acid after various oxygen exposures.

Figure 4.18 is a stacked plot of the CO_2 desorption peaks from 20 L of adsorbed formic acid after various oxygen exposures As all experiments were dosed with 20 L of formic acid and the intensity of the CO_2 desorption peak is related to the formic acid coverage, the CO_2 peaks should have the same intensities for all experiments. Fluctuations in the pumping speed and detector efficiency could account for the variation of peak intensities as seen above. The peak maxima appear within ± 4 K. A clear shoulder is observed on the leading edges especially those at high oxygen exposures.

Comparing the integrated areas of the CO_2 peak with the H_2O and H_2 peaks we notice that as the oxygen exposure increases the CO_2/H_2O ratio gets smaller (Figure 4.19) and the CO_2/H_2 ratio gets larger (Figure 4.20).

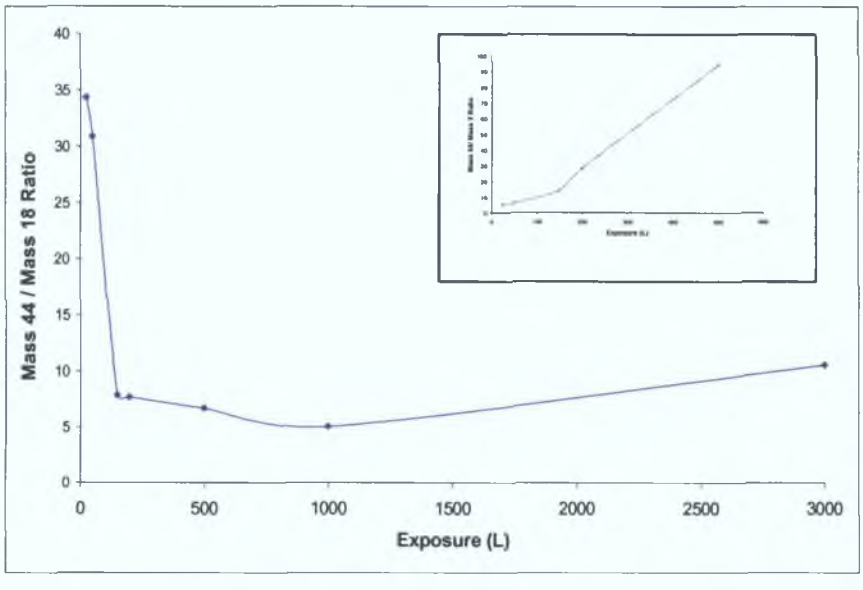

Figure. 4.19: Ratio of CO_2 versus H_2O desorption as a function of oxygen coverage.

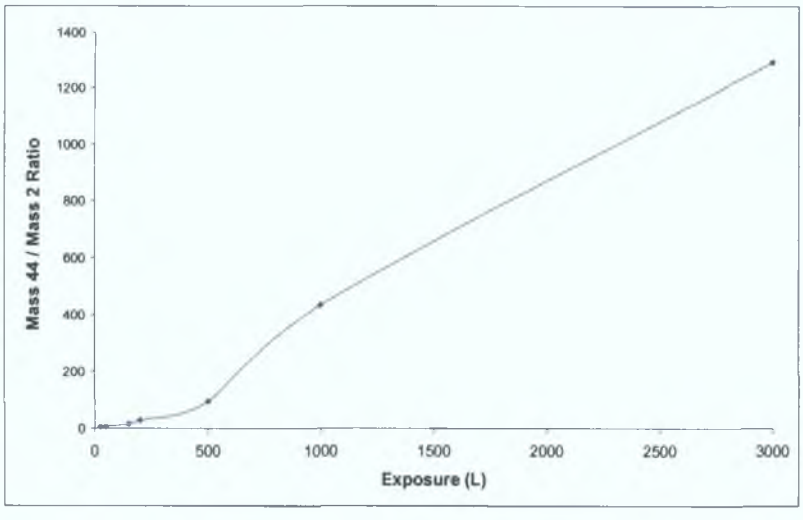

Figure. 4.20: Ratio of CO_2 versus H_2 desorption as a function of oxygen coverage. The inset shows the lower oxygen coverages blown up.

From the above results it is obvious that the presence of chemisorbed oxygen affects the decomposition of the formate intermediate on Cu(100). Unlike formate decomposition on clean Cu(100),which exhibits identical lineshapes for CO_2 and H_2 desorption, CO_2 evolution begins earlier on oxygen dosed Cu(100) due to the atomic hydrogen produced in the leading edge of the formate decomposition process being mopped up by a combination of reaction with chemisorbed oxygen to form H_2O and re-protonation of formate intermediate. It is only when all the reactive oxygen has been desorbed as water that we begin to see the presence of the H_2 peak once more.

The leading edge for the desorption of water appears at higher temperatures than that for CO_2. This delay could be associated with the formation of a hydroxy intermediate as the formate decomposes. With increasing temperature the hydroxy intermediate could become protonated by adsorbed atomic hydrogen causing the desorption of water. This theory would also explain the observed shoulder in the CO_2 peak. In the stacked CO_2 plot in Figure 4.18 this shoulder is most evident at high oxygen exposures. Comparing Figure 4.18 with Figure 4.13 it can be seen that this shoulder appears at the leading edge of the water peak.

The proposed reaction mechanism is therefore the following

$HCOOH_{(g)} + O_{(a)} \rightarrow HCOO_{(a)} + OH_{(a)}$

$HCOO_{(a)} + O_{(a)} \rightarrow CO_{2(g)} + H_{(a)}$

$H_{(a)} + OH_{(a)} \rightarrow H_2O_{(g)}$

Only when all the reactive oxygen is used up do the adsorbed hydrogen atoms recombine

$2H_{(a)} \rightarrow H_{2(g)}$

This mechanism is in agreement with Bowker and co-worker's TPD study on the O/Cu(110) system [10]

It is the water desorbing that causes the shoulder in the CO_2 peak The activation energy for the reaction is determined by the formate decomposition and so the water desorption is simply dependent on the formate decomposition

4 3 3 Decomposition of Formic Acid on the Oxygen Plasma Processed Surface

The somewhat aggressive technique of oxygen plasma processing allowed the oxygen coverage to be increased above 0 5 ML Figures 4 21 and 4 23 illustrate the TPRS spectra of the decomposition products from the 30 s and 120 s plasma processed surface after a 20 L formic acid exposure In both TPRS spectra there is an apparent delay in the leading edge of the water peak as was the case for the thermally oxidised Cu(100) surface The shoulder in the CO_2 peak associated with the water desorption is also present in the spectra below For the 120 s oxygen plasma treatment, the mass spectrometer was tuned to m/z = 30 to monitor if any formaldehyde desorbed However, none was observed

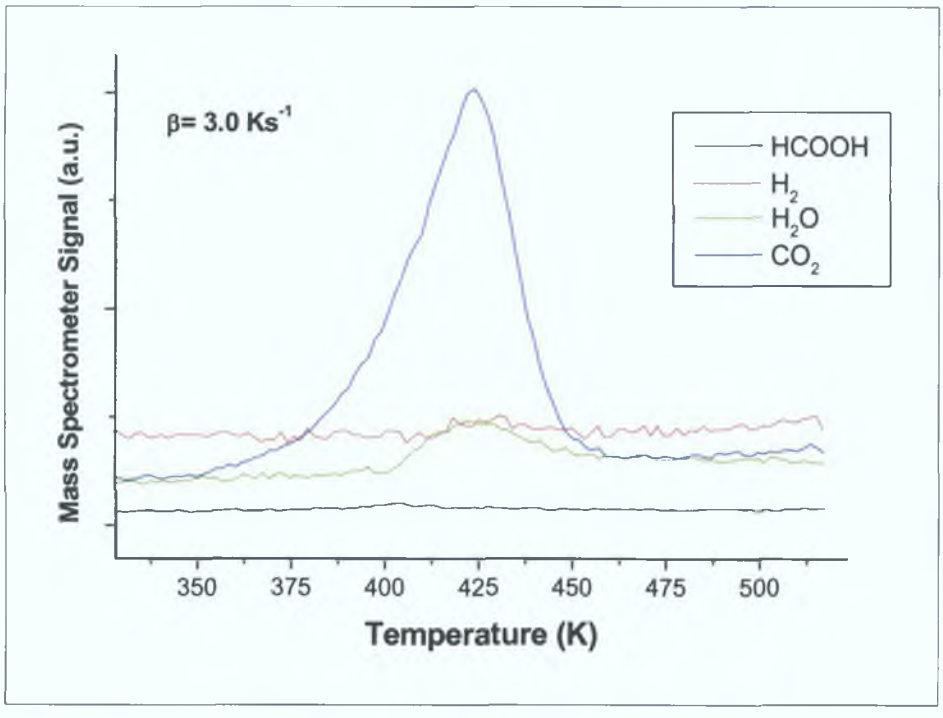

Figure. 4.21: TPRS spectrum of the decomposition products from the 30 s plasma processed surface after a 20 L formic acid exposure.

Exposure (s)	Area of H_2	Area of H_2O	Area of CO_2	CO_2 / H_2O Ratio
30	1.1E+05	4.6E+05	3.3E+06	7.2
120	2.9E+03	1.7E+05	1.5E+06	8.8

Figure. 4.22: Integrated area and ratios of the decomposition products after a 20 L formic acid exposure on the 30 s and 120 s oxygen plasma processed Cu(100) surface.

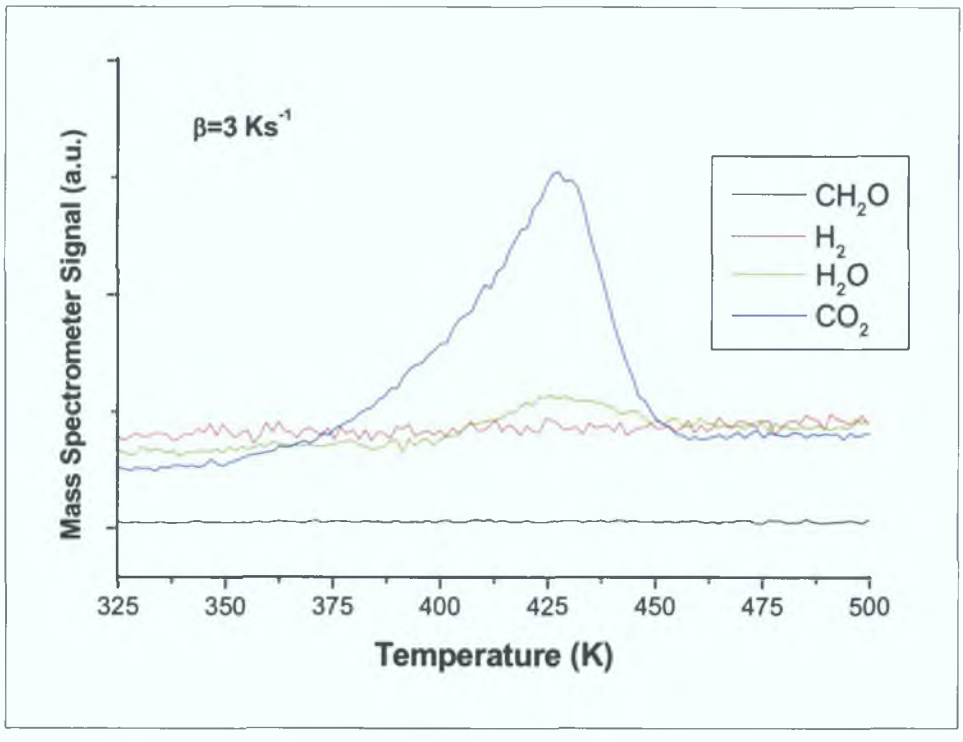

Figure. 4.23: TPRS spectrum of the decomposition products from the 120 s plasma processed surface after a 20 L formic acid exposure.

The intensity of the water peak for the 120 s plasma treatments was surprisingly weak. Perhaps at such high oxygen exposures a more stable copper oxide is formed and the oxygen atoms are less lightly to react off as water. To ensure that all the reactive oxygen was desorbed off as water another 20 L of formic acid was dosed on the surface and the experiments were repeated. The resulting TPRS spectra, showed CO_2 and H_2 desorption peaks similar to the decomposition of formic acid on clean Cu(100) indicating that even if there was oxygen left on the surface, it was not reactive. Consequently, TPRS studies are not enough for a conclusive investigation of the oxygen plasma-processed surface. Other surface science techniques would therefore be required. A combination of TPRS with Auger electron spectroscopy (AES) or X-ray photoelectron spectroscopy (XPS) would elucidate unambiguously whether there was any unreactive oxygen still adsorbed on the surface.

From the CO_2 / H_2O ratio in Figure 4.22 it is apparent that the water intensity did not significantly increase after an extra 90 s of oxygen plasma treatment. Although the

hydrogen intensity appears larger for the shorter plasma treatment, this could however, just be associated with extra signd noise

As for the thermally oxidised copper surface, the delay in the water desorption could be associated with the formation of a hydroxy intermediate after formate decomposition The observed delay could also, however, be related to the aggressive manner in which the oxygen is dosed on the surface The high-energy plasma beam may cause the oxygen atoms to become embedded into the copper surface Higher temperatures would then be required to free these oxygen atoms for bonding with hydrogen atoms

4 4 Conclusions

As the formic acid exposure on the clean Cu(100) surface increased

- The intensity of the desorbing molecules increased
- A shift to lower peak maxima was observed
- There was a decrease in the activation energy of desorpotion

TPRS analysis of the desorption of formic acid on the thermally dosed O/Cu(100) revealed that

- As the oxygen exposure increased, the water desorption increased
- Hydrogen desorption decreased with increasing oxygen exposures
- Only when all the reactive oxygen is reacted off as water will the production of hydrogen be observed
- The delay in the leading edge of the water peak may be associated with the formation of a hydroxy intermediate as the formate decomposes
- The observed shoulder in the CO_2 peak is a result of the desorption of water

In all experiments, only one 20 L dose of formic acid was required to remove all the reactive oxygen from the copper surface It would therefore be interesting to use smaller doses of formic acid, such as 10 L, to compare with the present study The necessary cooling facilities to dose oxygen at temperatures below 300K were unavailable for this study but it would be interesting to repeat our thermal experiments at lower temperatures to see how this affects the water desorption

The plasma work didn't reveal any new chemistry but it is a useful way of increasing the oxygen coverage above 0 5 ML Because of time restrictions, only experiments of 30 s and 120 s were performed It would be worthwhile to reconduct similar experiments at more frequent time intervals up to 120 s

AES or XPS work would need to be carried out in conjunction with TPRS analysis for both oxygen treatments to investigate possible unreactive oxygen remaining on the surface Low energy electron diffraction (LEED) or scanning tunnelling microscopy (STM) would shed more light on the binding sites of the formate on the Cu(100)-($2\sqrt{2}$ x $\sqrt{2}$)R45 °-O structure

References

[1] J Scholten and P Zwietering, Adv Catal 14, (1963) 35

[2] R J Madix, Adv Catal 29 (1980) 1

[3] D H S Ying and R J Madix, J Catal 61 (1980) 48

[4] J Mc Carty and R J Madix, J Catal 38 (1975) 402

[5] M Bowker, E Rowbotham F M Leibsle and S Haq, Surf Sci 349 (1996) 97

[6] K Pussi, M Lindroos, H Younis, E AlShamaileh, C J Barnes, to be published

[7] R Mayer, C S Zhang, K G Lynn, Phys Rev B 33 (1986) 8899

[8] D P Woodruff, J Phys Condens Matter, 6 (1994) 6067

[9] M Bowker and R J Madix, Surf Sci 102 (1981) 542

[10] M Bowker and R J Madix, Surf Sci 95 (1974) 190

CHAPTER 5

CONCLUSIONS & FUTURE WORK

CONCLUSIONS

Quantitative low-energy electron-diffraction (LEED) and Temperature Programmed Reaction Spectroscopy (TPRS) were successfully used in the determination and characterisation of the structures formed by adsorbing thin film platinum, formic acid and oxygen on Cu{100} single crystal TPRS is proved to be a powerful complementary method to LEED data and calculations The surface composition was also studied using Auger Electron Spectroscopy (AES)

The evolution of CO_2 from a clean Cu(100) upon decomposition of formate intermediate adsorbed on the surface has been monitored through the use of TPRS Spectroscopy The study has shown clearly the presence of repulsive lateral interactions between the adsorbates on the surface and has been identified

It has also been evidenced that platinum has a destabilising effect on the formate intermediate Peak temperature (T_p) for the CO_2 desorption spectra from copper-platinum model surfaces, appear around 40K lower than those from clean copper This suggests a much less stable surface alloy compared to the clean surface It was also observed that desorption is much more rapid from the copper-platinum than from clean copper More study is needed to fully understand these results

A Cu{100}-c(2x2)-Pt surface alloy structure formed by deposition of 1ML of Pt and thermal processing to 550K is shown to correspond to a copper-capped bimetallic surface-localised alloy with a sub-surface ordered c(2x2) CuPt layer The layerwise compositional profile has been extracted via ATA modelling resulting in an almost pure outermost copper monolayer with only a small Pt impurity concentration (10±10 at%) Layers 3 and 4 contained higher Pt concentrations of 20±20 and 30±30 at% respectively

Substitution of platinum into the selvedge results in a significant expansion in the surface interlayer spacings relative to clean Cu{100} and switches the weak oscillatory relaxation of clean Cu{100} to a strongly and non-uniformly expanded interlayer separation The outermost three interlayer spacings are strongly expanded

A Pt/Cu{100}-(2x2)-O surface alloy structure formed by deposition of a high Pt loading and thermal processing in oxygen atmosphere is shown to correspond to an oxygen overlayer on a copper-capped bimetallic surface-localised alloy with an

ordered c(2x2) CuPt monolayer in layers 2 and 4 Substitution of platinum into the selvedge results in a significant expansion in the surface interlayer spacings relative to Cu{100}-(2√2x√2)R45°-O due to the larger metallic radius of Pt and switches the weak oscillatory relaxation of Cu{100}-(2√2x√2)R45°-O to a strongly and non-uniformly expanded interlayer separation The outermost three interlayer spacings are expanded with a slight rippling in the first CuPt underlayer with Pt atoms rippled outwards towards the vacuum interface within the composite layer

FUTURE WORK

Several experiments are planned to be carried out as a continuation of this work They include the systems and projects described below

1 Coverage Dependent Structure and Reactivity of Cu{100}-c(2x2)-Pd-oxygen.

(a) Clean Cu{100} mass 44(CO_2) , mass 2(H_2), mass 18(H_2O), mass and mass 28(CO)
(b) Cu{100}/0 5ML Pd as above, but also mass 20(D_2O) to probe Pd like chemistry
(c) Cu{100}/1ML Pd as (b)
(d) Cu{100}/1 5L Pd as (b)

2 Structure and reactivity of Cu{100}-c(2x2)-K and Cu{511}/K Comparison Low Energy Electron Diffraction (LEED) and Temperature Programmed Desorption (TPD)

(a) Ion bombardment and annealing to high temperature about (600-700K)
(b) Calibrate K source with LEED
(c) Experiments for saturation exposure of formic acid (50L), TPRS of formic acid

(d) Temperature Programmed reaction spectroscopy (TPRS) of formic acid suggested potassium coverages 0 05L, 0 1L, 0 2L, 0 5L, 0 75L, 1 0L, 2L, 5L, 10L, 20L, and 50L In each case we can follow masses 2(H2), 18(H2O), 44(CO2), 28(CO) and 46(HCOOH)